

UNIVERSITY OF NAPLES FEDERICO II



DEPARTMENT OF PHARMACY

PhD programme in Pharmaceutical Sciences

Possible synergic interaction between endogenous lipids and natural products in the management of cardiovascular alterations, secondary to metabolic impairment

PhD student

Federica Comella

Coordinator

Prof.

ROSARIA MELI

Tutor

Prof.

GIUSEPPINA MATTACE RASO

XXXV CYCLE (2020-2022)

SUMMARY

ABSTRACT	1
INTRODUCTION.....	4
1. OLEOYLETHANOLAMIDE: an endogenous lipid	7
1.1 Origin and classification	8
1.1.1 Anabolic pathways.....	9
1.1.2 Catabolic pathways.....	11
1.2 PPAR- α : a key mediator of OEA effects	14
1.2.1 Role and expression of PPAR- α in kidney.....	16
1.2.2 Role and expression of PPAR- α in heart.....	18
1.2.3 Other converging mechanisms: TRPV1 and GPR119.....	19
1.3 Physiological and pharmacological effects	20
1.3.1 Effects of OEA on feeding	20
1.3.2 Effects of OEA in energy homeostasis: lipid and glucose metabolism.....	23
1.3.3 Effects of OEA on inflammation and fibrosis.....	25
1.3.4 Other actions of OEA	26
2. GINKGO BILOBA LEAVES: a natural extract	27
2.1 Phytochemistry and characterization	27
2.1.1 Flavonoids.....	28
2.1.2 Terpenoids	29
2.2 Bioactivities and clinical uses	30
2.2.1 Effect on vasculature	32
2.2.2 Antioxidant effect.....	33
2.2.3 Antidepressive effect.....	34
2.2.4 Metabolic effect	35
3. OBESITY-INDUCED CARDIORENAL DISEASE	37
3.1 Obesity: evidence, epidemiology and risk factor.....	37
3.2 Pathophysiological mechanisms in obesity: kidney-heart connection.....	38
3.2.1 Renometabolic alteration.....	40
3.2.2 Cardiometabolic alteration.....	42
3.3 Pharmacological approaches	47
3.3.1 Lifestyle modifications.....	48
3.3.2 Anti-obesity medications.....	48
3.3.3 Bariatric surgery.....	49
3.4 HFD-induced obesity in rodents: focus on cardiorenal alterations.....	50
4. CHRONIC KIDNEY DISEASE (CKD)	52
4.1 Definition, epidemiology and risk factors	52

4.2 Pathophysiological mechanisms	55
4.3 CKD management	57
4.3.1 Conventional care	58
4.3.2 Dialysis and kidney transplantation	59
4.3.3 Supportive care	60
4.4 FA-induced CKD animal model	60
5. METHODS.....	64
<i>In vivo models</i>	64
5.1 High fat diet-driven metabolic alterations in kidney and heart	64
5.2 Folic acid induced CKD: experimental setup	66
5.3 Oleoylethanolamide synthesis	69
5.4 Metabolic cages.....	71
5.5 Oral glucose tolerance test (OGTT)	72
5.6 Evaluation of cardiovascular parameters.....	73
5.7 Biochemical evaluations.....	73
5.8 Histological score analysis	74
5.9 Western blotting.....	74
5.10 Real Time PCR analysis	75
5.11 ROS assay.....	76
5.12 Lipidomic profile	77
<i>In vitro studies</i>	80
5.13 Cell culture and treatment	80
5.14 Assessment of cell viability.....	81
5.15 Protein and mRNA determinations	82
5.16 Data and statistical analysis.....	83
6. RESULTS	84
6.1 OEA limits metabolic impairment related to HFD-induced obesity	84
<i>Effect of OEA on cardiometabolic alteration related to obesity</i>	84
6.1.1 OEA counteracts metabolic alteration induced by HFD in mice	84
6.1.2 OEA ameliorates glucose homeostasis in obese mice	85
6.1.3 OEA balances the alteration of metabolic mediators in the heart	86
6.1.4 OEA increases myocardial glucose uptake activating AMPK-AKT-AS160 signalling.....	88
6.1.5 OEA effects on lipid profile in obese mice	89
6.1.6 OEA limits inflammatory and fibrosis in cardiac tissue.....	91
6.1.7 OEA involvement in cardiomyocyte autophagosome formation	93
<i>Effects of OEA on renal alteration related to obesity</i>	94
6.1.8 OEA recovers kidney function perturbed in obese mice	94
6.1.9 OEA limits inflammation and fibrosis induced by HFD	95
6.2 OEA counteracts FA-induced renal damage in mice	97

6.2.1 OEA improves renal function impaired by FA	97
6.2.2 OEA attenuates tubulointerstitial injury induced by FA.....	98
6.2.3 OEA inhibits proinflammatory parameters and cell recruitment in kidney of FA mice	100
6.2.4 OEA suppresses renal fibrotic response in FA mice	102
6.2.5 OEA counters oxidative stress related to FA-induced kidney damage ..	103
6.2.6 Effects of OEA on PPAR- α and TRPV1 transcription.....	104
6.3 PPARα involvement in OEA reno-protective effects	105
<i>In vivo experiments</i>	105
6.3.1 OEA fails in restoring kidney function in PPAR- α KO mice.....	106
6.3.2 PPAR- α blunting limits OEA anti-inflammatory and anti-fibrotic effects	107
<i>In vitro experiment</i>	108
6.3.3 Effects of OEA on TGF β 1-induced fibrosis in HK-2 cells	108
6.3.4 PPAR- α involvement in the inhibition effect of OEA on fibrosis and inflammation induced by TGF- β 1 exposure	110
6.3.5 OEA inhibits effect on the TGF- β 1/Smad and MAPK signaling pathways in HK-2 cells through the PPAR- α	111
SUPPLEMENTARY RESULTS	113
6.4 OEA and EGb association does not show synergistic effects.....	113
<i>In obese mouse model</i>	113
6.4.1 OEA and EGb combination fails to restore the metabolic alteration in HFD mice	113
<i>In CKD mouse model</i>	114
6.4.2 OEA and EGb association does not regenerate kidney impairment in FA mice	114
6.4.3 OEA and EGb combination does not limits kidney inflammation and fibrosis in FA mice.....	115
6.4.4 EGb can not restore inflammation, fibrosis, and oxidative stress in FA mice	116
7. DISCUSSION	118
7.1. Lack of synergy between OEA and EGb on kidney damage.....	119
7.2. OEA protective effect in HFD-induced heart damage	121
7.3. OEA effect on kidney damage.....	125
8. GENERAL CONCLUSIONS	131
9. KEY POINTS	133
10. REFERENCES	134

ABSTRACT

The interaction between the kidneys and the heart has been recognized as a clinical entity called cardiorenal syndrome (CRS). CRS represents concomitant cardio-vascular and renal disorders that result from systemic diseases with common pathophysiological pathways. Whether in the heart or the kidney, fibrosis is the expected consequence of inflammation and oxidative stress-related endothelial dysfunction in hypertension, diabetes mellitus, and obesity, ultimately leading to cardiovascular disease (CVD), heart failure, and chronic kidney disease (CKD).

Peroxisome proliferator-activated receptor (PPAR)- α is a member of the nuclear hormone receptor family of ligand-activated transcription factors and is mainly involved in regulating inflammation, fibrogenesis, and lipid oxidation [Lin et al., 2022].

Oleylethanolamide (OEA), belonging to the family of N-acylethanolamines, is an endogenous lipid mediator derived from the monounsaturated fatty acid oleic acid. OEA, a PPAR- α high-affinity agonist, controls feeding behaviour, body weight, and lipid metabolism [Bowen et al., 2017].

This study aimed to investigate OEA potential in counteracting cardiorenal alterations in a mouse model of obesity induced by a high-fat diet (HFD) and to evaluate the possible OEA synergic effect with Ginkgo Biloba leaf extract (EGb).

In our experimental conditions, after 12 weeks of HFD feeding, EGb alone or combined with OEA did not show any significant effect after 6-week treatment. No difference was shown among HFD-fed mice and EGb- or

EGb and OEA-treated mice in metabolic, cardiovascular, and renal function parameters. Similarly, the evaluation of molecular markers related to macrophage recruitment or fibrosis in the kidney did not show any potential of EGb or EGb/OEA combination in damping renal damage. However, long-term administration of OEA (2.5mg/kg/day) in obese mice limited metabolic alterations and heart and kidney damage. In particular, OEA normalizes cardiac metabolic factors, modulates tissue lipid profile, and reduces inflammatory and fibrotic markers. OEA also improved functional renal readouts, accompanied by a reduction of kidney inflammatory factors.

Furthermore, to assess the direct effect of this acylethanolamide on kidney function and damage, regardless of its metabolic activity, its antifibrotic and anti-inflammatory effects were investigated in a mouse model of CKD induced by a high dose of folic acid (FA).

In FA-induced CKD, short-term administration of OEA (2.5mg/kg/day) for eleven days prevents inflammation, fibrosis, and oxidative stress. All those OEA effects were blunted in FA-challenged PPAR- α KO mice, indicating a pivotal involvement of PPAR- α in the OEA renoprotective effect. *In vitro* experiments on human proximal tubular cells HK-2 exposed to transforming growth factor (TGF)- β 1 confirmed the direct and specific impact of OEA, which reduced the inflammatory and fibrotic processes. The *in vitro* activity of OEA on HK-2 was contingent on PPAR- α activation since the preincubation with a PPAR- α specific antagonist blunted OEA effects.

These results indicate that OEA may be a promising molecule for treating cardiometabolic alterations and kidney dysfunction, limiting the molecular mechanisms associated with the transition toward chronic diseases.

Keywords: Oleoylethanolamide (OEA); Obesity; Cardiorenal syndrome; Fibrosis; Chronic Kidney Disease (CKD); PPAR- α .

INTRODUCTION

The prevalence of obesity, according to World Health Organization (WHO) estimates, has been steadily increasing over the past several decades. The interactive metabolic maladaptive mechanisms due to obesity determine cardiovascular and kidney disease risk factors, including insulin resistance, hypertension, and dyslipidemia that constitute the cardiorenal metabolic syndrome (CRMetS) [Connell et al., 2014]. The bidirectional relationship between the heart and kidney can be direct or indirect and includes an intricate feedback system in which the dysfunction in one organ affects the other. Whether in the heart or the kidney, fibrosis is the expected consequence of inflammation and oxidative stress-related endothelial dysfunction in hypertension, diabetes mellitus, and obesity, ultimately leading to cardiovascular disease, heart failure, and chronic kidney disease (CKD) [Zannad et al., 2018]. Therefore, there is a need to develop new therapeutic strategies for treating and preventing cardiovascular damage sustained by metabolic diseases.

The pathogenesis of obesity involves regulating calorie utilization, appetite, and physical activity; however, it has complex interactions with the socio-economic status and underlying hereditary and environmental factors. Fat accumulation is driven by an energy imbalance between food intake and energy-expended calories, which leads to excessive adipose tissue accumulation [Lin et al., 2021]. Fibrosis is a common consequence of inflammation- and oxidative stress-related endothelial dysfunction, obesity, diabetes mellitus, ischemia, and organ injury. It is a common feature in heart failure and chronic kidney disease. Therefore, we suggest that fibrosis may be a marker and the primary driver of the

pathophysiology of several cardiorenal syndromes. Interstitial fibrosis in the heart, large arteries, and kidneys may play a key role in the pathophysiology of the cardiorenal syndrome continuum [Zannad et al., 2018].

Peroxisome proliferator-activated receptors (PPARs) are nuclear receptors that modulate the functions of many target genes. Three isoforms of PPARs, have been identified, namely PPAR- α , β/δ , and γ . PPAR- α is involved in fatty acid oxidation (FAO) and is expressed in the liver, kidney, brown adipose tissue, and cardiac muscle. The pleiotropic role of this receptor in metabolism and inflammatory response supports the idea that the modulation of its signalling may contribute to managing the comorbidities secondary to metabolic impairment. Whereas metabolic effects of PPARs are mediated by activation of a PPAR-responsive element present in the promoter region of different genes, the cardiovascular protective actions may result from anti-inflammatory and antioxidant actions mediated by transrepression of proinflammatory and pro-oxidant genes [Lee et al., 2015].

A potent PPAR- α agonist, oleoylethanolamide (OEA), is a lipid mediator and bioactive endogenous fatty acid ethanolamide that exerts several distinctive homeostatic properties such as appetite control and food intake, and anti-inflammatory activity. OEA indeed regulates energy homeostasis and handles lipid and glucose metabolism [Sihag et al., 2018; Tutunchi et al., 2020].

EGb 761 is a standardized *Ginkgo biloba* leaf extract that contains a well-defined concentration of flavone glycosides and terpene lactones (24% and 6%, respectively). Although the exact mechanism of the extract is

overlooked, evidence accumulated *in vitro* and *in vivo* shows that EGb has several benefits, including the improvement of hemodynamics, the suppression of platelet-activating factor, and the scavenging of ROS, and the relaxation of the vasculature [Tabassum et al., 2022].

This study aimed to evaluate the effect of OEA on cardiorenal metabolic syndrome and its possible synergistic effect when administered in combination with EGb. Furthermore, an in-depth study was carried out to investigate the mechanisms underlying OEA effect, using models of renal damage *in vivo* and *in vitro*.

1. OLEOYLETHANOLAMIDE: AN ENDOGENOUS LIPID

1.1 ORIGIN AND CLASSIFICATION

Oleoylethanolamide (OEA) is an endogenous lipid mediator belonging to **N-acylethanolamines (NAEs)**, a class of naturally occurring bioactive signaling molecules synthesized by animal and plant tissues [Ueda et al., 2010]. NAEs, consisting of an acyl chain linked by an amide bond to ethanolamine, differ in the length and unsaturation degree of the acyl chain. Although sharing the same basic scaffold, NAEs can bind to several different receptors and exert a plethora of biological effects, including anti-inflammatory, analgesic, neuroprotective and anorectic ones (Table 1.1) [Mock et al., 2022.]. Examples of NAEs, besides OEA, include arachidonoylethanolamide (AEA) or anandamide, palmitoylethanolamide (PEA), docosahexaenoylethanolamide (DHEA), stearoylethanolamide (SEA) and linoleoylethanolamide (LEA).

Derived from the omega-9 monounsaturated fatty acid, OEA is widely distributed among organs and has been detected in the gastrointestinal tract (e.g. small intestine, stomach, colon), brain, adipose tissue, liver, kidney, lung, spleen, pancreas, salivary gland, muscle, and heart. The concentration of OEA in the small intestine of vertebrates is regulated by the fed and fasted metabolic states [Igarashi et al., 2015]. OEA was initially isolated from chocolate and cocoa powder, but not from white chocolate or brewed espresso, and has since been identified in unfermented cocoa beans and other plant-based foods (e.g., oatmeal, hazelnuts, soybeans, and millet), as well as human breast milk [Di Marzo et al., 1998].

Name	Structure	Receptor	Bioactivity
PEA (16:0)		PPAR- α [2] GPR55 [3] GPR119 [4]	Anti-inflammatory [5] Neuroprotective [6] Anti-epileptic [7] Analgesic [8] Anorectic [9]
SEA (18:0)		GPR119 [4]	Anti-inflammatory [10] Anorectic [11]
OEA (18:1- ω 9)		PPAR- α [12] GPR119 [4]	Anti-inflammatory [13] Anorectic [9] Analgesic [14] Neuroprotective [15]
LEA (18:2- ω 6)		PPAR- α [16] GPR119 [17]	Anorectic [18] Neuroprotective [19]
AEA (20:4- ω 6)		CB ₁ [20] CB ₂ [21] TRPV1 [22]	Neurotransmission [23] Orexigenic [24] Analgesic [25] Anxiolytic [26] Memory formation [27] Neuroprotective [28]
DHEA (22:6- ω 3)		GPR110 [30]	Fertility [29] Neurogenesis [31] Anti-inflammatory [32]

Abbreviations: PEA = *N*-palmitoylethanolamine, SEA = *N*-stearoylethanolamine, OEA = *N*-oleoylethanolamine, LEA = *N*-linoylethanolamine, AEA = *N*-arachidonylethanolamine, DHEA = *N*-docosaheptaenoylethanolamine, PPAR- α = peroxisome proliferator-activated receptor α , GPR = G protein coupled receptor 55/110/119, CB = cannabinoid receptor 1/2, TRPV1 = Transient receptor potential vanilloid 1.

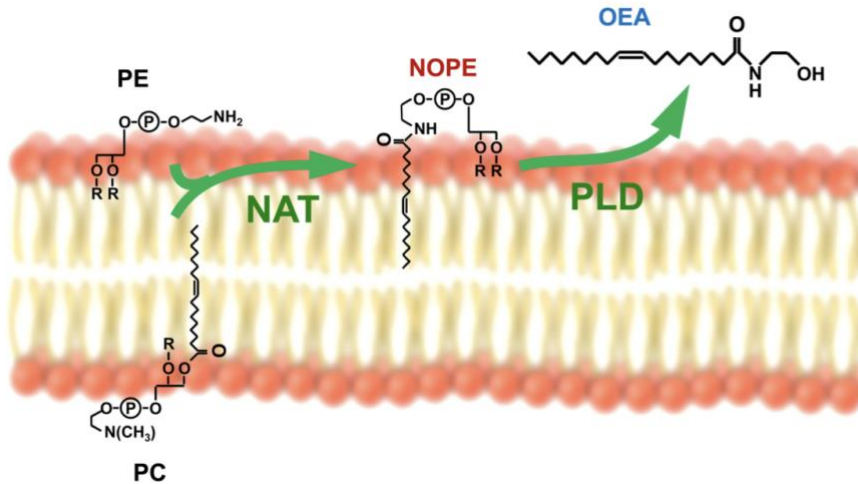
Mock et al. 2022.Prog Lipid Res.

Table 1.1|N-acylethanolamine (NAE) family members and their reported biological activities. NAE family members and their reported biological activities and receptors interaction. NAEs participate in the control of multiple physiological functions, including pain, inflammation and exert neuroprotective and anorectic effects.

1.1.1 ANABOLIC PATHWAYS

OEA synthesis in the intestine is well characterized and is stimulated by diet-derived oleic acid [Schwartz et al.,2008]. Circulating levels of OEA are generally lower than those of organs [Tellez et al., 2013; Balvers et al., 2013], suggesting that OEA may act as a paracrine rather than an endocrine signalling molecule [Fu et al., 2007]. Its presence in plasma is probably due to the “spill-over” of the mediator from peripheral tissues [Annuzzi et al., 2010]. In addition, OEA, like all NAEs, is not stored in the cells but instead synthesized in a stimulus-dependent manner. Their levels

are tightly regulated by their biosynthetic and degradation enzymes. The sympathetic nervous system controls the endogenous mobilization of OEA [LoVerme et al., 2006; Fu et al., 2011]. OEA biosynthesis involves two concerted steps; the first one is the transfer of an oleic group from the stereospecific numbering-1 (sn-1) position of a membrane phospholipid, for example, phosphatidylcholine (PC) to the amine group of a second membrane phospholipid, namely phosphatidylethanolamine (PE) (Figure 1.1). This N-acylation, catalyzed by the N-acyltransferase enzyme (NAT), is calcium-dependent. Different pathways have been proposed to form of N-acyl-phosphatidylethanolamine (NAPE) by inter- or intra-molecular N-acylation from PE or PC. However, evidence suggested that rather than simple precursors to NAEs, NAPEs can be defined as signalling lipids, able to control pivotal biological functions by themselves [Wellner et al., 2013]. In OEA synthesis, its NAPE precursor is N-oleoyl-phosphatidylethanolamine (NOPE). The second reaction is catalyzed by N-acyl-phosphatidylethanolamine phospholipase D (NAPE-PLD), which cleaves NAPEs to produce OEA and other NAEs. The enzyme specifically hydrolyzes NAPE, but not PE or PC. The primary structure of NAPE-PLD shows that this enzyme belongs to the metallo- β -lactamase family and has no sequence similarity to other PLDs, which typically hydrolyze PC to phosphatidic acid and choline. Thus, NAPE-PLD is distinct from other PLDs in both structure and catalytic function.



Romano et al., 2015, *Frontiers in Pharmacology*

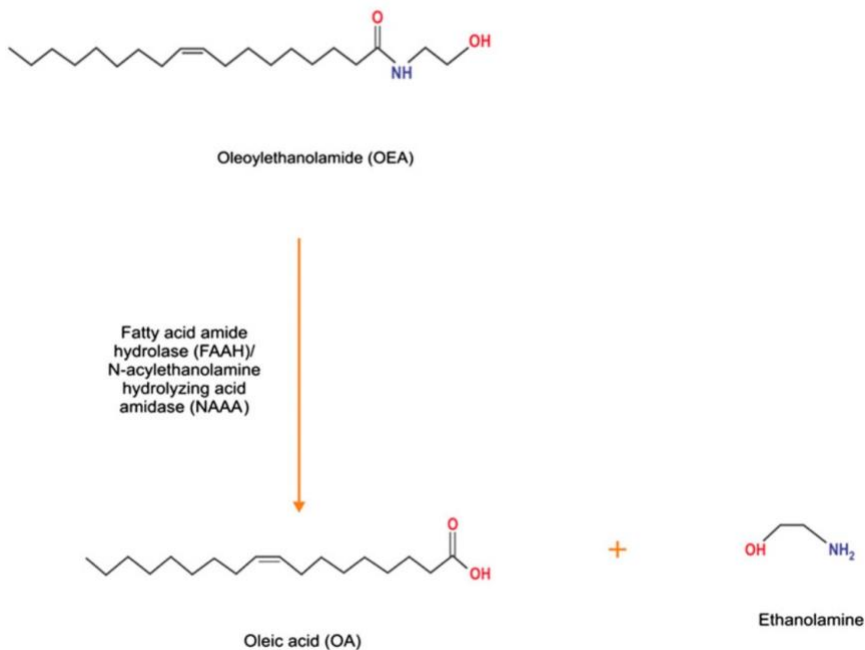
Fig.1.1|OEA biosynthesis. Two concerted reactions mediate OEA synthesis: The first one is the N-acylation of phosphatidylethanolamine (PE) from the phospholipid bilayer of the cell membrane, mediated by a N-acyltransferase (NAT) to form N-oleoyl-phosphatidyl ethanolamine (NOPE) and the second reaction is the phospholipase D (PLD)-mediated hydrolysis of NOPE.

1.1.2 CATABOLIC PATHWAYS

The primary biological mechanism for terminating the cellular signalling cascade of NAEs is catabolism by enzymatic hydrolyses, such as OEA, into oleic acid and ethanolamine. The enzymes identified in the degradation of NAEs are fatty acid amide hydrolase (FAAH) and N-acylethanolamine-hydrolyzing acid amidase (NAAA) (Figure 1.2). FAAH is an integral membrane protein that belongs to the amidase signature family and functions as a general inactivating enzyme for all NAEs [McKinney et al., 2005]. However, FAAH prefers the AEA substrate [Wei et al., 2006]. NAAA is an additional NAE hydrolyzing enzyme that belongs to the lysosomal choloylglycine hydrolase family [Tsuboi et al., 2007; Ueda et al., 2010]. This enzyme likely provides a minor contribution to OEA catabolism, as it has a

significant preference for PEA over OEA in substrate-specificity experiments [Tai et al., 2012].

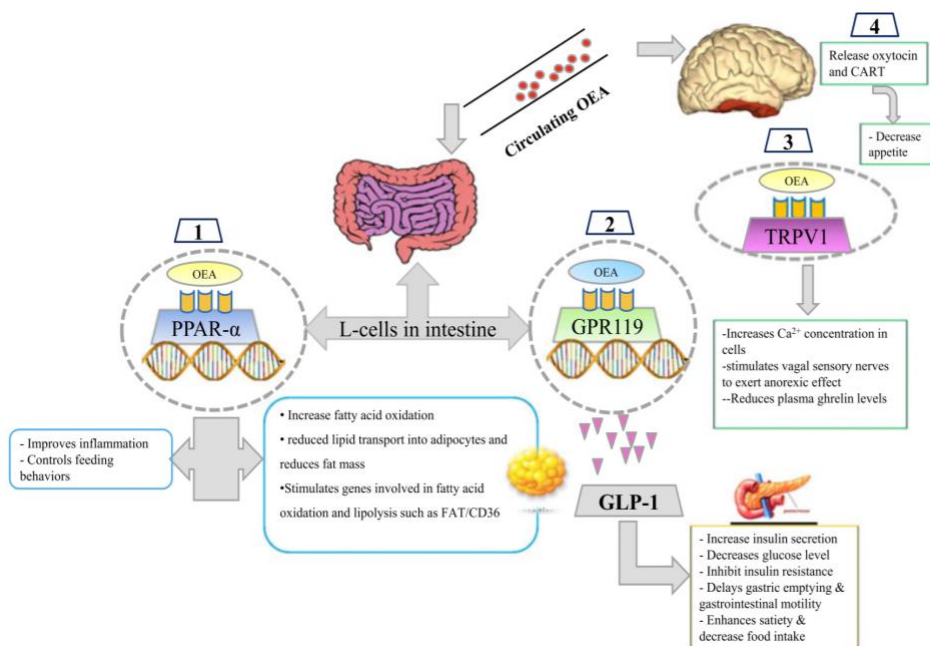
FAAH is ubiquitously distributed, with the highest activity in the liver, brain, and small intestine [McKinney et al., 2005]. FAAH exhibits the most increased activity toward AEA, LEA, and OEA, while NAAA preferentially hydrolyses PEA [Ueda et al., 2013]. Also, their optimal pH is different, 4.5-5.0 for NAAA versus 8.5–10.0 for FAAH. This supports that NAAA is mainly found in the lysosomes [Ueda et al., 2001], while FAAH is located in the endoplasmic reticulum.



Sihag et al., 2018 Obesity reviews

Fig.1.2|OEA degradation Two enzymes hydrolyze OEA: fatty acid amide hydrolase (FAAH) and N-acylethanolamine-hydrolyzing acid amidase (NAAA), into oleic and ethanolamine.

Among NAEs, OEA is a potent mediator of satiety, exerting an anorectic effect. OEA has been described as a mediator of lipid metabolism, insulin secretion, energy expenditure and gastrointestinal motility based upon its mechanism of action and its main target receptors: the PPAR- α . Additional anti-inflammatory and neuroprotective actions of OEA have been suggested. However, its activity may also be mediated by other receptors, such as GPR119 and the transient receptor potential vanilloid one channel (TRPV)-1 (Figure 1.3).



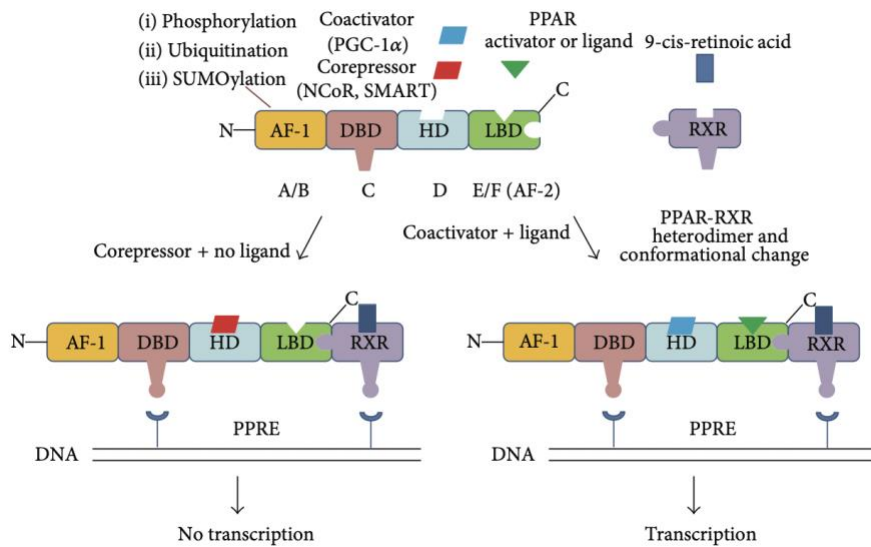
Laleh et al., 2018. Journal of cellular physiology

Fig 1.3|Schematic diagram illustrating the proposed mechanisms of OEA action. The primary mechanism of OEA is regulating energy homeostasis and feeding behaviour through interaction with these receptors. OEA, as a ligand of PPAR- α , GPR119, and TRPV1 receptors, suppresses appetite, modulates lipid abnormality, and decreases inflammatory cytokines.

1.2 PPAR- α : A KEY MEDIATOR OF OEA EFFECTS

PPAR- α was first discovered in the early 1990s and belonged to the PPAR subfamily, consisting of three isotypes: α , β , and γ . PPARs are orphan nuclear receptors that belong to the thyroid, steroid, and retinoid hormone receptor superfamilies of ligand-activated nuclear hormone receptors [Michalik et al., 2006; Bookout et al., 2006; Berger et al., 2002;]. PPAR isoforms possess five or six structural regions within four functional domains, termed A/B, C, D, and E/F (Figure 1.4) [Usuda et al., 2014; Guo et al., 2006]. After binding to their respective ligands, PPARs translocate to the nucleus, undergo a conformational change, interact with transcriptional cofactors, and regulate gene transcription [Rogue et al., 2011; Willson et al., 2000].

Like all other nuclear receptors, PPARs possess a highly conserved DNA-binding domain that recognizes peroxisome proliferator response elements (PPREs) in the promoter regions of target genes [Chan et al., 2009]. After ligand binding, PPARs heterodimerize with the retinoid-X receptor (RXR). PPAR–RXR heterodimers bind to PPRE to initiate the transcriptional regulation of target genes that participate in nutrient metabolism and regulate cellular and whole-body energy homeostasis during lipid and carbohydrate metabolism, cell growth, cancer development, and so on [Lee et al., 2015; Hong et al., 2019].



Lee et al., 2015 PPAR Research

Fig 1.4|Structure of PPAR and its transactivation or transrepression process. Without a ligand, the PPAR-RXR heterodimer recruits the corepressors (left process). After ligand binding, conformational change in PPAR-RXR induces the dissociation of the corepressor complex. PPAR binds to PPPE and assembles coactivator complexes (right process). Active transcriptional complex assembles with coactivator proteins.

PPAR- α tissue expression is ubiquitous, albeit at a different level. PPAR- α is mainly expressed in tissues with high rates of fatty acid catabolism, i.e., those involved in digestive function (liver, stomach, enterocytes) and muscular activity (heart, skeletal muscle, kidney at proximal tubules). In the nervous system, the expression is moderated (low in the retina or lacking expression in the central nervous system). Low expression is found in the pancreas and adipose tissue [Braissant et al., 1996], while in the brain, PPAR- α is located at the highest levels in neurons, followed by astrocytes, and is weakly expressed in microglia [Warden et al., 2016; Tufano et al., 2020] most likely, to upregulate the expression of several

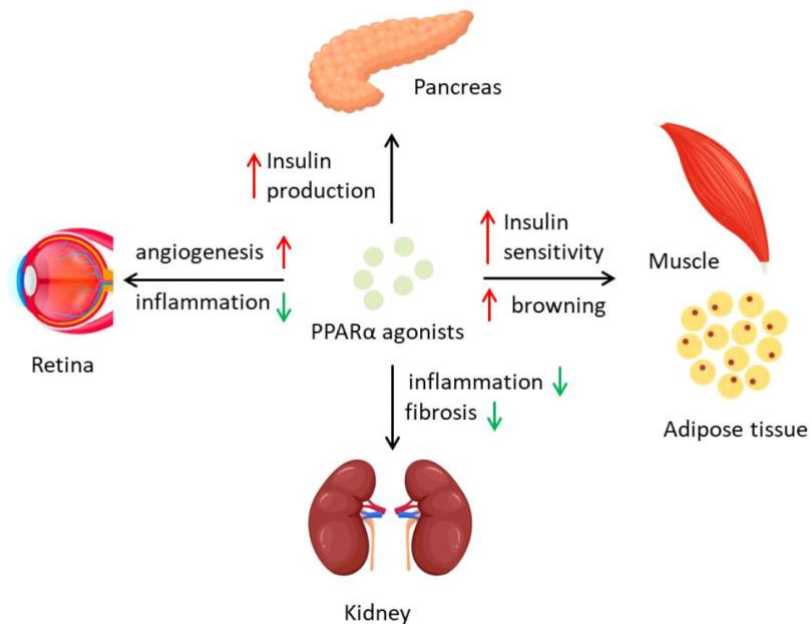
synaptic related genes encoding proteins engaged in excitatory neurotransmission and neuroprotective mechanism [Mariani et al., 2017; Mattace Raso et al., 2011; Roy et al., 2013]. In the immune system, PPAR- α expression is detected in the spleen, monocytes/macrophages, and neutrophils [Marx et al., 2004]. In addition, expression is seen in reproductive organs and the epidermis.

1.2.1 ROLE AND EXPRESSION OF PPAR- α IN KIDNEY

PPAR- α is highly expressed in tissues with high mitochondrial and FAO activity levels, including those of the liver, kidney, intestinal mucosa, and heart [Dixon et al., 2021]. Lower levels of PPAR- α expression have also been detected in several other tissues. Within the kidney, PPAR- α is abundant in the proximal tubules and medullary thick ascending limbs, with much lower levels in glomerular mesangial cells [Guan et al., 1997; Kamijo et al., 2002]. Given the high levels of expression in proximal tubules and medullary thick ascending limbs, PPAR- α has been implicated in the metabolic regulation of the kidney. It has been reported that the activation of renal PPAR- α regulates the transcription of several genes involved in FAO and inflammatory response and significantly induces the expression of β -oxidation enzymes in the renal cortex. Mice deficient in PPAR- α have poorer kidney function with sepsis-induced AKI, which is also related to reduced FAO and increased inflammation [Iwaki et al., 2019]. In proximal tubular epithelial cells in mice, PPAR- α was sufficient to maintain FAO and protect renal function and morphology in AKI [Li et al., 2009]. In models of

unilateral ureteral obstruction, preservation of PPAR- α expression led to a reduction in tubulointerstitial fibrosis and inflammation.

Further analysis reveals decreased production of transforming growth factor (TGF)- β , IL-1 β , IL-6, and TNF- α , and reduced macrophage infiltration [Li et al., 2013].



Lin et al., 2022 Frontiers

Fig 1.5 | PPAR- α activation regulates diabetes and diabetic complications. PPAR- α agonists act on different organs to counter diabetes and its complications. PPAR- α activation preserves the function of insulin-producing islets and promotes energy expenditure of adipose tissue and insulin sensitivity of muscle. Inflammation of the kidney and retina could be inhibited by PPAR- α agonists.

PPAR- α also plays an important role in glomerulonephritis. Plasma-free fatty acid and triglyceride levels were elevated in relation to a decrease in

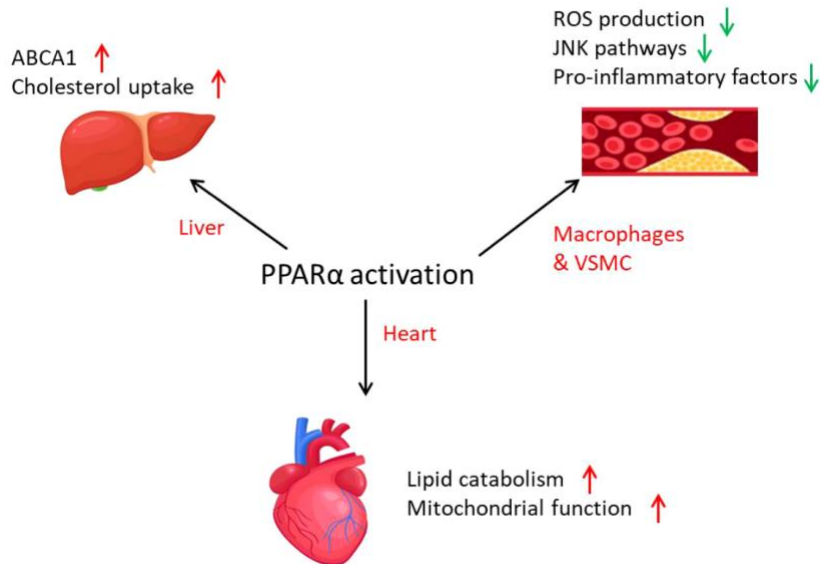
PPAR- α expression in high-fat diet (HFD) models of renal damage. In these models, treatment with fenofibrate increased PPAR- α expression, prevented HFD-induced renal lipotoxicity, reduced oxidative stress and lipid accumulation in the glomeruli, and prevented the development of albuminuria and glomerular fibrosis [Tanaka et al., 2011; Chung et al., 2018].

1.2.2 ROLE AND EXPRESSION OF PPAR- α IN HEART

PPAR- α is a crucial regulator of substrate utilization in the heart. Fatty acids are a primary energy source for the heart, and β -oxidation of fatty acids provides nearly 70% of cardiac ATP; the rest is mainly obtained from glycolysis and lactate oxidation [Stanley et al., 2005]. PPAR- α regulates fatty acid metabolism in the heart by stimulating the transcription of genes related to fatty acid uptake, transport, and oxidation. Moreover, cardiovascular expression of PPAR- α has anti-inflammatory and antioxidant effects, and activation of inflammatory signalling pathways is important in cardiomyocyte hypertrophy [Guellich et al., 2007]. Accordingly, PPAR- α agonists have helped repress inflammation caused by cardiovascular disease (Figure 1.6). Pretreatment of neonatal cardiomyocytes with PPAR- α agonist significantly decreases lipopolysaccharide (LPS)-stimulated TNF- α release, interleukin (IL)-1-induced IL-6 secretion, and PG and cyclooxygenase-2 expression [Takano et al., 2000].

The functions of cardiac PPAR- α were evaluated in PPAR- α KO mice. Loss of PPAR- α in mice results in impaired PPAR- α target gene expression, FA

utilization, and contractile function, indicating that PPAR- α is essential for cardiac function and FA utilization in the healthy heart [Lee et al., 2015].



Lin et al., 2022 Frontiers

Fig 1.6|The role of PPAR- α in cardiovascular diseases. PPAR- α is involved in cardiovascular diseases through the activation of lipid metabolism and the inhibition of inflammation. PPAR- α activation promotes mitochondrial function, lipid catabolism in the heart and cholesterol uptake in the liver. In atherosclerosis, PPAR- α activation leads to decreased inflammation in macrophages and VSMCs.

1.2.3 OTHER CONVERGING MECHANISMS: TRPV1 AND GPR119

Another receptor target for OEA is the transient receptor potential vanilloid type-1 (TRPV1), a capsaicin-sensitive receptor highly expressed in vagal sensory afferent neurons [Ahern et al., 2003; Wang et al., 2005]. OEA has been shown to activate TRPV1 in a phosphorylation-dependent manner, requiring phosphorylation of the receptor by protein kinase C for

subsequent OEA activation [Ahern et al., 2003]. OEA can also directly excite the cell bodies of vagal sensory neurons through TRPV1 with a rise in calcium and, thus, membrane depolarization. Chemical removal of peripheral sensory fibers, as well as direct intracerebroventricular injection of OEA, renders OEA ineffective in energy intake experiments [Rodriguez de Fonseca et al., 2001]. Furthermore, OEA administration reduces short-term food intake in wild type, but not in TRPV1 null mice [Wang et al., 2005]. These findings indicate that the peripheral nervous system and TRPV1 provide a link between intestinal OEA and food intake control in the central nervous system and TRPV1 acts in diet-mediated regulation of OEA.

Finally, OEA is also an endogenous agonist of GPR119, a G protein-coupled receptor expressed in rodent and human pancreatic and intestinal cells [Overton et al., 2006]. Nevertheless, the utility of this interaction is uncertain. For example, OEA administration to GPR119 deficient mice resulted in food intake suppression like wild-type mice [Lan et al., 2009]. GPR119 as a receptor for OEA-mediated satiety is unlikely, and future research is needed to determine its role in lipid metabolism.

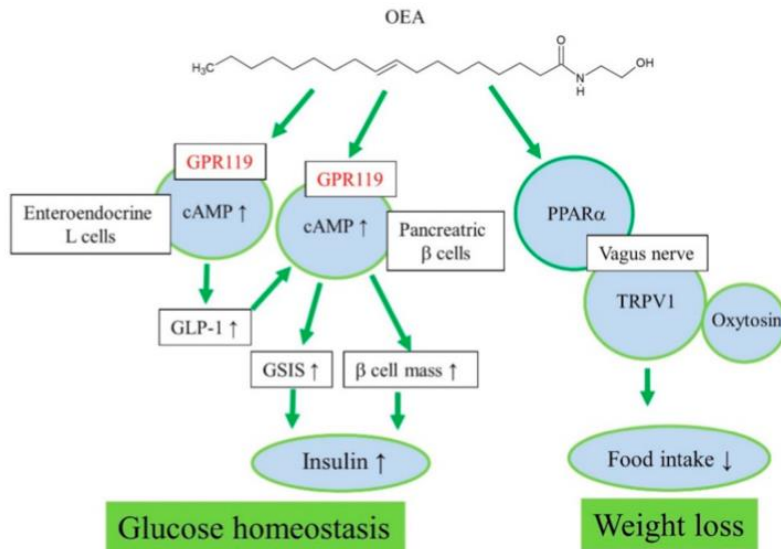
1.3 PHYSIOLOGICAL AND PHARMACOLOGICAL EFFECTS

1.3.1 EFFECTS OF OEA ON FEEDING

OEA is synthesized in the small intestine of various vertebrate species, where its level decreases during food deprivation and increases upon re-feeding [Astarita et al., 2006; Rodriguez de Fonseca et al., 2001; Petersen

et al., 2006]. The rise in plasma OEA level after feeding could be due to the presence of OEA in food [Di Marzo et al., 1998], but the concentrations of OEA in food products are very low (below 2 µg/g of food), suggesting that a part of the increase in the level of OEA is linked to an activated endogenous synthesis. In the small intestine, where its functions have been extensively studied, OEA is generated postprandially from diet-derived oleic acid [Schwartz et al., 2008] and acts as a local messenger to promote satiety [Gaetani et al., 2003; Proulx et al., 2005; De Fonseca et al., 2001]. Feeding stimulates cells in the mucosal layer of the duodenum and jejunum to produce OEA [Fu et al., 2007, 2008], suggesting that this lipid messenger participates in satiety induction. Specifically, OEA regulates appetite by delaying the onset of meals and reducing their size as well as increasing intervals between meals [Gaetani et al., 2003; Oveisi et al., 2004]. OEA modulates appetite in the central nervous system through the release of hypothalamic neuropeptides involved in energy homeostasis such as oxytocin [Gaetani et al., 2010; Serrano et al., 2011]. Various OEA doses have been tested with intraperitoneal injection (i.p.) administration ranging from 5 to 20 mg/kg of body weight, leading to a dose-dependent decrease in food intake. A significant reduction in food intake was observed for 4 h after i.p. injection of OEA at 5 mg/kg and for all 9 days of the experiment in rats [Yang et al., 2007]. Rodriguez de Fonseca et al. [2001] first described the anorexigenic effect of OEA in rats and reported the systemic administration of OEA. This anorexic action is explained by the ability of OEA to engage PPAR-α [Fu et al., 2003], implicated in the regulation of absorption, storage, and utilization of dietary fat [Bookout et al., 2006; Lefebvre et al., 2006]. The satiating

properties of OEA can also be partially explained by its action on the gastrointestinal tract. Indeed, OEA delays gastric emptying [Aviello et al., 2008] and slows intestinal motility [Capasso et al., 2005]. It has been demonstrated that the anorexic effects of OEA are mediated by PPAR- α activation [Fu et al., 2003]. In parallel, studies were performed in wild-type and PPAR- α KO mice to establish how OEA, a potent endogenous PPAR- α agonist, can regulate food intake and body weight gain. This study showed that OEA reduces food intake, inhibits body weight gain, and lowers plasma cholesterol levels in wild-type mice, whereas it has no such effects in PPAR- α mutant mice [Fu et al., 2005]. This implication of PPAR- α in the mechanism of action of OEA has also been confirmed with some *in vitro* gene reporter assays on cell cultures [Astarita et al., 2006]. Investigation of the mechanism of action revealed that OEA stimulates the vagal nerve through the capsaicin receptor TRPV1. To confirm TRPV1 involvement in OEA effects on food intake, wild-type mice and TRPV1-null mice were injected with OEA (12.5 mg/kg). Short-term feeding was significantly reduced in the control group but not in the TRPV1-null group, showing the role of this receptor in regulating feeding behavior [Ahern et al., 2003; Wang et al., 2005]. OEA has been shown to regulate the activity of TRPV1 indirectly, and activation of this receptor leads to the excitation of peripheral vagal sensory nerves involved in the nervous control of food intake (Figure 1.7).



Dong-Soon Im, *Int. J. Mol. Sci.* 2021

Fig 1.7| Proposed mechanisms of action of OEA for glucose homeostasis and weight loss regulation. The anorectic action of OEA seemed to be mediated mainly through PPAR- α and peripheral vagal sensory nerves. OEA-induced glucose homeostasis can be mediated by the GPR119 receptor, which influences GLP-1 release from L-cells and insulin secretion from β -cells.

1.3.2 EFFECTS OF OEA IN ENERGY HOMEOSTASIS: LIPID AND GLUCOSE METABOLISM

Besides controlling food intake, OEA is involved in the peripheral control of energy balance. Thus, in rodent adipocytes and adipose tissue, acute or chronic OEA treatments reduced lipogenesis and enhanced lipolysis and FAO [Guzmán et al., 2004; Fu et al., 2005; Serrano et al., 2008; Thabuis et al., 2011; Suárez et al., 2014].

PPAR- α is a ligand-activated transcription factor involved in various tissues' lipid metabolism. Indeed, it enhances the expression of lipid transporters and lipid-metabolizing enzymes in enterocytes [Bünger et al.,

2007; Fu et al., 2003; Yang et al., 2007]. *In vivo* rodent models indicate OEA increases the expression of PPAR- α and PPAR- α target genes encoding for proteins involved in lipid metabolism [Bowen et al., 2017]. Results from *in vitro* studies and *in vivo* animal models demonstrate that OEA enhances lipid utilization by stimulating fatty acid uptake, intracellular transport, intracellular lipolysis and fat oxidation and may also modulate lipid levels in tissues and circulation. Moreover, OEA-stimulated β -oxidation of fatty acids has been demonstrated in both *in vitro* and *in vivo* rodent models. Guzman et al. [2004] measured FAO in skeletal muscle, heart, and liver cells incubated with OEA. Rat soleus muscle strips incubated with OEA exhibited elevated FAO in a concentration-dependent manner. This evidence suggests that high OEA levels modulate energy metabolism by utilizing fatty acids for energy, possibly with a decrease in hepatic lipogenesis.

PPAR- α activation by OEA in the adipocyte promotes lipolysis of triglyceride lipid droplets, releasing fatty acids from the adipocyte for uptake into oxidative tissues. OEA can bind to PPAR- α in the liver and muscle to promote fat utilization through increased fatty acid uptake and β -oxidation, as well as elevated fatty acid transport to muscle and enhanced breakdown of liver lipid droplets. PPAR- α increases the uptake, esterification, and trafficking of cellular fatty acids and regulates lipoprotein metabolism genes. PPAR- α promotes the adaptive response to fasting by controlling fatty acid transport, FAO and ketogenesis. [Montaigne et al., 2021].

The identified biological functions of OEA also include the regulation of glucose metabolism. Ren et al. [2020] show that OEA treatment increased

glycogen synthesis and storage and inhibited gluconeogenesis and endogenous glucose production in primary hepatocytes and liver tissue via the LKB1/AMPK pathway. OEA efficiently suppressed hyperglycemia and hyperinsulinemia in HFD/STZ-induced diabetic PPAR- α KO mice, which supports a PPAR- α -independent mechanism of blood sugar regulation by OEA in diabetes.

1.3.3 EFFECTS OF OEA ON INFLAMMATION AND FIBROSIS

Beyond the regulation of appetite and metabolism, various effects are attributed to exogenously administered OEA, including antifibrotic and anti-inflammatory effects and control of oxidative stress. An *in vitro* study revealed that OEA suppressed the activation of TGF- β 1, the expression of α -smooth muscle actin (α SMA), and the expression of collagen type 1a/3a, which greatly contributes to hepatic fibrosis progression [Chen et al., 2015]. Moreover, preclinical studies have shown that OEA is an anti-inflammatory and antioxidant compound with neuroprotective effects in alcohol abuse. Exogenous administration of OEA blocks the alcohol-induced TLR4-mediated pro-inflammatory cascade, reducing the release of proinflammatory cytokines and chemokines, oxidative and nitrosative stress, and ultimately, preventing the neural damage in the frontal cortex of rodents [Jin et al., 2015; Sayd et al., 2014; Antón et al., 2017].

Furthermore, Yang et al. [2016] demonstrate that OEA exerts anti-inflammatory effects by enhancing LPS-triggered PPAR- α signalling, inhibiting the TLR4-mediated NF- κ B signalling pathway, and interfering

with the ERK1/2-dependent signalling cascade (TLR4/ERK1/2/AP-1/STAT3), suggesting that OEA may be a therapeutic agent for inflammatory diseases.

1.3.4 OTHER ACTIONS OF OEA

Evidence accumulated over the years highlights that OEA also exerts analgesic and neuroprotective effects.

Suardiaz et al. [2007] showed OEA analgesic properties in two nociceptive experimental animal models of inflammatory and visceral pain. In these studies, i.p. injection of OEA induced a significant analgesic effect in a dose-dependent manner not only in the early phase but also in the early part of the late phase in mice through a mechanism independent of PPAR- α activation. Previous studies have shown that OEA exhibited potent neuroprotective effects in animal models of neurological disorders [Sun et al., 2007; Zhou et al., 2012]. It exerts a partial and dose-dependent neuroprotection of dopaminergic neurons of the substantia nigra [Galan-Rodriguez et al., 2009]. Gonzalez-Aparicio et al. [2014] found that systemic OEA leads to the neuroprotection of the nigrostriatal system in an experimental model of Parkinsonism.

2. GINKGO BILOBA LEAVES: A NATURAL EXTRACT

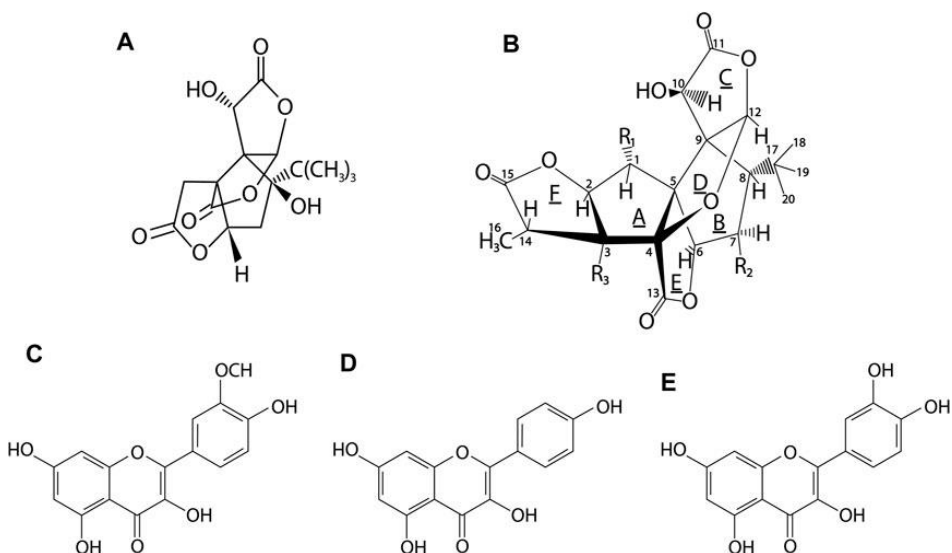
2.1 PHYTOCHEMISTRY AND CHARACTERIZATION

Ginkgo biloba (Syn.: *Salisburia adiantifolia* or *Pterophyllus salisburiensis*) is a deciduous tree commonly known as a “living fossil”; it is the only species in the genus of Ginkgoaceae which has survived until today. The genus name “*biloba*” refers to the tree’s two separate lobes, and the genus name Ginkgo is a phonetic translation of the tree’s Japanese name [Mohanta et al., 2012]. Though its natural habitat is in China, Japan and Korea, its origin is believed to be the remote mountainous valleys of the Zhejiang province of eastern China [Kramer et al., 1990; Ridge et al., 1997]. *Ginkgo biloba* has been used as a traditional medicinal plant for longer than 2000 years in China and other parts of the world [Singh et al., 2008] and is currently grown in Europe, Asia, Argentina, North America, and New Zealand [Belwal et al., 2019].

Among all commercialized extracts of *Ginkgo biloba* (EGb), EGb 761 is the most used standardized extract that contains ~24% flavone glycosides (primarily quercetin, isorhamnetin, and kaempferol) and 6% terpene lactones (bilobalide 2.6–3.2%), and ginkgolides A, B, C (~2.8–3.4%) and 2.6–3.2% bilobalide, with a ginkgolic acid content less than 5 ppm (Figure 2.1) [Chan et al., 2007]. Concerning the original composition of *Ginkgo biloba* leaves, EGb 761 is enriched with pharmacologically active ingredients such as flavonoids and terpene lactones and depleted of any toxic components, mainly ginkgolide acids. EGb can be used for food, medicine, material, greening and ornamental purposes [Liu et al., 2022].

Due to its wide-ranging medicinal use, almost every portion of EGb has been subjected to considerable chemical research.

The therapeutic mechanisms of action of the Ginkgo leaf extract are suggested to be through its antioxidant, antiplatelet, antihypoxic, antiedemic, hemorrhheologic, and microcirculatory activities, where the flavonoid and the terpenoid constituents may act in an integrative manner [Mahadevan et al., 2008; Boateng et al., 2022].



Belwal et al., 2019 Nonvitamin and Nonmineral Nutritional Supplements

Fig 2.1|Chemical structures of the major active compounds in *G. biloba* leaves. Bilobalide(A), ginkgolide (B), isorhamnetin(C), kaempferol (D), quercetin(E). Ginkgolides contained in EGb belong to the group of diterpenes, whereas bilobalide to sesquiterpenes. The main flavonols of EGb are kaempferol, quercetin and isorhamnetin.

2.1.1 FLAVONOIDS

The main key components of EGb are flavonoids, whose content reaches 24%, while terpenoids are present in a smaller percentage and classified in ginkgolides and bilobalide (Figure 2.2). Lots of flavonoids have been

identified from EGb, including monoflavonoids, diflavones, flavonoid aglycones, flavanones and flavonoid glycosides [Ji et al., 2017]. Flavonoid glycosides of EGb are mainly metabolized in two parts of the body: one is the liver, where a series of reactions occur under the action of CYP450 to produce metabolites with higher water solubility; the second is the intestinal tract, where flavonoid glycosides are hydrolyzed into aglycon under fermentation of intestinal microbiota.

Flavonoids, the prominent ingredient in EGb, exhibit various pharmacological activities such as antioxidant, free radical scavenging, anti-tumour, hepatic and cardio-cerebral blood vessel protection. Biflavonoids, including ginkgetin, isoginkgetin, bilobetin, also have various pharmacological activities, such as anti-cancer and anti-bacterial effects [Patel et al., 2022].

2.1.2 TERPENOIDS

The main terpenoids in EGb are terpene lactones, usually composed of several lactonic rings, including diterpene lactones and sesquiterpenelactones [Yang et al., 2016]. Ginkgolides A, B, and C are three different forms of ginkgolides that have diverse pharmacological actions. Ginkgolide A, one of the active ginkgolides from *G. biloba*, could reduce the inflammatory response induced by lipopolysaccharide [Li et al., 2017]. Ginkgolide B is used to treat inflammatory and neurological illnesses by acting as antagonist at platelet-activating factor receptors. Ginkgolides A and B also regulate peripheral benzodiazepine receptors, indicating neuroprotective properties. It is worth noting that ginkgolides

are specific compounds in EGb and have not been found in other natural plants; they have been known for neuroprotective, antioxidative, anti-inflammatory, anti-ischemic, and cardiovascular protective activities [Mohammad Nabavi et al., 2022]. Whereas bilobalides protect the central nervous system from ischemia, traumatic brain injury, and cerebrovascular disease [Feng et al., 2019].

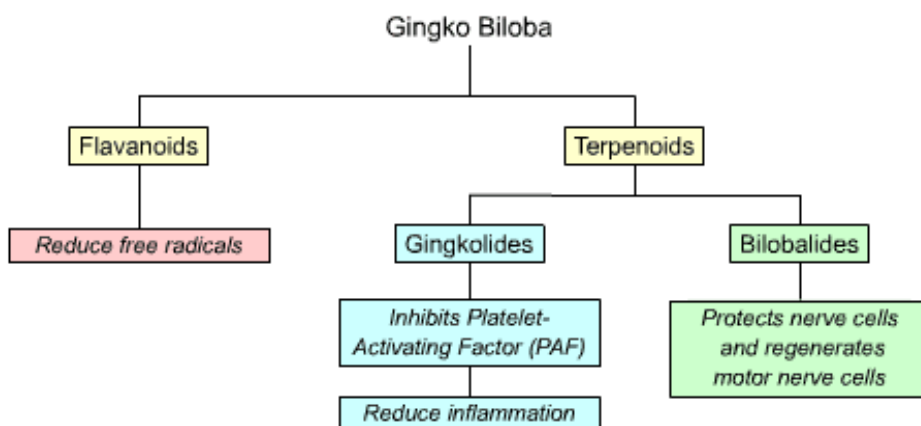
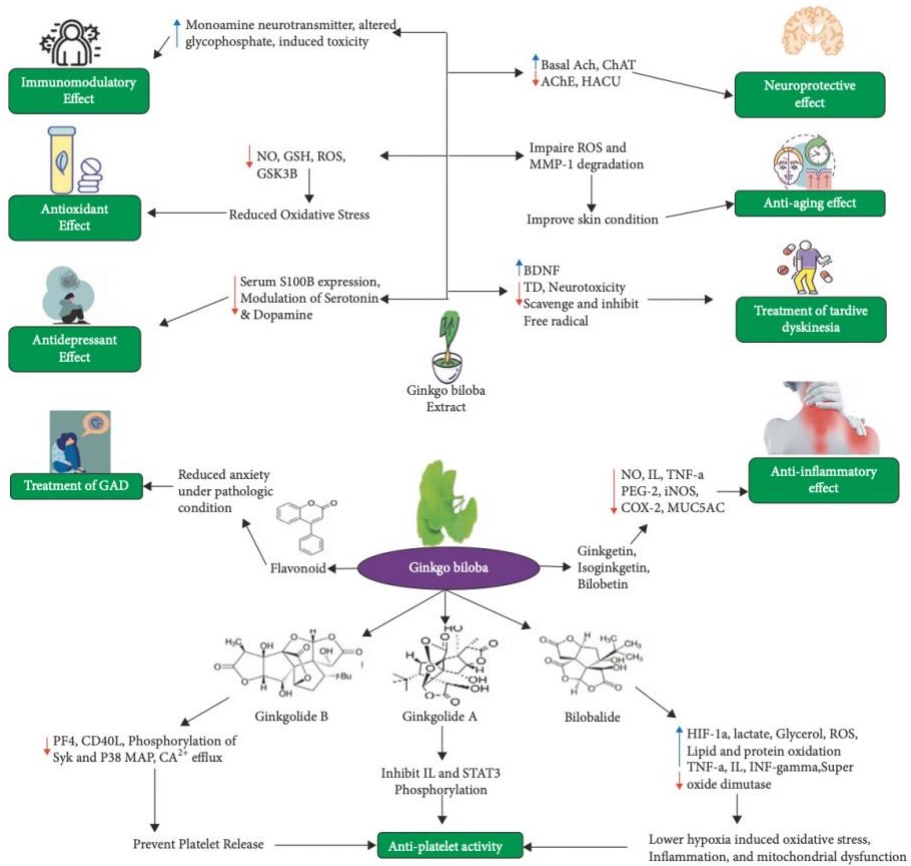


Fig 2.2|The schematic effect of the various component of *Ginkgo biloba*. Flavonoids mainly possess antioxidant properties, while ginkgolides primarily inhibit PAF and reduce inflammation. Bilobalides, on the other hand, have neuroprotective effects.

2.2 BIOACTIVITIES AND CLINICAL USES

Although the exact mechanism of the extract is overlooked, evidence accumulated shows that EGb has beneficial effects in the amelioration of hemodynamics, suppression of platelet-activating factor, scavenging of ROS, and the relaxation of the vasculature (Fig. 2.3). Furthermore, EGb is a medical tool for ameliorating memory loss, blood circulation, and

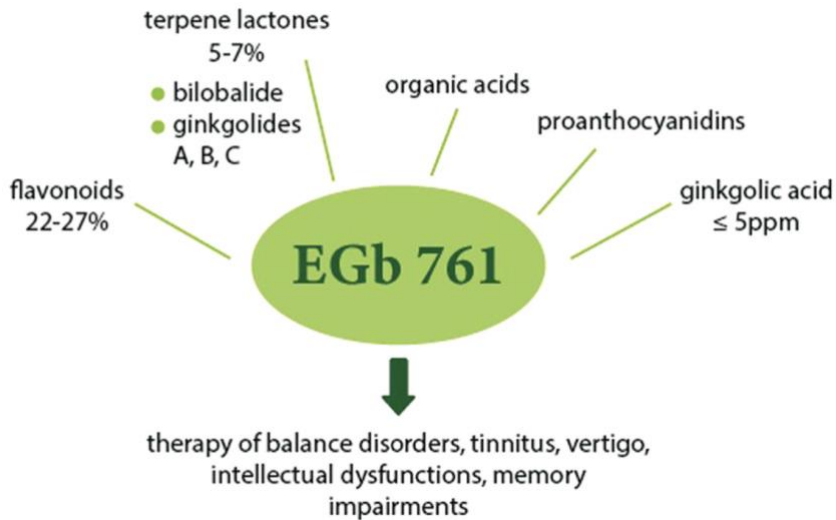
respiratory function [Chan et al., 2007], while in current Chinese medicine, mainly used to calm wheezing, stop the pain, and treat hypercholesterolemia, hypertension, coronary artery disease, angina pectoris, and cerebrovascular disease [Tao et al., 2019].



Tabassum et al., 2022 Evidence-Based Complementary and Alternative Medicine

Fig 2.3| Therapeutic potential of *Ginkgo biloba*. EGb has been reported to have immunomodulatory neuroprotective, antioxidant, cardioprotective, stress alleviating, and memory-enhancing effects.

Clinically, it has been prescribed to treat dementia, macular degeneration, vaso-occlusion, memory deficit and cochleovestibular disorders (Figure 2.4) [Saper et al., 2014].



Novak et al., 2021 *Frontiers in pharmacology*

Fig 2.4|The main components of EGb 761 and their possible uses. EGb 761 is enriched with active substances and contains flavonoids, terpene lactones group including bilobalide and ginkgolides A, B and C, organic acids, proanthocyanidins, with a reduced content of ginkgolic acid. The extract could be applied to treat balance disorders, tinnitus, vertigo, cognitive dysfunction, memory impairment and others.

2.2.1 EFFECT ON VASCULATURE

EGb is used primarily in the treatment of hearing and balance disorders, tinnitus and dizziness resulting from impaired local blood flow, as well as for cognitive dysfunction [Novak et al., 2021; Radunz et al., 2020], and it is recommended for the treatment of geriatric memory disorders, including vascular and neurodegenerative dementia. Several clinical studies have

repeatedly shown the efficacy of EGb 761 in the treatment of mild-to-moderate dementia of different aetiology [Schneider et al., 2005; Napryeyenko et al., 2007]. According to that, EGb 761 also substantially alleviated tinnitus in dementia patients, as demonstrated in a meta-analysis of the available studies, including 773 tinnitus patients [Spiegel et al., 2018].

Moreover, multiple studies demonstrate EGb's protective effects against platelet aggregation. Drieu et al. [2000] tested the effects of EGb on platelet activation factor (PAF)-induced aggregation of washed human platelets. They demonstrated that EGb competitively inhibits platelet aggregation in a concentration-dependent manner. Additionally, the study by Simon et al. [1987] confirmed that competitive inhibition by EGb of PAF-induced platelet aggregation was receptor-mediated.

Furthermore, EGb 761 promotes vasodilation, increasing blood flow via the veins, arteries, and capillaries; it prevents platelet aggregation and decreases bleeding [van Beek et al., 2002].

2.2.2 ANTIOXIDANT EFFECT

Terpenes, flavonoids, and bioflavonoid components are thought to contribute to the antioxidant capabilities of EGb, which has been shown to be beneficial against various free radical-generating substances, including oxyferryl, superoxide, hydroxyl, NO, and peroxy radicals. The antioxidant properties of EGb contribute to protecting the cardiovascular system, brain, and retina from free radical damage associated with ageing. The antioxidant capabilities and flavonol contents of EGb crude extracts

were investigated; Kaur et al. [2015] found that ginkgolide B derived from EGb 761 applied to human neuroblastoma IMR-32 and SHSY5Y cells reduced ROS/RNS production by prooxidant A β 25–35 peptides. MDA and NO levels increased with age but were suppressed by pretreatment with EGb 761. By controlling oxidative stress, EGb 761 can protect against ischemic injury [Zhou et al., 2017]. Aydin et al. [2016] utilized cisplatin to promote oxidation in the rat brain and observed that EGb 761 reduced GSH and NO levels in brain tissue, which decreased oxidative stress. It has also been used as an antioxidant to treat neurodegenerative diseases [Yu et al., 2021]. Besides, Liu et al. [2019] found that the antioxidant effects of ginkgolides and bilobalide from EGb against cerebral ischemia injury are through activating the Akt/Nrf2 pathway. Song et al. [2019] also found that the EGb could relieve cerebral ischemia-reperfusion injury by decreasing serum MDA levels and elevating activity levels of SOD and GSH-PX.

2.2.3 ANTIDEPRESSIVE EFFECT

In addition, the positive effect of EGb 761 on depression and anxiety as a comorbidity of dementia is very well documented [Bachinskaya et al., 2011; Nacu and Hoerr, 2016; Scripnikov et al., 2007]. In a meta-analysis of all available clinical studies with a total of 1628 patients, a very pronounced effect on anxiety and depression, among other neuropsychiatric symptoms, was found in favour of EGb 761 compared to placebo [Savaskan et al., 2018]. Besides effects on neuropsychiatric symptoms, EGb 761 may also act centrally by improving cerebral perfusion in areas involved in auditory processing. For instance, the cerebral

perfusion rate of the auditory cortex increased when rats received 130 mg/kg of EGb 761 intravenously [Krieglstein et al., 1986].

2.2.4 METABOLIC EFFECT

Findings from *in vivo* and *in vitro* studies suggest that EGb intake may improve glycemic control through various mechanisms, including preserving pancreatic β -cell functions by enhancing antioxidant defence mechanisms in pancreatic islets [Kudolo, 2001; Tabrizi et al., 2020], a decrease in insulin resistance, an increasing pattern of glucose transport to peripheral tissue, and ameliorating obesity-induced insulin signalling impairment [Banin et al., 2014; Rhee et al., 2015]. Moreover, Tanaka et al. [2004] showed that the hypoglycemic effect of EGb may be attributed to its inhibitory effect on α -amylase and glucosidase enzymes. In two trials by Aziz et al. [2018] and Shi et al. [2019], EGb administration to diabetic patients with doses of 120 mg/day for 3 months and 72 mg/day for 24 months led to a significant reduction in fasting blood sugar and HbA1c levels. However, discrepant results in other studies showed no improvement in fasting blood sugar [Jie & Hai, 2005; Li et al., 2009; Zhao et al., 2016] or HbA1c [Kudolo, 2001; Lasaite et al., 2014; Zhao et al., 2016] levels after EGb intake.

EGb administration has been shown to regulate lipid levels mainly by inhibiting adipogenesis and stimulating lipolysis in animal models [Dell'Agli & Bosisio, 2002; Kang, 2017; Yao et al., 2004]. In addition, in a study of male rabbits, EGb treatment dramatically decreased plasma cholesterol and TG levels while significantly increasing HDL-C levels compared with the

control group. Furthermore, in aortic tissue, EGb has been found to lower MDA levels while raising glutathione (GSH) levels [Kang et al., 2017].

3. OBESITY-INDUCED CARDIORENAL DISEASE

3.1 OBESITY: EVIDENCE, EPIDEMIOLOGY AND RISK FACTOR

Obesity is a complex multifactorial chronic and metabolic disease with an excessive accumulation of fat mass that leads to adverse effects on health. In line with The Obesity Atlas 2022 estimates, it is the epidemic of our era, and its incidence is increasing by more than 30% by 2030 [The Obesity Federation 2022]. The Global Burden of Disease study, which includes data from 195 countries, reports that obesity has more than doubled since 1980 and parallels global trends in the prevalence of type 2 diabetes mellitus (T2DM) [Afshin et al., 2017; Gregg et al., 2017]. The emerging pandemic of obesity is thought to be triggered by sociologic/environmental factors that include an increasingly sedentary lifestyle with physical inactivity and excess compact caloric consumption. The obesity rate has dramatically enhanced in both males and females, and across all ages, with proportionally higher prevalence in older persons and women [World Health Organization, 2020]. While this trend exists globally, absolute prevalence rates vary across regions, countries, and ethnicities. In low- and middle-income countries, rates of overweight and obesity are rising, especially in urban areas.

Obesity is associated with an increased risk of a series of metabolic alterations, constituting the 'metabolic syndrome', predisposing to T2DM and its related co-morbidities, especially the micro- and macro-vascular diseases [Ginsberg et al., 2009]. The effects of obesity have a critical impact on different clinical areas, particularly endocrinology, cardiology, and nephrology. Indeed, it is an increasingly common cause of insulin

resistance and long-term associated complications, such as cardiovascular disease (CVD), fatty liver disease, overt type 2 diabetes mellitus and chronic kidney disease (CKD).

Obesity is the central driver in this constellation of heart and kidney disease risk factors. There is currently a vigorous discussion on whether the risk is cumulative, additive, or synergistic. Still, most experts agree that the risk intensifies with increasing detrimental factors for CVD and CKD.

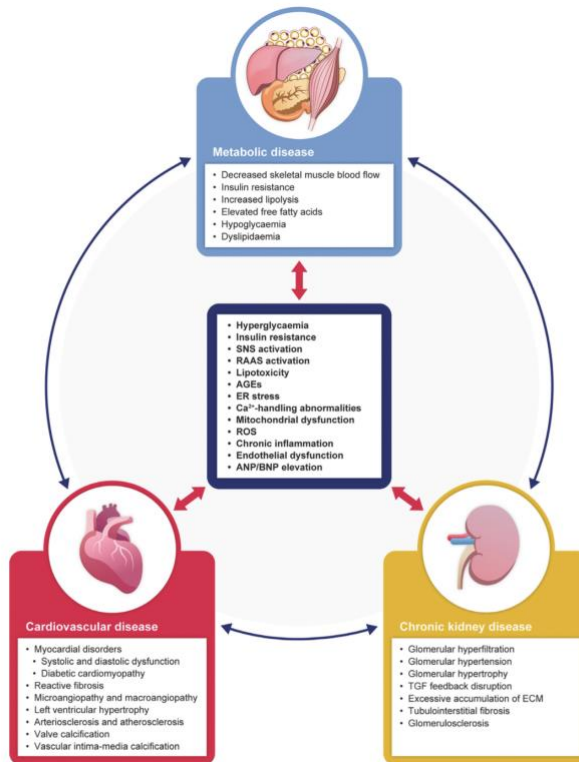
3.2 PATHOPHYSIOLOGICAL MECHANISMS IN OBESITY: KIDNEY-HEART CONNECTION

Cardiovascular, renal, and metabolic diseases such as T2DM interact at the pathophysiological level, resulting in the overlap between these conditions.

Mechanisms by which obesity and T2DM exert pathophysiological effects on the heart and kidneys include hyperglycaemia, production of advanced glycation end products (AGEs), insulin resistance, hyperactivity of the renin-angiotensin-aldosterone system (RAAS), lipotoxicity, endoplasmic reticulum (ER) stress, abnormalities in calcium handling, mitochondrial malfunction and deficits in energy production, oxidative stress, and chronic inflammation [Kadowaki et al., 2022]. The resulting pathophysiological interplay between metabolic disease, the heart and the kidneys forms a vicious cycle of CRMetS disease (Figure 3.1) [Connell et al., 2014].

Indeed, the kidney is one of the most fuel-hungry organs in the human body; the kidney and heart showed higher resting metabolic rates than the brain or other organs [Bhargava et al., 2017]. The kidney requires the

second highest mitochondrial density and oxygen consumption after the heart to provide energy for a variety of cellular functions and processes, including removing waste products, reabsorbing nutrients, balancing the body's fluids, and regulating blood pressure [Pagliarini et al., 2008; Bhargava et al., 2017].



Kadowaki et al., 2022 Diabetes Obes Metab

Fig 3.1| Molecular and pathophysiological interplay between cardiovascular disease, chronic kidney disease and metabolic disease. Cardiorenal syndrome represents concomitant cardio-vascular and renal disorders that result from systemic diseases with common pathophysiological pathways. These distinct processes converge and, over time, promote organ damage and dysfunction in both the heart (e.g., diastolic dysfunction, heart failure with preserved ejection fraction, heart failure with reduced ejection fraction, left ventricular hypertrophy) and kidney (acute kidney injury, chronic kidney disease).

3.2.1 RENOMETABOLIC ALTERATION

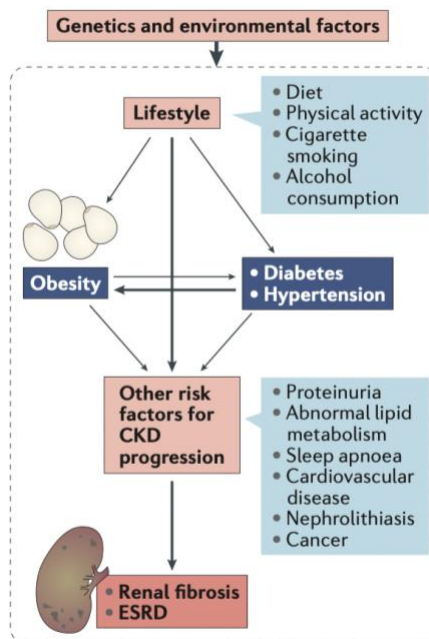
Obesity is associated with unfavorable hormonal changes, which are reflected in insulin resistance and hyperinsulinemia, abnormal renal lipid metabolism, hyperaldosteronism, increase in systemic arterial blood pressure, volume expansion and renal fibrosis [Lakkis et al., 2018].

The links between obesity and chronic kidney disease are numerous, bidirectional, and complex; shared pathophysiological pathways may explain this complexity (e.g., chronic inflammation, increased oxidative stress, and hyper-insulinemia), shared clusters of risk factors as well as associated diseases (e.g., insulin resistance, hypertension and dyslipidemia) [Stasi et al., 2022].

Overall, several mechanisms are closely related to the onset and progression of CKD in the general population, including changes in renal hemodynamics, neurohumoral pathways, renal adiposity, local and systemic inflammation, dysbiosis of microbiota, insulin resistance, and fibrotic process [Stasi et al., 2022]. In this scenario, many mechanisms have been proposed to elucidate the pathophysiology of obesity-related chronic renal failure. Briefly, a combination of hemodynamic players, mainly hypertension and metabolic disorders exacerbate renal damage in obese patients. Furthermore, visceral adiposity promotes cellular accumulation of free fatty acids (FFA) and triglycerides (TG), leading to oxidative stress and lipotoxicity [Cignarelli et al., 2007]. Additionally, the production of inflammatory mediators, such as adipokines and cytokines, and profibrotic factors increase inflammation, endothelial dysfunction, and renal injury. Ultimately, obesity and CKD share a close association;

however, the pathophysiology of obesity-related CKD is seemingly multifactorial [Prasad et al., 2022].

Increased adiposity is associated with enhanced lipogenesis as a result of a positive caloric balance, and the abundance of lipids results in increased systemic availability and ectopic tissue accumulation of free fatty acids; this results in tissue lipotoxicity (e.g., liver) with secondary organ damage as well as dyslipidemia [Izquierdo-Lahuerta et al., 2016]. Lipotoxicity in the kidney occurs with deposition of excess TG, most prominently in the glomeruli and proximal renal tubules [Bobulescu et al., 2010], and results in the glomerular basement membrane and podocyte injury [Joles et al., 2000] with a resultant increase in membrane permeability. Renal lipotoxicity also enhances insulin resistance, oxidative stress, endothelial dysfunction, and pro-inflammatory status [Martínez-García et al., 2015].



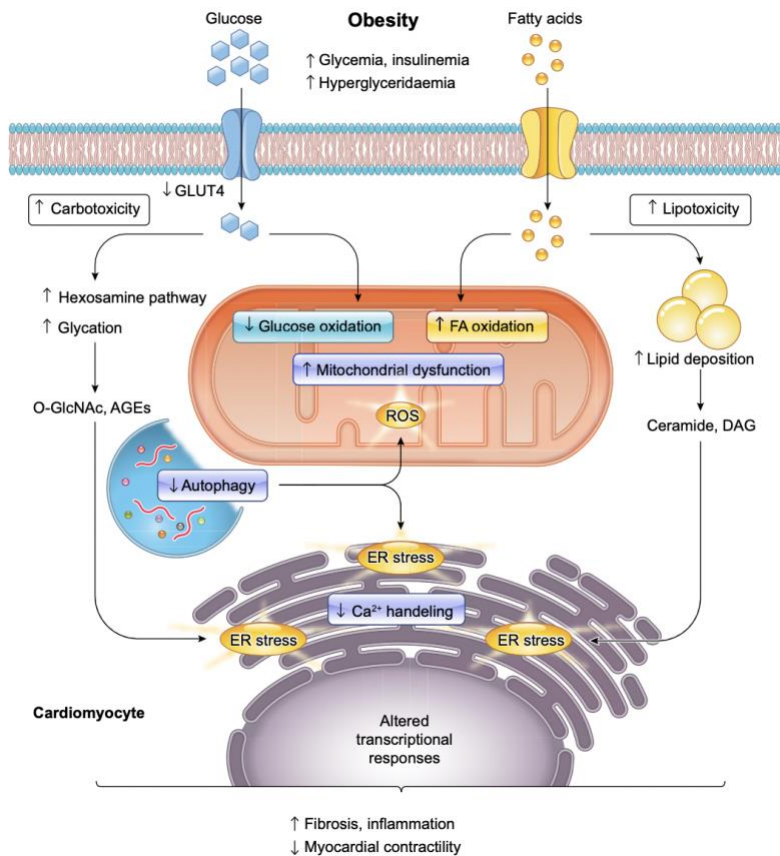
Câmara et al., 2017. NATURE REVIEWS | NEPHROLOGY

Fig.3.2|The influence of obesity on progression of renal fibrosis. Lifestyle factors, such as poor diet, physical inactivity, smoking, and alcohol consumption, are associated with an increased risk of obesity, diabetes, hypertension, and renal dysfunction. Further risk factors, such as sleep apnea and cardiovascular disease, increase the risk of end-stage renal disease (ESRD) progression. Genetic and environmental factors influence all these processes.

3.2.2 CARDIOMETABOLIC ALTERATION

As shown in metabolic syndrome, impaired body energy homeostasis leads to inadequate energy transfer to vital organs such as the heart, skeletal muscle, and liver. The heart derives its energy for contraction from the oxidative metabolism of fatty acids and carbohydrates. The healthy heart readily switches from fatty acids to carbohydrates when stressed and from carbohydrates to fatty acids when plasma fatty acid levels increase (e.g., fasting). This phenomenon is termed “metabolic flexibility of the heart”. It occurs, for example, during the transition when the adaptation of the heart to a changed physiologic milieu progresses to maladaptation [Taegtmeyer et al., 2004].

Moreover, reduced intracellular glucose levels resulting from insulin resistance in cells that take up glucose in an insulin-dependent manner may shift metabolism towards free fatty acid oxidation, a less efficient process. In the diabetic heart, decreased adenosine triphosphate (ATP) production from glucose metabolism may cause compensatory increases in free fatty acid uptake and accumulation of triacylglycerols, which may exceed mitochondrial respiratory capacity, resulting in a build-up of toxic lipid metabolites and mitochondrial dysfunction [Forbes et al., 2013; Jia et al., 2016; Lopaschuk et al., 2021].



Ren et al., 2021. American physiological society

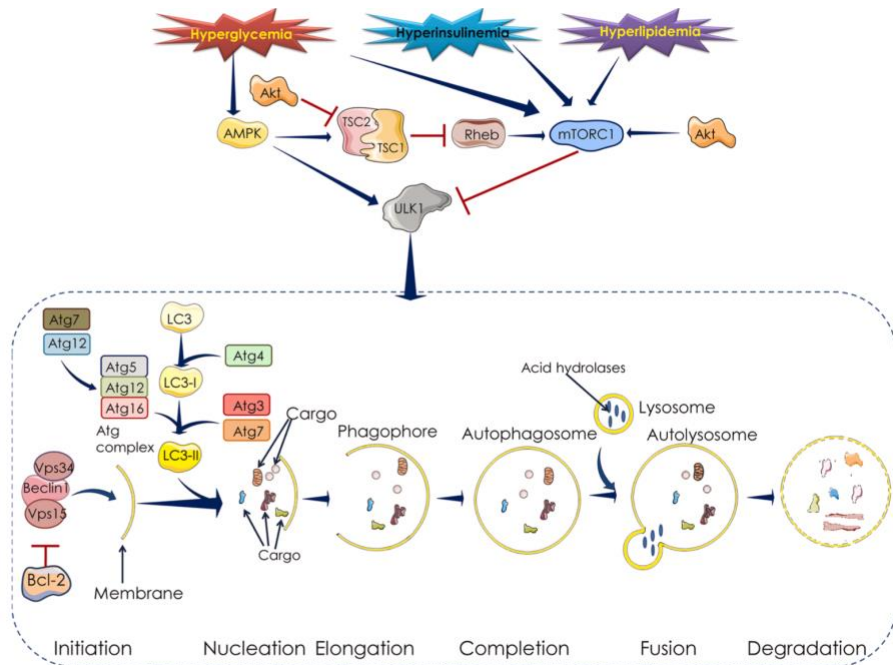
Fig 3.3|Metabolic stress and organelle dysfunction in obesity cardiometabolic alteration. Metabolic stress and organelle dysfunction in obesity cardiometabolic alteration. Obesity leads to decreased myocardial glucose uptake and oxidation, increased FAO, and altered cardiomyocyte gene expression. Increased accumulation of triglycerides and their products, such as ceramides and DAG, cause the majority of lipotoxicity in hearts. Different metabolic pathways, such as hexosamine and (AGE), have been identified as pro-oxidative processes and are usually elevated in obesity. Autophagy activity in the heart declines with obesity, and its insufficiency is involved in accumulating reactive oxygen species (ROS) and developing endoplasmic reticulum (ER) stress, leading to obesity-related cardiometabolic diseases.

Furthermore, oxidative stress in the heart is directly correlated to its reduced performance and dysfunction [Fiorentino et al., 2013]. It is well

known that oxidative stress is implicated in the production of inflammatory mediators, and in turn, inflammation is involved in the generation of oxidative stress through the generation of ROS (Figure 3.3) [Oguntibeju et al., 2019]

It is also widely accepted that inflammation is involved in the pathogenesis of cardiac damage [Kenny et al., 2019]. The various pathogenic pathways contributing to the development of MetS culminate in a pro-inflammatory state that explains the elevation in different inflammatory markers such as IL-6, C-reactive protein (CRP), and TNF α [Suryavanshi et al., 2017]. This latter cytokine acts on various tissues, leading to a prothrombotic state by increasing fibrinogen levels and promoting the expression of vascular cell adhesion molecules (VCAMs), leading to cardiac hypertrophy, inflammation, fibrosis, apoptosis and extracellular matrix remodelling.

Another process impaired in the metabolic syndrome is autophagy, which is highly sensitive to changes in the micronutrient environment and regulates nutrient uptake, cell metabolism and recycling of essential nutrient components [Evans et al., 2022; Kimmelman & White, 2017; Saxton & Sabatini, 2017]. It plays a pivotal role in maintaining cellular homeostasis in diligent cardiac tissues; in fact, it is involved in the recycling/clearing the damaged organelles, cytoplasmic contents, and aggregates, which are frequently produced in cardiomyocytes.



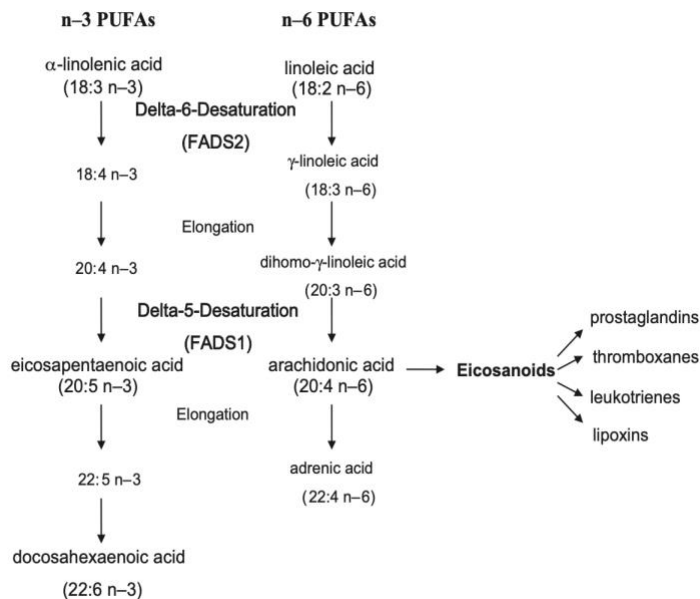
Dewanjee et al., 2021 Ageing Research Reviews

Fig.3.4|The cellular and molecular aspects of cardiac autophagy in the diabetic milieu. The cellular and molecular aspects of cardiac autophagy in the diabetic milieu. Blue arrows indicate downstream cellular events; black arrows were used for labelling; red lines indicate inhibition. Akt: protein kinase B, AMPK: adenosine 5'-monophosphate-activated protein kinase, Atg: autophagy-related, Bcl-2: B-cell lymphoma 2, LC3: microtubule-associated protein 1 light chain 3, LC3-I: the cytosolic form of LC3, LC3-II: a membrane-bound form of LC3, mTORC1: mechanistic target of rapamycin kinase complex 1, Rheb: Ras homolog enriched in brain, TSC: tuberous sclerosis complex, Vps: vacuolar protein sorting.

Cardiac metabolic dysregulation also involves altering the levels and activity of lipids and enzymes in regulating PUFA desaturase and elongase of fatty acids, whose role in cardiovascular physiology and pathophysiology is of great importance. PUFAs are essential components of cell membranes and influence cell functions by regulating metabolic

pathways and the synthesis of inflammatory mediators [Das et al., 2006]. Therefore, adequate stretch and desaturation of fatty acids are essential in maintaining cardiac metabolic homeostasis, whereby alterations of these processes could cause critical functional consequences.

Arachidonic acid (ARA; 20:4n-6) is the precursor of important molecules involved in inflammation, such as eicosanoids, and is believed to play a role in the atherosclerotic process [De Caterina et al., 2004]. ARA derives from the diet or is obtained through the elongation-desaturation process of its precursor, linoleic acid (LA; 18:2n-6). The d-5 (D5D) and d -6 (D6D) desaturases are key enzymes of this pathway (Figure 3.5): D6D catalyzes the conversion of LA to γ -linolenic acid (18:3n-6), which is converted in dihomono- γ -linolenic acid (20:3n-6), which in turn is desaturated to ARA by D5D.



Martinelli et al., 2008 Am J Clin Nutr

Fig.3.5| The n-3 and n-6 fatty acid metabolism pathways. The biological membranes' unsaturation degree is modulated by the action of the desaturation and elongation enzymes mediating fatty acid biosynthesis and metabolism.

Furthermore, other categories of essential lipids are sphingomyelins (SM). Beyond their role as structural membrane components, they have crucial functions as signalling molecules in many biological processes [Kikas et al., 2018]. The decrease in the SM pool in diabetes could potentially contribute to increased oxidative stress and reduced insulin secretion, resulting in hyperglycaemia secondary to an inability to compensate for the reduced insulin sensitivity [Xu et al., 2013].

3.3 PHARMACOLOGICAL APPROACHES

The defining components of cardiorenal metabolic syndrome are central obesity; insulin resistance; hypertension; metabolic dyslipidemia (low HDL levels, high triglyceride levels and small LDL increase; albuminuria and decreased glomerular filtration rate (< 60 ml/min) [Connell et al., 2014]. In treating "cardio-renal metabolic syndrome", it must be considered that this is a condition in which the essential alteration is purely metabolic and is responsible for the coexisting cardiac and renal complications [Zoccali & Mallamaci 2013].

The complications associated with obesity, diabetes and cardio-vascular complications are not independent conditions but are a more complex picture requiring a multidisciplinary approach [Mattina et al., 2022]. However, the primary pharmacological aim is to counteract obesity.

3.3.1 LIFESTYLE MODIFICATIONS

Given the lack of specific pharmacological interventions, ‘lifestyle modification’ remains the cornerstone of obesity management [Swinburn et al., 2011]. Individuals with obesity are suggested to lose at least 10% of body weight via diet, physical activity, and behavioural therapy [Obesity Guidelines 2013]. A portion-controlled diet can achieve significant short-term weight loss [Lee et al., 2018]. Long-term weight control can be achieved via high levels of physical activity and continued patient–practitioner contact. In many cases, lifestyle modification results in dramatic body weight loss, significantly reducing cardiovascular risk [Nguyen et al., 2019].

3.3.2 ANTI-OBESITY MEDICATIONS

Pharmacotherapy is recommended for those whose BMI is ≥ 30 (or a BMI ≥ 27 with comorbid conditions) and who are unable to lose weight using lifestyle modification alone [Telles et al., 2016]. The U.S. FDA (Food and Drug Administration) approved some new pharmacotherapy drugs for short-term obesity treatment (Table 3.1). Since Lorcaserin was withdrawn, there are only four treatments, namely Naltrexone-Bupropion (Contrave), Orlistat (Xenical, Alli), Liraglutide (Saxenda) and Phentermine-Topiramate (Qsymia)] approved in addition to Gelesis which is now the fifth, approved for long-term use [Greenway et al., 2019; Gomez et al., 2018; Rebello et al., 2020]. The FDA also approved the MC4R agonist-Setmelanotide for use in individuals with severe obesity due to either POMC, PCSK1 (proprotein

convertase subtilisin/kexin type 1), or leptin receptor LEPR deficiency at the end of 2020 [Yeo et al., 2021].

In addition, 11 different components have been identified from 54 families of the plants to have anti-obesity potential. These families include Celastraceae, Zingiberaceae, Theaceae, Magnoliaceae, and Solanaceae [Karri et al., 2019]. Traditional Chinese medicine delivers unique solutions to treat obesity, such as regulating fat metabolism, enhancing hormone levels and regulating intestinal microbiota, among other pathways [Gong et al., 2020].

Weight-loss medication	Approved for	How it works
Orlistat (Xenical) Available in lower dose without prescription (All)	Adults and children ages 12 and older	Works in the gut to reduce the amount of fat the body absorbs from food
Liraglutide (Saxenda) Available by injection only	Adults	May decrease hunger or increase feelings of satiation. A lower dose under a different name of Victoza was approved to treat T2DM.
Phentermine-Topiramate (Qsymia)	Adults	A mix of topiramate, which is used to treat migraine headaches or seizures, and phentermine, which lessens appetite. May decrease hunger or increase feeling of satiation.
Naltrexone-Bupropion (Contrave)	Adults	A mix of naltrexone and bupropion. May decrease hunger or increase feelings of satiation.
Gelesis (Plenity) (84)	Adults	The gel pieces increase the volume and elasticity of the stomach and small intestine contents, contributing to a feeling of fullness and inducing weight loss.
Setmelanotide (Imcivree) (85)	Adults and children ages 6 and older	An agonist of the MC4R, used in individuals with severe obesity due to either POMC, PCSK1, or LEPR deficiency, and should not be used for other types of obesity such as general obesity.
Other medications that curb your desire to eat include	Adults	Increase chemicals in the brain to make depress feelings of hunger or increase feelings of satiation.
<ul style="list-style-type: none"> •Phentermine (Adipex, Superenza) •Benzphetamine (Regimex, Didrex) •Diethylpropion (Tenuate) •Phendimetrazine (Bontril PDM) 		

Lin et al., 2021 *Frontiers in Endocrinology*

Table 3.1 Medications approved for obesity treatment. The U.S. FDA (Food and Drug Administration) approved some new pharmacotherapy drugs for obesity treatment.

3.3.3 BARIATRIC SURGERY

For individuals with a BMI > 40 or BMI > 35 with comorbidities who cannot lose weight by lifestyle modifications or pharmacotherapy, bariatric surgery or weight loss surgery is another option [Telles et al., 2013].

Studies have reported that the benefits of bariatric surgery go beyond just weight loss and include the reduction of chronic inflammation involved in obesity [Osto et al., 2013; Al-Rubaye et al., 2019; Kops et al., 2020]. Standard bariatric operations, including BPD (Biliopancreatic diversion), SG (sleeve gastrectomy), RYGB (Roux-en-Y gastric bypass), and AGB (adjustable gastric banding), benefit individuals' metabolic profiles to varying degrees [Aminian et al., 2015].

3.4 HFD-INDUCED OBESITY IN RODENTS: FOCUS ON CARDIORENAL ALTERATIONS

High-fat diets (HFD) are commonly used in research to model human metabolic syndrome [Wali et al., 2020]. In particular, C57BL/6J mice fed HFD has been extensively used as a model of diet-induced obesity (DIO) to study the mechanisms of insulin resistance, as they are comparatively more susceptible to metabolic impairment [Wang et al., 2012]. In fact, the C57BL/6 strain is more prone to develop obesity and insulin resistance than A/J, C57BLKS/J, BALB/c, FVB/N, and 129S6 mice [Fontaine et al., 2016; Reuter 2007; Small et al., 2018]. The two commonly used sub-strains of C57BL/6 mice used in DIO studies are C57BL/6J (from JAX lab) and C5BL/6N (from NIH). The C57BL/6J mice contain a mutation in the nicotinamide nucleotide transhydrogenase gene, gain more body weight, and have higher blood glucose levels and glucose tolerance than C57BL/6N mice on HFD [Nicholson et al., 2010].

The HFDs used in metabolic research typically provide 40–60% of calories from fat, and the commonly used sources of fat include lard and beef

tallow, which are rich in saturated fatty acids [Wali et al., 2020]. Male mice are mostly used in experiments as they are more prone to HFD-induced insulin resistance than females [Pettersson et al., 2012].

An HFD can induce glomerular hypertrophy, fibrosis, and kidney scarring [Ruggiero et al., 2011; Sun et al., 2020; Kuwahara et al., 2016]. HFD leads to renal lipid accumulation in renal tubules and accelerates the development of obesity-related nephropathy [Chen et al., 2019]. Accumulated lipids also induce mitochondrial fission and apoptosis in renal cells, suggesting that HFD causes renal cell injury, which may be attributed to oxidative stress and mitochondrial dysfunction, promoting excess programmed cell death [Sun et al., 2020]. Moreover, it is well documented that diet-induced obesity may lead to profound changes in heart lipid composition due to its limited capacity for de novo fatty acid synthesis and, therefore, reliance on the exogenous supply of fatty acids [Dirkx et al., 2011].

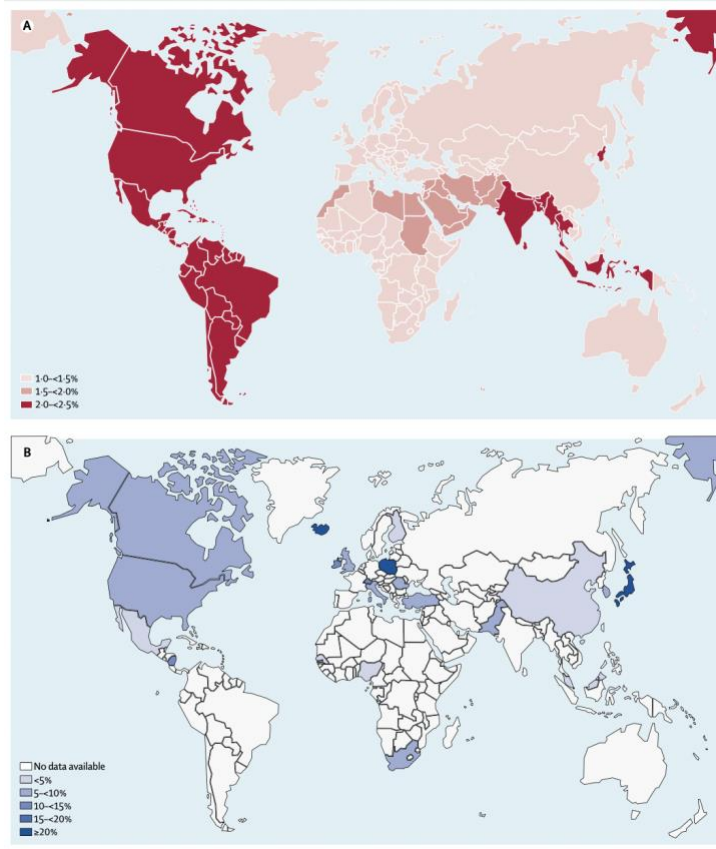
4. CHRONIC KIDNEY DISEASE (CKD)

4.1 DEFINITION, EPIDEMIOLOGY AND RISK FACTORS

Chronic kidney disease (CKD) is a syndrome defined as the persistent alteration of the function and/or structure of the kidney due to various causes; the evolution is slow, progressive, and irreversible and is associated with a higher risk of cardiovascular disease, could lead to end-stage renal disease (ESRD) and death [Zoccali et al., 2017].

The global burden of chronic kidney disease is substantial and growing; approximately 10% of adults worldwide are affected by some form of chronic kidney disease [Bikbov et al., 2021; Xie et al., 2018]. By 2040, CKD is estimated to become the fifth leading cause of death globally—one of the largest projected increases of any major cause of death [Foreman et al., 2018]. This trend can be partially attributed to the expanding ageing population globally [Stevens et al., 2010].

This pathology is usually insidious, and the patients remain asymptomatic most of the time, presenting the typical complications typical of renal dysfunction only in more advanced stages (i.e., eGFR of less than 30 mL/min per 1.73 m²).



Webster et al., 2017. Lancet

Fig 4.1 Burden of kidney disease globally. (A) The proportion of total mortality attributed to kidney disease. (B) Prevalence of chronic kidney disease.

The rate of loss of kidney function varies by aetiology, exposures, and interventions, but in most cases, progression to kidney failure typically takes months and decades to develop. Signs and symptoms of kidney failure result from progressive uraemia, anaemia, volume overload, electrolyte abnormalities, mineral and bone disorders, and acidaemia and inevitably lead to death if left untreated [Zarantonello et al., 2021]. Renal replacement therapy, either chronic dialysis or kidney transplantation, is a life-sustaining treatment for people with kidney failure.

There are currently over 1.4 million patients on renal replacement therapy worldwide. One way to reduce the economic burden of chronic kidney disease would be early intervention. To achieve this, it is crucial to identify people with an increased risk of kidney disease. An individual's genetic and phenotypic makeup predisposes them to risk for kidney disease. Factors such as race, gender, age and family history are crucial. For example, being of African-American descent, having older age, having low birth weight, and having a family history of kidney disease are considered decisive risk factors for CKD. Furthermore, smoking, obesity, hypertension, and T2DM can also lead to kidney disease. An uncontrolled diabetic and/or hypertensive patient can easily and quickly become a patient with end-stage renal disease. Exposure to heavy metals, excessive alcohol consumption, smoking and analgesic drugs pose risks. Experience of acute kidney injury, a history of cardiovascular disease, hyperlipidemia, metabolic syndrome, hepatitis C virus, HIV infection, and malignancy are additional risk factors. Determination of serum creatinine levels and urinalysis in patients at risk for CKD is usually sufficient for initial screening [Kazancıoğlu et al., 2013].

The kidney is involved in several complex processes critical in the homeostasis of blood, bone integrity, acid–base balance, electrolyte levels and blood pressure. As nephron number declines, patients experience complications associated with dysregulation of many of these exchange systems, such as metabolic acidosis, anaemia, mineral bone disorder (MBD, which is associated with vitamin D deficiency, hyperparathyroidism, hyperkalaemia and hyperphosphataemia), arterial hypertension, hyperuricaemia and expansion of effective circulating fluid volume.

Dyslipidaemia, endocrine abnormalities and growth impairment in children can also occur. Of these complications, CVD is the leading cause of death in patients with CKD worldwide and is associated with dyslipidaemia, hyperuricaemia and hypertension [Saland et al., 2010]

4.2 PATHOPHYSIOLOGICAL MECHANISMS

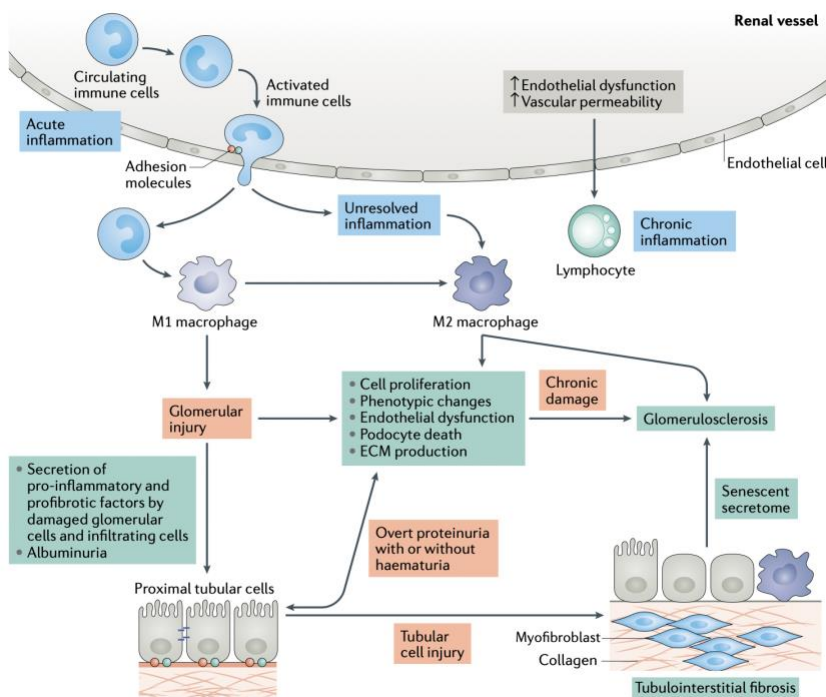
CKD is a chronic renal dysfunction syndrome characterized by nephron loss, inflammation, myofibroblasts activation, and extracellular matrix (ECM) deposition, the main processes of the initial and progression of renal fibrosis [Yuan et al., 2022].

Fibrosis is part of the normal repair process triggered in response to injury and preserves the architecture and functional integrity of the tissue. However, the deregulation of this process leads to the pathological accumulation of ECM proteins, mainly collagens [Zeinsber et al., 2012]. In CKD, loss of podocytes and their replacement by ECM (termed glomerulosclerosis), tubular cell injury and subsequent tubulointerstitial fibrosis contribute to nephron loss [Hodgkins et al., 2012; Meng et al., 2014]. These processes result in the replacement of parenchymal tissue by ECM — the pathological hallmark of fibrosis — and concomitant irreversible damage. Thus, regardless of aetiology, CKD progresses to tubulointerstitial fibrosis, which correlates more strongly with proteinuria and disease severity than histological glomerular injury [Wehrmann et al., 1990]. Tubulointerstitial diseases also lead to glomerulosclerosis, although the molecular pathways are less well characterized than those that underlie the link between glomerular injury and tubulointerstitial fibrosis.

The primary pathological mechanism that links oxidative stress, inflammation and CKD progression is characterized by an initial injury in the kidney due to the activities of intra- and extracellular oxygen-derived radicals and the resultant inflammatory response. Radicals such as superoxide and hydroxyl radicals readily interact with the molecular components of a nephron [Kao et al., 2010].

Proinflammatory cytokines, such as $\text{TNF}\alpha$, trigger signalling pathways that activate $\text{NF}\kappa\text{B}$ transcription factors [Esteban et al., 2004]. The translocation of $\text{NF}\kappa\text{B}$ dimers to the nucleus prompts the transcription of genes involved in systemic inflammatory responses, thereby encouraging a downstream generation of free radicals via phagocytic activity (often referred to as “respiratory bursts” or “oxidative bursts”) [Tucker et al., 2015].

Renal fibrosis, including nephrosclerosis and tubulointerstitial fibrosis, constitutes the final common pathway of renal injuries, regardless of etiologies. EMT is the principal mechanism promoting renal fibrosis, and myofibroblasts are the primary cell type that produces the extracellular matrix [Hu et al., 2022]. The fibrotic microenvironment triggers renal resident cells such as fibroblasts, pericytes, TECs, and endothelial cells, and bone marrow-derived cells like macrophages and mesenchymal stem cells transdifferentiate into myofibroblasts [Boor et al., 2012]. The activation and proliferation of myofibroblasts produce a large amount of ECM. Interstitial ECM expansion accelerates hypoxia and nephron loss [Liu et al., 2011; Humphreys et al., 2018].



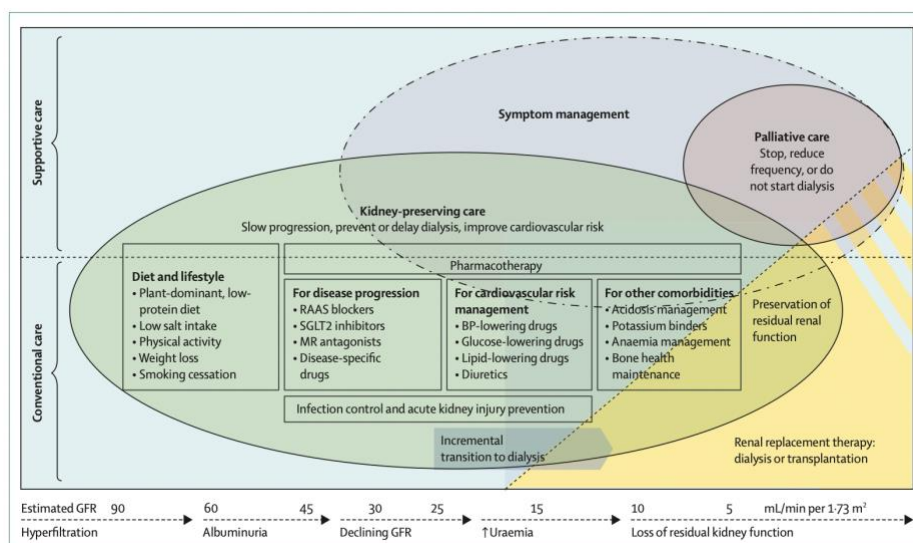
Ruiz-Ortega 2020. Nature Reviews | Nephrology

Fig 4.2 | Glomerular injury and fibrosis. Glomerular injury is associated with the recruitment of inflammatory cells, including macrophages and lymphocyte populations, with characteristic cytokine secretion patterns that can lead to tubular cell injury and interstitial fibrosis through diverse mechanisms, including the secretion of inflammatory and profibrotic factors. Conversely, tubulointerstitial injury can eventually lead to glomerulosclerosis via mechanisms that likely involve inflammatory cells and spill-over of pro-inflammatory and profibrotic cytokines from the interstitium.

4.3 CKD MANAGEMENT

CKD is a progressive disease with no cure and high morbidity and mortality commonly occurring in the general adult population, especially in people with diabetes and hypertension. Preservation of kidney function can

improve outcomes and can be achieved through non-pharmacological strategies (e.g., dietary and lifestyle adjustments) and chronic kidney disease-targeted and kidney disease-specific pharmacological interventions [Kalantar-Zadeh et al., 2021].



Kalantar-Zadeh 2021. Lancet

Fig 4.3| Conservative and preservative management of CKD. The bottom half of the chart represents conventional (life-prolonging and kidney-prolonging) strategies. In contrast, the top half represents supportive care, including palliative and hospice care, in which dialysis is often avoided or withdrawn.

4.3.1 CONVENTIONAL CARE

A plant-dominant, low-protein, and low-salt diet may help mitigate glomerular hyperfiltration and preserve renal function for longer, possibly leading to favourable alterations in acid-base homeostasis and the microbiota. Pharmacotherapies that alter intrarenal haemodynamics (e.g., renin–angiotensin–aldosterone pathway modulators and SGLT2

inhibitors) can preserve kidney function by reducing intraglomerular pressure independently of blood pressure and glucose control. In contrast, other novel agents (e.g., non-steroidal mineralocorticoid receptor antagonists) might protect the kidney through anti-inflammatory or antifibrotic mechanisms. Some glomerular and cystic kidney diseases might benefit from disease-specific therapies. Managing CKD-associated cardiovascular risk, minimizing the risk of infection, and preventing acute kidney injury are crucial interventions for these patients, given the high burden of complications, associated morbidity and mortality, and the role of non-conventional risk factors in chronic kidney disease. When renal replacement therapy becomes inevitable, an incremental transition to dialysis can possibly be considered and proposed to preserve residual kidney function.

4.3.2 DIALYSIS AND KIDNEY TRANSPLANTION

Renal replacement therapy, including hemodialysis and peritoneal dialysis, is a potential treatment modality in patients with ESRD. It is essential to consider the timing of dialysis initiation concerning eGFR and residual renal function and the resulting impact on quality of life [Rivara et al., 2017].

When available, however, eligibility for kidney transplantation should be assessed based on age and comorbidities, although it may take months or even years to complete [Abramowicz et al., 2015]. To verify eligibility, potential donors must undergo a comprehensive health evaluation, including testing for blood type and human leukocyte antigen

compatibility with the potential recipient, GFR measurements, imaging of the kidneys and urinary tract, cardiac tests and other tests depending on the medical history. Such rigorous testing is recommended to ensure the donor's short- and long-term well-being after donation. Comorbidities such as cancer, chronic infections, cardiac or peripheral vascular disease, and the risk of medical noncompliance are carefully assessed in this trial.

4.3.3 SUPPORTIVE CARE

Kidney replacement therapy might not be available or affordable, but it might not be advisable for medical reasons. Particularly in very old patients with ESRD and comorbidities, dialysis does neither increase lifespan nor improve quality of life. Supportive care in the setting of kidney disease represents palliative care that, as defined by the WHO, is an approach that improves the quality of life through the prevention and relief of suffering by employing early identification and assessment and managing the symptoms of uremia [Davison et al., 2015].

4.4 FA-INDUCED CKD ANIMAL MODEL

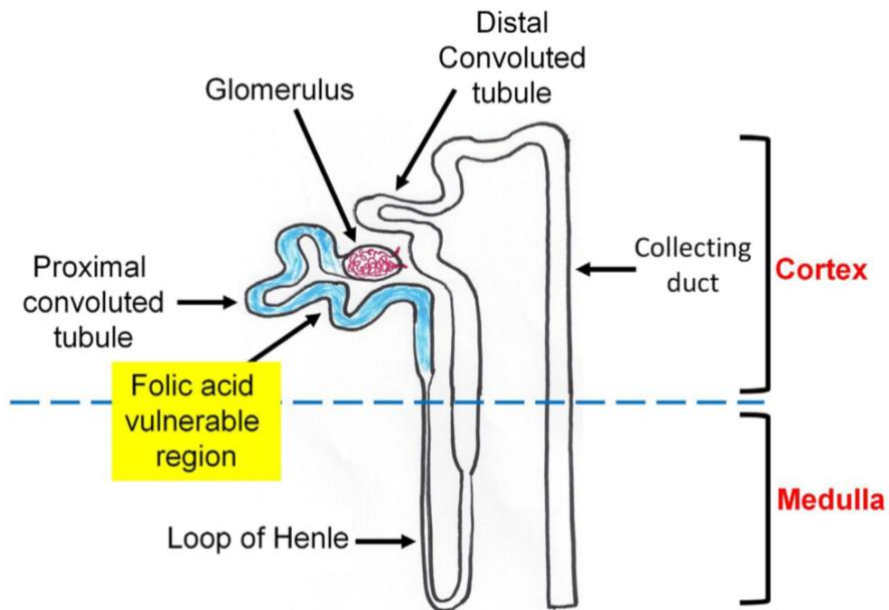
FA is also known as vitamin B9 [Lobos et al., 2021; Goossens et al., 2021]. It is a cofactor in one-carbon metabolism essential for cellular proliferation and growth [Samodelov et al., 2019; Ducker et al., 2017; Lieberman et al., 2013].

While low doses of FA (usually less than 10 mg/day) are beneficial and against oxidative stress [Schneider et al., 2011; Hwang et al., 2011; Akgun et al., 2021], high doses of FA, e.g., 150-250 mg/day, as widely used in the

induction of animal kidney disease, are highly toxic [Doi et al., 2006]. The first report of kidney injury induced by FA was published in 1969 [Brade et al., 1969]. These studies led to the concepts of “renal folate toxicity” and “folate nephropathy” in the 1970s [Hsueh et al., 1973; Kirschbaum et al., 1979]. Now, the procedures of FA-induced kidney injury in mice and rats are well-established and widely used. In both mouse and rat models of acute kidney injury, a single injection of FA at a dosage of 150-250 mg/kg body weight intraperitoneally can cause AKI [Nikolic et al., 2020; González-Guerrero et al., 2018; Kumar et al., 2015], resulting in proteinuria and increased blood urea nitrogen (BUN) and creatinine [Jiang et al., 2019], AKI can be studied within 72 h of FA administration [Aparicio-Trejo et al., 2020] If left untreated, CKD will develop and can be studied more than four weeks or beyond after FA injection.

Progression of AKI to CKD can also be investigated after a single high-dose FA injection [Aparicio-Trejo et al., 2019]. Therefore, FA-induced kidney disease can cover AKI, CKD, and the AKI–CKD transition [Burgos-Silva et al., 2015]. Additionally, as FA is water-soluble and the injection is intraperitoneal, the procedure of kidney disease induction is simple and straightforward, without the need for surgery. Importantly, FA-induced kidney disease can recapitulate the clinical symptoms of human kidney disease, and the model is highly reproducible [Gupta et al., 2012]. The cisplatin model, the diphtheria toxin model and the aristolochic acid model require repeated dosing of the animals; the Unilateral Ureteral Obstruction (UUO) model, conversely, involves surgery [Ewees et al., 2021; Bao et al., 2018]. Concerning which site or region in the nephron is vulnerable to FA-induced damage, it has been well established that FA

damage occurs mainly in the proximal tubular epithelial cells (Figure 4.4) [Zhu et al., 2017; Ortega et al., 2006; Jung et al., 2018].



Yan et al., 2021. Anim Models Exp Med

Fig 4.4| FA vulnerable region in the kidney. Diagram showing the proximal convoluted tubule in the nephron as the most vulnerable region to FA-induced damage. The blue highlighted tubule depicts the proximal convoluted region.

After a high dose of FA administration via i.p. injection, FA can quickly form crystals in the kidney within renal tubules, followed by acute tubular necrosis, epithelial regeneration, and renal cortical scarring, culminating in renal injury reflected by renal inflammation, renal fibrosis and induction of tubular injury and cell death (Figure 4.5) [Jiang et al., 2018]. FA induced a remarkable increase in creatinine and BUN in plasma and a higher urinary volume [Aparicio-Trejo et al., 2019].

Moreover, numerous studies demonstrate a redox imbalance status induced by FA injection [Aparicio-Trejo et al., 2020]. Gupta et al. [2012]

found a decreased level of the reduced form of glutathione and SOD activity; meanwhile, levels of hydrogen peroxide were increased.

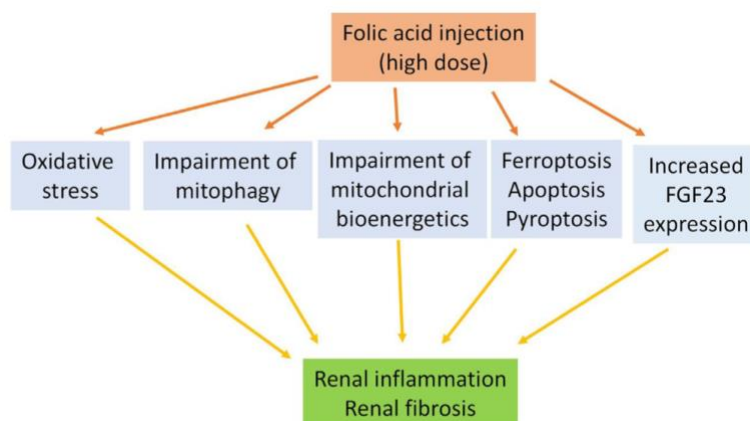


Fig 4.5| Major pathological mechanisms of FA-chronic kidney disease (CKD). These include oxidative stress, impairment of mitophagy and mitochondrial bioenergetics, ferroptosis, apoptosis, and increased expression of fibroblast growth factor 23 (FGF23). These mechanisms result in renal inflammation and fibrosis, eventually leading to renal dysfunction or kidney disease.

5. METHODS

IN VIVO MODELS

5.1 HIGH FAT DIET-DRIVEN METABOLIC ALTERATIONS IN KIDNEY AND HEART

Male C57Bl/6J mice at 6 weeks of age were housed in stainless steel cages in a room kept at $22 \pm 1^\circ\text{C}$ with a 12:12 hours light-dark cycle. The animals were randomly divided into five groups as reported below: (i) control group (STD) receiving chow standard diet and vehicle; (ii) HFD group receiving vehicle; (iii) HFD group treated with OEA (HFD+OEA 2,5 mg/kg/die i.p.), (iv) HFD group treated with EGb (100 mg/kg/die) and (v) HFD group treated with OEA and EGb (HFD+OEA+EGb, 2,5 mg/kg/die i.p. and 100 mg/kg/die *per os*, respectively). The standard chow diet had 17% fat without sucrose, while HFD had 45% energy derived from fat and 7% sucrose. OEA was suspended in water/PEG/TWEEN 80 (90/5/5 v/v), while EGb was suspended in water. Treatments started after 12 weeks of HFD feeding and are conducted concurrently with the HFD. Two experiments were conducted, the first in which the treatment with OEA and EGb alone and in the association was carried out and lasted 6 weeks (Fig 5.1) and the second experiment in which the treatment with OEA lasted 8 weeks (Fig 5.2).

During the experimental period, body weight was assessed weekly. In addition, in the first experiment, blood pressure was recorded weekly during treatment. Moreover, to evaluate water intake and collection of 24-h urine, all mice were placed in individual metabolic cages. Before sacrifice, bioelectrical impedance analysis (BIA) was performed to

measure fat body composition using BIA 101 analyzer modified for the mouse (Akern, Florence, Italy). Fat-free mass was calculated, and fat mass content was determined as the difference between body weight and fat-free mass. At the end of the experiment, blood was collected from all animals, and the heart and kidneys were removed. All samples were frozen and stored at -80°C for subsequent determinations.

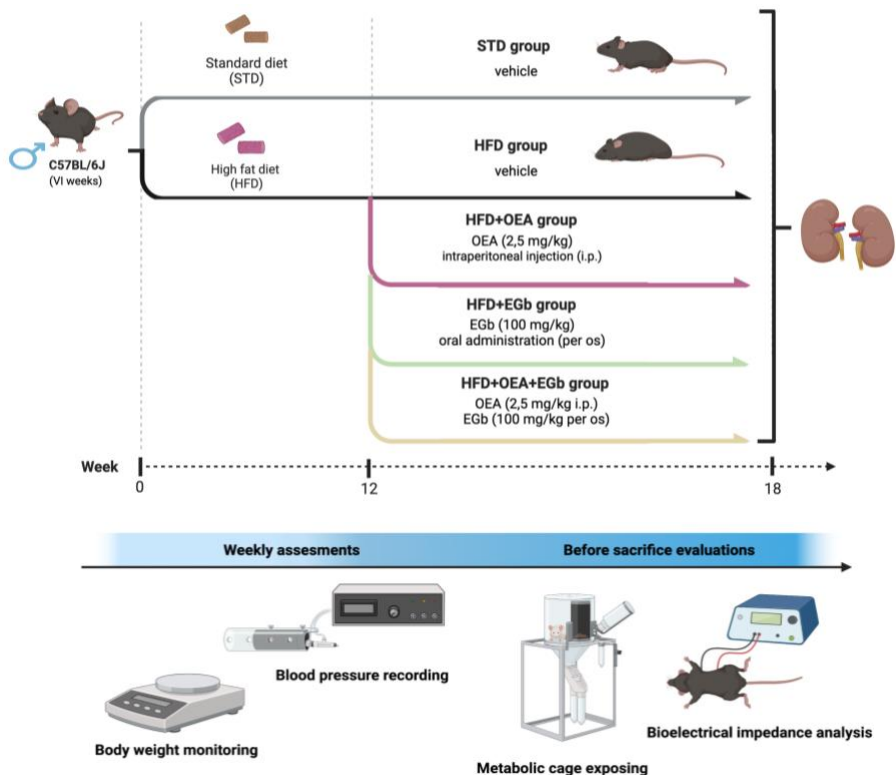


Fig 5.1| Experimental protocol of HFD-induced kidney damage (I experiment). The animals were randomly divided into five groups: control group (STD) receiving standard chow diet and vehicle; HFD group receiving vehicle; HFD group treated with OEA (HFD+OEA 2,5 mg/kg/die i.p.), HFD group treated with EGb (HFD+EGb 100 mg/kg/die) and HFD group treated with OEA and EGb (HFD+OEA+EGb). Treatments started after 12 weeks of HFD feeding and lasted 6 weeks along with HFD.

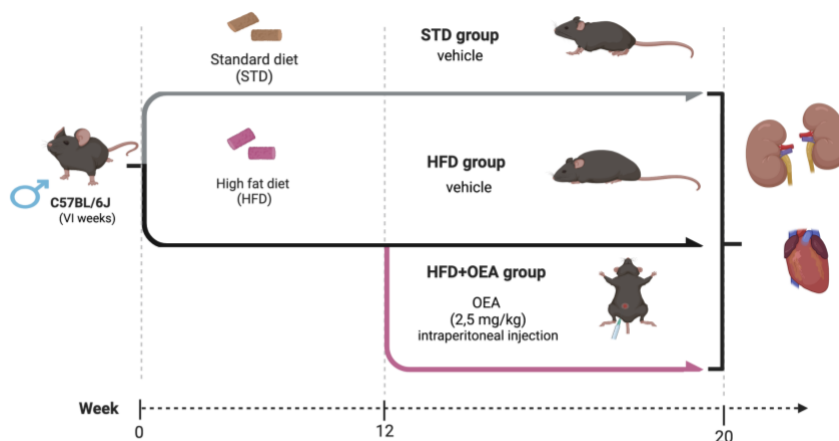


Fig 5.2| Experimental protocol of HFD-induced cardiorenal metabolic alterations (II experiment). The animals were randomly divided into control group (STD) receiving standard chow diet and vehicle; HFD group receiving vehicle; HFD group treated with OEA (HFD+OEA 2,5 mg/kg/die i.p.). Treatments started after 12 weeks of HFD feeding and lasted 8 weeks along with HFD.

5.2 FOLIC ACID INDUCED CKD: EXPERIMENTAL SETUP

Male C57Bl/6J (Charles River, Wilmington, MA, USA) and $PPAR\alpha^{-/-}$ (B6.129S4-SvJae-Ppar-atm1Gonz; Jackson Laboratories) mice (21 weeks) weighing approximately 28–30g were housed in stainless steel cages in a room kept at $22\pm 1^{\circ}\text{C}$ with a 12:12 hours lights-dark cycle (from 7 a.m. to 7 p.m.). The $PPAR-\alpha^{-/-}$ mice colony was established and maintained by heterozygous crossing. Mice were genotyped as described on the supplier webpage (<http://jaxmice.jax.org>) using the RedExtract kit (Sigma e Aldrich, Italy). Mice were allowed food and water ad libitum.

Nephropathy was induced chemically with a single intraperitoneal injection of FA (150 mg/kg) dissolved in 0.3 mol/L sodium bicarbonate.

Control mice received sodium bicarbonate alone. The dose of FA was critical for the induction of severe renal damage and was chosen after preliminary studies.

In the first experiment setting, mice were randomly assigned to one of the following groups: (i) control group (CON) receiving vehicle; (ii) mice insulted by FA (150 mg/kg i.p.) receiving vehicle; (iii) FA group treated with OEA (FA+OEA, 2,5 mg/kg/die i.p.), (iv) FA group treated with EGb (FA+EGb, 100 mg/kg/die per os) and (v) FA group treated with OEA and EGb (FA+OEA+EGb, 2,5 mg/kg/die i.p. and 100 mg/kg/die per os, respectively). The treatment started 3-day after FA injection and lasted until day 14.). OEA and EGb were prepared as reported above. FA was obtained from Sigma–Aldrich (St. Louis, MO).

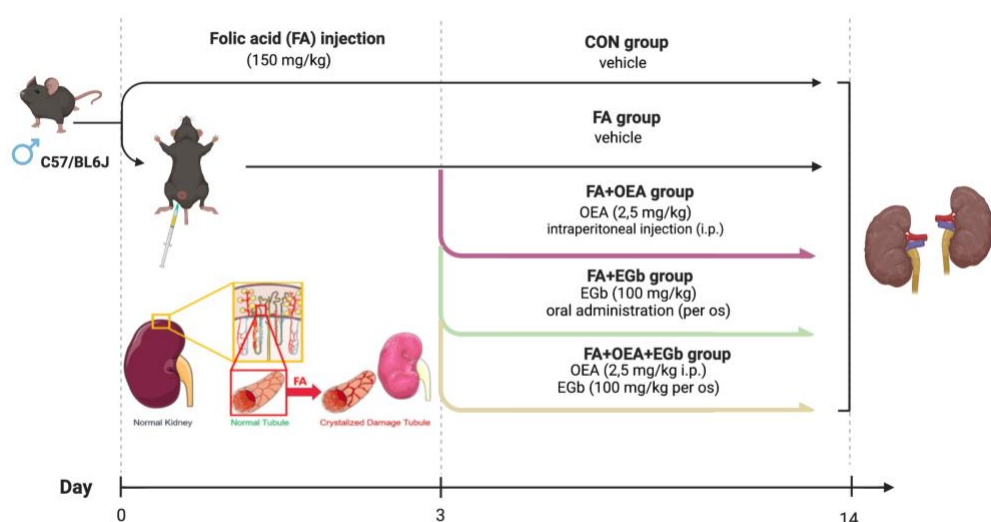


Fig 5.3| Experimental protocol of FA-induced kidney damage (I experiment). Mice were randomly assigned to one of the following groups: (i) control group (CON) receiving vehicle; (ii) control group treated with OEA (2,5 mg/kg daily i.p.) (CON+OEA); (iii) mice insulted by FA (150 mg/kg) receiving vehicle; (iv) FA group treated with OEA (FA+OEA), FA group treated with EGb (FA+EGb) and FA group treated with OEA and EGb (FA+OEA+EGb). The treatment started 3 day-after of FA injection and lasted until day 14.

In the second experiment, mice were divided into 4 groups: (i) control group (CON) receiving vehicle; (ii) control group treated with OEA (2,5 mg/kg daily i.p.) (CON+OEA); (iii) mice insulted by FA (150 mg/kg) receiving vehicle and (iv) FA group treated with OEA (FA+OEA, 2,5 mg/kg daily i.p.).

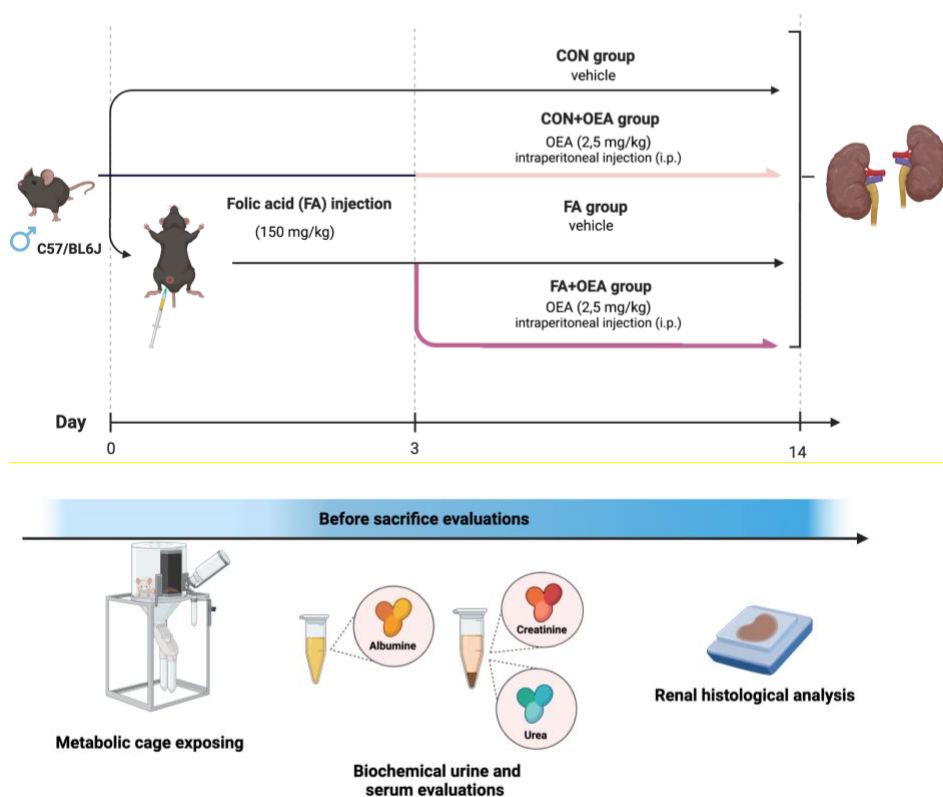


Fig 5.4| Experimental protocol of FA-induced kidney damage (II experiment). In the second experiment, mice were divided into 4 groups: (i) control group (CON) receiving vehicle; (ii) control group treated with OEA (CON+OEA); (iii) mice insulted by FA (150 mg/kg) receiving vehicle and (iv) FA group treated with OEA (FA+OEA). The treatment started 3-day after of FA injection and lasted until day 14.

Concurrently, PPAR- $\alpha^{-/-}$ mice were divided as follows: (i) control group (CON) receiving vehicle; (ii) mice insulted by FA (150 mg/kg) receiving vehicle and (iii) FA group treated with OEA (FA+OEA, 2,5 mg/kg daily i.p.).

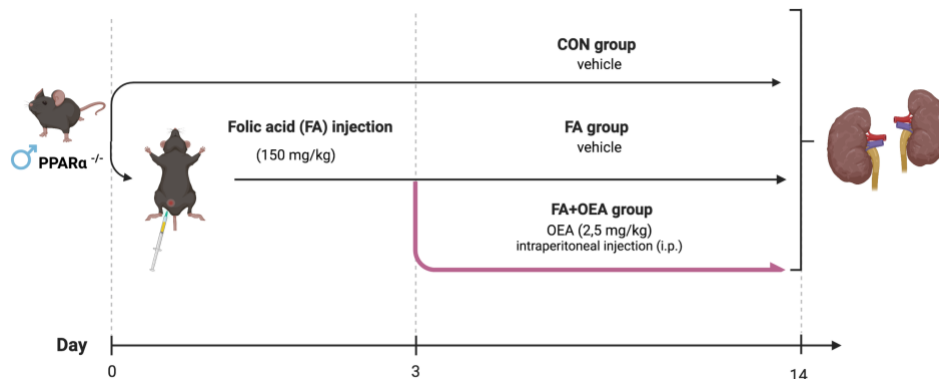


Fig 5.5| Experimental protocol of FA-induced kidney damage in PPAR α null mice. PPAR α null mice were divided into 3 groups: (i) control group (CON) receiving vehicle; (ii) mice insulted by FA (150 mg/kg) receiving vehicle; and (iii) FA group treated with OEA (FA+OEA). The treatment started 3-day after of FA injection and lasted until day 14.

In all sets of experiments, mice were euthanized 14 days after FA injection. Before sacrifice, all mice were placed in individual metabolic cages for a water intake evaluation and collection of 24-h urine. At the end of the experiment, blood was collected, and mice were sacrificed by an i.p. injection of a mixture of ketamine/xylazine followed by cervical dislocation. Left kidneys were removed and snapped frozen for the isolation of RNA or protein and stored at -80°C . Right kidneys were kept in 10% buffered formalin for histological examination.

5.3 OLEOYLETHANOLAMIDE SYNTHESIS

The procedure for the OEA synthesis is under that described by Han D. *et al.* [2017] but with appropriate modifications in the purification step.

To oleic acid (2 g, 7.09 mmol) in DCM dry 5 mL at 0°C, oxalyl chloride was added dropwise (1.87 mL, 21.27 mmol) followed by 5 drops of DMF dry. The reaction was stirred under nitrogen and allowed to warm to room temperature for over 5 hours. The solvent was removed via rotary evaporation, and the obtained residue was washed with DCM dry (10 mL) two times. To the orange semi-solid dissolved in DCM dry (5 mL) was added ethanolamine (4.25 mL, 70.9 mmol) dissolved in turn in DCM dry (5 mL) and was stirred for 15 minutes. The reaction mixture was washed with water (2 × 15 mL), 1 M HCl (2 × 15 mL), water (2 × 15 mL), 1 M NaOH (2 × 15 mL), and brine (2 × 15 mL), then dried over anhydrous Na₂SO₄ and concentrated to dryness. Purification of the residue via silica gel chromatography, using DCM/MeOH (NH₃sat) (98/2, v/v) as the eluent, gave target compound OEA as a white solid (1.797 g, 76%). ¹H NMR (600 MHz, CDCl₃) δ = 5.94 (bs, 1H), 5.37 – 5.29 (m, 2H), 3.69 – 3.73 (m, 2H), 3.41 (dd, *J* = 10.1, 5.3 Hz, 2H), 2.75 (bs, 1H), 2.21 – 2.17 (m, 2H), 2.02 – 1.97 (m, 4H), 1.65 – 1.59 (m, 2H), 1.33 – 1.22 (m, 20H), 0.86 (t, *J* = 6.9 Hz, 3H). ¹³C NMR (150 MHz, CDCl₃) δ = 174.7, 130.2, 130.0, 62.8, 42.6, 36.82, 32.1, 29.9, 29.8, 29.7, 29.5, 29.4, 29.3, 27.4, 27.3, 25.9, 22.83, 14.3. ESI-MS [M+H]⁺: *m/z* 326.6.

All reactions involving air-sensitive reagents were performed under nitrogen in oven-dried glassware using the syringe-septum cap technique. All chemicals used for synthesis were purchased from commercial sources (Sigma-Aldrich). All solvents were purified and degassed before use. Chromatographic separation was carried out under pressure using Merck silica gel 60 using flash-column techniques. Reactions were monitored by thin-layer chromatography (TLC) performed on 0.25 mm silica gel-coated

aluminium plates (60 Merck F₂₅₄) using a solution of potassium permanganate and iodine vapor as visualizing agents. All reagents were used as received without further purification except oleic acid. Before being used as the starting reagent, oleic acid was purified by flash column chromatography using petroleum ether/dichloromethane (70/30 v/v) acidified with acetic acid (1%) as eluent. Dichloromethane (DCM) used for the reactions was dried over P₂O₅ and was freshly distilled under nitrogen prior to use. *N,N*-dimethylformamide (DMF) dry was stored over 3 Å molecular sieves. ¹H and ¹³C NMR spectra were recorded at room temperature on a JEOL ECZ-R 600 at 600 and 150 MHz, respectively, and calibrated using SiMe₄ as an internal reference. Chemical shifts (δ) are given in parts per million (ppm) and the coupling constants (*J*) in Hertz (Hz). The following abbreviations were used to designate the multiplicities: s = singlet, dd = doublet of doublet, t = triplet, m = multiplet, bs = broad singlet. ESI spectra were recorded on a Micromass Quattro API micro (Waters Corporation, Milford, MA, USA) mass spectrometer. Data were processed using a MassLynxSystem (Waters).

5.4 METABOLIC CAGES

To determine the metabolic profile, mice from all groups were placed individually in metabolic cages the day before the sacrifice. This procedure allows monitoring of several parameters, such as food and water intake, by weighing pellets and the dispenser of water at the beginning and end of the 24-hour experiment. In addition, metabolic cages made it possible to evaluate the urinary output for 24 hours and to collect urine samples for functional measurements.

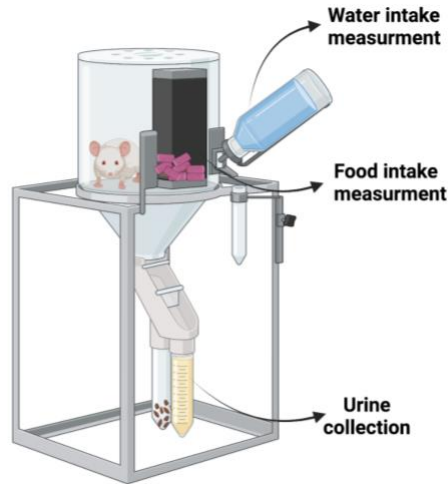


Fig 5.6| Metabolic cage. The cages are available for single mice (with a single chamber feeder) and have been designed to measure food and water intake and separate and collect feces and urine.

5.5 ORAL GLUCOSE TOLERANCE TEST (OGTT)

At the beginning of the 8th week of OEA treatment, an oral glucose tolerance test (OGTT) was performed on different sub-groups of mice (8 animals/each group). OGTT was performed in overnight fasted animals receiving glucose (1 g/kg, Sigma-Aldrich, St Louis, MO, USA). Blood glucose levels were measured at selected time points after injection (0,30,60,90,120 minutes). During this test, mice have free access to drinking water. The area under the curve (AUC) related to glucose level during the time was calculated from time 0 as an integrated and cumulative measure of glycemia up to 120 minutes for all animals. Glucose levels were measured by the glucometer One Touch Ultrasmart (Lifescan, Milpitas, CA).

5.6 EVALUATION OF CARDIOVASCULAR PARAMETERS

The blood pressure of the animals of all groups was monitored throughout the pharmacological treatment period. The systolic blood pressure (SBP) was monitored using a non-invasive methodology, using a tail-cuff system instrument (Ugo Basile, Biological Research Apparatus, 21025 Comerio, Italy). Two weeks before the start of the measurements, the animals were preliminarily trained in this experimental procedure. The mice were housed for 30 minutes in a preheated room between 28-30 ° C where thermoneutrality is established. The sensor was then positioned approximately 2 cm away from the base of the tail to measure the blood parameters. The SBP was measured during all weeks of treatment between 9.00h and 12.00h, and the analyzed values resulted from at least three consecutive measurements for each animal.

5.7 BIOCHEMICAL EVALUATIONS

The blood, collected at the end of the experimental period by cardiac puncture, was centrifuged at 2500 rpm at 4 °C for 12 min to obtain the serum samples on which urea, creatinine, and cholesterol levels were measured. Urea was expressed in the form of BUN obtained by dividing the concentration of urea in the blood by 2.14 (i.e. the ratio between the molecular weight of urea and urea nitrogen). The formula is $BUN = [urea] / 2.14$.

These parameters were quantified using commercially available kits according to the manufacturer's instructions. All samples and standards were analyzed in doublet to avoid intra-test variation.

Urine albumin and creatinine were measured in spot urine samples to calculate urine UACR. Urine albumin was measured using ELISA kit (abcam ab241017).

5.8 HISTOLOGICAL SCORE ANALYSIS

Kidneys were fixed in 10% neutral-buffered formalin and dehydrated through graded alcohols before being embedded in paraffin wax. Sections were cut at the 5-micron thickness and were stained with hematoxylin–eosin (HE) or Masson’s trichrome. For each case, the percentage of tubules with necrosis, epithelial vacuolization, tubular dilation, and cast formation was evaluated using a 4-point score system as follows: (0) none; (1) <20%; (2) 20–50%; (3) 50–70%; and (4) >70%. Similarly, the severity of fibrosis was graded, based on the ratio between fibrosis and total area examined, into the following categories: (0) none; (1) <20%; (2) 20–50%; (3) 50–70%; and (4) >70%. The inflammation was graded into the following categories: 0 (absent), 1 (mild inflammation), 2 (moderate inflammation), and 3 (severe inflammation). The differences in the distribution of the semiquantitative histologic scores among groups were compared using the Kruskal-Wallis and Mann–Whitney U test (IBM SPSS Statistics - Version 25).

5.9 WESTERN BLOTTING

Kidney and heart after homogenization with a homogenizer (Ultra-Turrax T8; IKA Labortechnik, Staufen, Germany) were lysed, and total protein lysates were undergone to SDS-PAGE. The blot was performed by a Trans-Blot Turbo transfer system (Bio-Rad Laboratories, Segrate, Milan, Italy), transferring proteins from a slab gel to a nitrocellulose membrane. The

following parameters were set: 10 min of blotting time, 1.3 mA (circa 25 V). The filter was then blocked with 1X phosphate buffer solution (PBS) and 5% non-fat dried milk for 45 minutes at room temperature and probed with rabbit polyclonal antibody against SOD2 (1:1000; Cell Signaling cat#13141), Phospho-AMPK α (Thr172)(1:1000; Cell Signaling cat#2531), AMPK α (1:1000; Cell Signaling cat #2532), Phospho-AKT (Thr308) (1:1000; Cell Signaling Cat #4056), Phospho-AKT (Ser473) (1:1000; Cell Signaling Cat #9271), AKT (1:1000; Cell Signaling Cat #9272), Phospho-AS160 (Ser588)(1:1000; Cell Signaling Cat #8730); AS160 (1:1000; Cell Signaling Cat #2670); LC3B (1:1000; Cell Signaling Cat #2775); SQSTM1/p62 (1:1000; Cell Signaling Cat #5114). Western blot for anti- β -actin (1:5000; Sigma-Aldrich Cat #A5441) or GAPDH (1:8000; Sigma-Aldrich Cat #G9545) was performed to ensure equal sample loading. The filter detection was performed by ChemiDoc Imaging System (Bio-Rad Laboratories, Hercules, CA, USA).

5.10 REAL TIME PCR ANALYSIS

Total RNA was isolated from the kidney or cells using TRIzol Reagent (Bio-Rad Laboratories, Hercules, CA, USA). cDNA was obtained using High-Capacity cDNA Reverse Transcription Kit from 8 μ g total RNA. PCRs were performed with a Bio-Rad CFX96 Connect Real-time PCR System instrument and software. PCR conditions were 15 min at 95 °C followed by 40 cycles of two-step PCR denaturation at 94°C for 15 s, annealing extension at 55°C for 30 s and extension at 72°C for 30 s. Each sample contained 500 ng cDNA in 2X QuantiTect SYBR Green PCR Master Mix and

primers pairs to amplify collagen type I alpha 1 chain (*Col1a1*), collagen type III alpha 1 chain (*Col3a1*), collagen type IV alpha 1 chain (*Col4a1*), fibronectin 1 (*Fn1*), fibrillin-1(*Fbn1*) EGF-like module containing mucin like hormone receptor like 1(*Emr1*), also known as F4/80, interleukin (IL)-1 β (*Il1b*), IL-6 (*Il6*), tumor necrosis factor alpha (*Tnfa*) transforming growth factor beta 1 (*Tgfb1*), interferon gamma (*Ifng*), chemokine (C-C motif) ligand 2 is also referred to as monocyte chemoattractant protein (MCP)1 (*Ccl2*), chymase 1, mast cell (*Cma1*), tryptase beta-2 (*Tpsb2*), cluster of differentiation 36 (*Cd36*), toll like receptor 4 (*Tlr4*), nuclear factor kappa B Subunit 1 (*Nfkb1*), Peroxisome Proliferator Activated Receptor Alpha (*Ppara*), transient receptor potential cation channel subfamily V Member 1 (*Trpv1*), adiponectin (*AdipoQ*), meteorin-like protein (*Metrn1*) (Qiagen, Hilden, Germany), Kidney injury molecule (KIM)-1 (*Havcr1*) and Neutrophil gelatinase-associated lipocalin (NGAL) (*Lcn2*) in a final volume of 50 μ l. The relative amount of each studied mRNA was normalized to GAPDH or 18s as a housekeeping gene, and data were analysed according to the $2^{-\Delta\Delta CT}$ method.

5.11 ROS ASSAY

An appropriate volume of freshly prepared kidney tissue homogenate was diluted in 100 mM potassium phosphate buffer (pH 7.4) and incubated with a final concentration of 5 μ M dichlorofluorescein diacetate (Sigma–Aldrich) in dimethyl sulfoxide for 15 min at 37°C. The dye-loaded samples were centrifuged at 12 500 \times g for 10 min at 4°C. The pellet was mixed at ice-cold temperatures in 5 mL of 100 mM potassium phosphate buffer (pH

7.4) and incubated for 60 min at 37°C. The fluorescence measurements were performed with an HTS-7000 Plus plate reader spectrofluorometer (Perkin Elmer, Wellesley, MA, USA) at 488 nm for excitation and 525 nm for emission wavelengths. ROS was quantified from the dichlorofluorescein standard curve in dimethyl sulfoxide (0–1 mM).

5.12 LIPIDOMIC PROFILE

Metabolite extraction

Metabolite extraction was accomplished by fractionating the cardiac tissue samples into pools of species with similar physicochemical properties, using appropriate combinations of organic solvents. The following methods were used according to the target analytes' chemical class:

Proteins were precipitated by adding H₂O (15:1, v/w), methanol containing the internal standards used for platform 1 (50:1, v/w), chloroform: methanol (2:1) containing internal standards used for platform 2 (4:1, v/w) and chloroform (40:1, v/w) to the cardiac tissue (50 mg). The homogenization of the resulting mixture was then performed using a Precellys 24 homogenizer at 6500 rpm for 35 seconds x 2 rounds. Samples were incubated at -20°C for 1 hour, and after vortexing them, 500 µl were collected for each platform:

- Platform 1: Fatty acyls, steroids and lysoglycerophospholipids profiling Supernatants were collected after centrifugation at 18,000 x g for 15 minutes at 4°C, dried under vacuum, reconstituted in

methanol, and resuspended with agitation for 20 minutes. Samples were then centrifuged at 18,000 x g for 5 minutes at 4°C and were transferred to plates for UHPLC-MS analysis.

- Platform 2: cholesteryl esters, sphingolipids and glycerophospholipids profiling. Samples were mixed 100µl water, vortexed and incubated for 10 minutes at 4°C. After centrifugation at 18,000 x g for 5 minutes at 4°C; the organic phase was collected and dried under vacuum. Dried extracts were then reconstituted in acetonitrile/isopropanol (1:1), resuspended with agitation for 10 minutes, centrifuged at 18,000 x g for 5 minutes at 4°C, and transferred to plates for UHPLC-MS analysis.

Additionally, different types of quality control (QC) samples were used to assess the data quality¹:

- QC calibration sample: It is a pool of all samples used to correct the different response factors between and within batches. These samples are extracted and analyzed simultaneously as individual samples.
- QC Validation sample: It is a reference liver sample used to assess how well the data pre-processing procedure improved the data quality. As in the case of the QC calibration sample, these samples were extracted and analyzed at the same time as the individual samples.
- QC blank sample: It is a blank sample with extraction performed for biological samples.
- QC system suitability blank: It is a blank sample of the solvents in which biological samples are reconstituted.

For each analytical platform, randomized sample injections were performed, with each QC calibration and validation extract uniformly interspersed throughout the entire batch run.

LC-MS analysis

Mass spectrometry coupled to ultra-high performance liquid chromatography (UHPLC-MS) is well suited to metabolic profiling analyses due to its high sensitivity, large coverage over different classes of metabolites, high throughput capacity, and wide dynamic range. Two UHPLC-MS methods were used for each platform to analyze the lipidome of mouse cardiac tissue samples. Chromatographic separation and mass spectrometric detection conditions employed are summarized in Table 5.1. The overall quality of the analysis procedure was monitored using repeat extracts of the QC samples. Retention time stability throughout the run is generally < 6 s variation (injection-to-injection), and mass accuracy is generally < 5 ppm for m/z 400-1000 and < 1.2 mDa for m/z 50- 400.

	Platform 1	Platform 2
Column type	UPLC BEH C18, 1.0 x 100 mm, 1.7 μ m	UPLC BEH C18, 1.7 μ m 2.1x100mm
Flow rate	0.14 ml/min	0.40 ml/min
Solvent A	H ₂ O + 0.05% Formic Acid	H ₂ O:ACN (2:3) + 10mM Ammonium Formate
Solvent B	ACN + 0.05% Formic Acid	ACN:IPA (1:9) + 10mM Ammonium Formate
(%B), time	0%, 0 min	40%, 0 min
(%B), time	50%, 2 min	100%, 10 min
(%B), time	100%, 13 min	40%, 15 min
(%B), time	0%, 18 min	
Column temperature	40 °C	60 °C
Injection volume	2 μ l	1 μ l
Source temperature	120 °C	120 °C
Nebulization N₂ flow	600 l / hour	1000 l / hour
Nebulization N₂ temperature	350 °C	500 °C
Cone N₂ flow	30 l / hour	30 l / hour
Capillary voltage	2.8 kV	3.2 kV
Cone voltage	50 V	30 V

Table 5.1 UHPLC-MS analysis methods

IN VITRO STUDIES

5.13 CELL CULTURE AND TREATMENT

The human proximal tubular cell line (HK-2 cells) was obtained from ATCC (Manassas, VA). HK-2 cells were grown in (Dulbecco's Modified Eagle Medium) DMEM 1.0 g/L glucose supplemented with 10% FBS, penicillin (100 U/ mL) and streptomycin (100 mg/mL) and maintained at 37 °C in a 5% CO₂ incubator. All cultures used in the experiment were between passages 22 and 30. When cells reached 60–70% of confluence, the medium was replaced with 2% FBS in DMEM, and the cells were stimulated. To determine the gene expression of inflammatory and fibrotic markers, HK-2 cells were incubated with the selective PPAR- α antagonist GW6471 (4 μ M) in 0.1% DMSO for 30 min before the 12h pre-treatment with OEA (5 μ M) and then stimulated with TGF- β 1 (10 ng/mL)

for 24 h. While to better estimate protein phosphorylation of SMAD3, ERK and p38 pathways, the cells were incubated with GW6471 (4 μ M) for 30 min before the 1h pre-treatment with OEA (5 μ M) and then stimulated with TGF- β 1 (10 ng/mL) for 30 minutes. At the end of the stimulation period, the cells were lysed. Before lysis, cell morphology was assessed to evaluate the epithelial appearance and an elongated and spindle-shaped morphology.

5.14 ASSESSMENT OF CELL VIABILITY

Cell viability was analyzed using the MTT assay. This is a colorimetric metabolic activity assay that allows us to evaluate cell viability and that uses a salt called 3-[4,5-dimethylthiazol-2-yl]-2,5 diphenyl tetrazolium bromide (MTT) that has a yellow color when it is dissolved in buffer solutions or in a culture medium without phenol red and is capable of penetrating the living cell and being metabolized in the mitochondria, producing a color change. Inside the mitochondria, the MTT compound will be reduced by the NAD(P)H-dependent cellular oxidoreductase (or dehydrogenase) enzymes, which remove the tetrazolium ring and form an insoluble, purple crystal called formazan, which will be measured spectrophotometrically at a wavelength of 550 nanometers (nm). The principle of this simple, precise, and reproducible test is that in the vital cell, the mitochondrial activity is constant, such that a variation in the number of vital cells regulates in linear proportion the mitochondrial activity [van Meerloo et al., 2011]. Therefore, an increase in the number of living cells implies an increase in the amount of MTT metabolized by dehydrogenases in mitochondria.

This assay was carried out to determine if OEA affects the mitochondrial activity of HK-2 cells. Were seeded 10,000 HK-2 cells in 0.32 cm² wells of 96-well culture plates (cell density 46,875 cells/cm²) and incubated at 37 °C and 5% CO₂ for 24 hours. After incubation, washes were performed with a volume of 100 µl of 2% FBS DMEM culture medium for 6 hours. After the serum deprivation process, the DMEM culture medium was removed, and the treatment was carried out for 24 hours with the 1 mM and 30 ng/mL doses of OEA. Four hours before the end of OEA treatment, 25 µl of MTT was added at a concentration of 5 mg/mL. When the treatment ended, 100 µl of the solubilizing agent was added, containing sodium dodecyl sulfate (SDS), which is necessary to lyse cells, dissolve the formazan crystals, and estimate the amount of MTT metabolized. It was incubated at 37°C and 5% CO₂ for 24 hours to subsequently read the absorbance at 550 nm using a microplate reader (Multiskan go, Thermo Scientific). The results were expressed as a percentage of the mean of control cell values.

5.15 PROTEIN AND MRNA DETERMINATIONS

Hk-2 cells were lysed, and total protein lysates were undergone to SDS-PAGE, as described above. The filter was then probed with rabbit polyclonal antibody against Phospho-p38 MAPK (Thr180-Tyr182) XP[®] (1:1000; Cell Signaling cat#4511), p38 MAPK XP[®] (1:1000; Cell Signaling cat #8690), Phospho-p44/42 MAPK (Erk1/2) (Thr202/Tyr204) (1:1000; Cell Signaling Cat #9101), p44/42 MAPK (Erk1/2) (1:1000; Cell Signaling Cat #9102), Phospho-Smad3 (Ser423/425) (1:1000; Cell Signaling Cat #9520), Smad3 (1:1000; Cell Signaling Cat #9523). Western blot for anti-β-actin (1:5000; Sigma-Aldrich Cat #A5441) was performed to ensure equal sample loading.

The detection of the filter was performed by ChemiDoc Imaging System (Bio-Rad Laboratories, Hercules, CA, USA).

Total RNA, isolated from the Hk2 cells, was extracted using TRIzol Reagent (Bio-Rad Laboratories, Hercules, CA, USA). cDNA was obtained using High-Capacity cDNA Reverse Transcription Kit from 2 µg total RNA. PCRs were performed with a Bio-Rad CFX96 Connect Real-time PCR System instrument and software. PCR conditions were 15 min at 95 °C followed by 40 cycles of two-step PCR denaturation at 94°C for 15 s, annealing extension at 55°C for 30 s and extension at 72°C for 30 s. Each sample contained 500 ng cDNA in 2X QuantiTect SYBR Green PCR Master Mix and primers pairs to amplify Collagen Type IV Alpha 1 Chain (*Col4a1*), Fibronectin 1 (*Fn1*), Interleukin-1β (*Il1b*), chemokine (C-C motif) ligand 2 is also referred to as monocyte chemoattractant protein (MCP)1 (*Ccl2*), (Qiagen, Hilden, Germany), in a final volume of 50 µl. The relative amount of each studied mRNA was normalized to 18s ribosomal subunit as a housekeeping gene, and data were analysed according to the $2^{-\Delta\Delta CT}$ method.

5.16 DATA AND STATISTICAL ANALYSIS

Data are presented as means ± SEM and subjected to one-way variance analysis (ANOVA) for multiple comparisons followed by Bonferroni's post hoc test, using GraphPad Prism 8 (GraphPad Software, San Diego, CA, USA). Differences among groups were considered significant at values of $p < 0.05$.

6. RESULTS

6.1 OEA LIMITS METABOLIC IMPAIRMENT RELATED TO HFD-INDUCED OBESITY

EFFECT OF OEA ON CARDIOMETABOLIC ALTERATION RELATED TO OBESITY

6.1.1 OEA COUNTERACTS METABOLIC ALTERATION INDUCED BY HFD IN MICE

To investigate the effect of OEA on obesity, we fed C57BL/6J mice with an HFD for 12 weeks to acclimatize the obese phenotype. Then mice were treated with OEA for eight weeks along with HFD feeding. The body weight of animals from all groups was evaluated weekly throughout treatment, starting 12 weeks after HFD feeding. As expected, the HFD group showed a higher body weight gain than that of mice on the STD diet (Fig 6.1A and B). OEA gradually and significantly reduced body weight (Fig 6.1 A) and weight gain (Fig 6.1 B) compared to untreated HFD mice. The body weight data were also analyzed as the area under the curve (AUC) of body weight recorded throughout the treatment period. Consistently, obese mice showed a significant increase in AUC of body weight and weight gain that was markedly reduced in the OEA group.

Long-term HFD consumption caused an increase in food intake that was significantly reduced in OEA-treated mice, consistent with the literature (Hansen et al., 2009; Kleberg et al., 2014) (Fig.6.1 C). At the end of the experimental period, HFD mice showed a significant increase in serum cholesterol levels (Fig.6.1 D), markedly reduced in OEA-treated mice. Moreover, to assess the effect of OEA on body composition for fat mass

estimation, bioelectrical impedance analysis (BIA) was conducted on all mice of each group. The increased fat mass shown by HFD mice was reduced in OEA-treated mice (Fig 6.1 E).

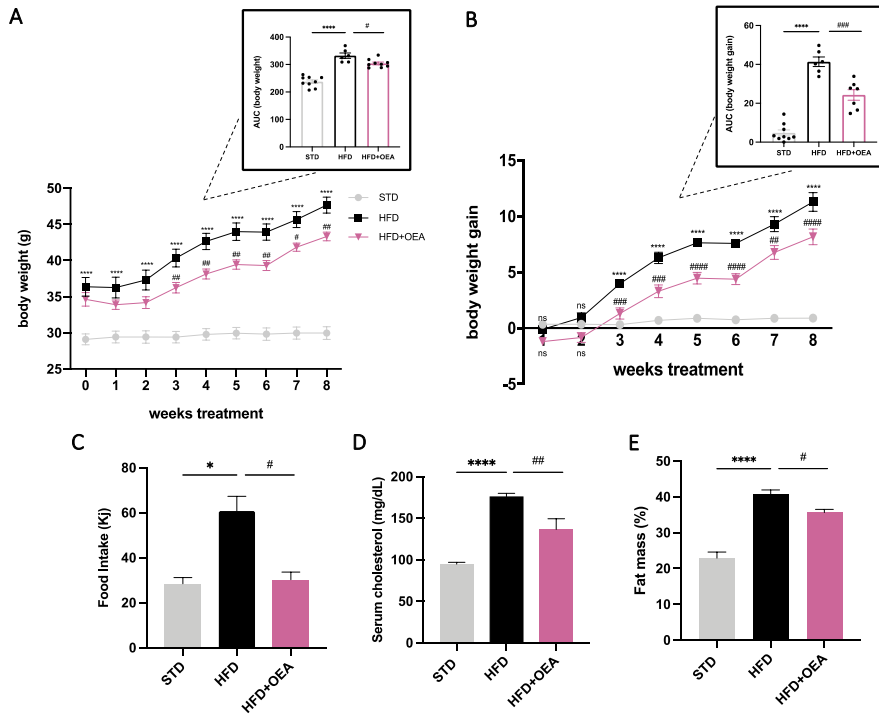


Fig 6.1 OEA treatment regains metabolic parameters altered by HFD. Body weight was measured weekly during the treatment period. OEA markedly decreases body weight (A) and weight gain (B), significantly increasing in HFD mice. Similar results were obtained by evaluating the respective AUCs. Moreover, OEA reduced food intake, expressed in Kilojoule (Kj) (C), serum cholesterol (D) and fat mass (E). Results are shown as mean \pm S.E.M (* P <0,05 and **** P <0,0001 vs STD; # P <0,05, ## P <0,01, ### P <0.001, and #### P <0,0001 vs HFD).

6.1.2 OEA AMELIORATES GLUCOSE HOMEOSTASIS IN OBESE MICE

To characterize the metabolic phenotype and to specifically assess alterations in glucose metabolism, we performed the OGTT (Fig. 6.2). In

the STD group, the peak of the blood glucose level of approximately 200 mg/dL was reached around 30 min after glucose administration and immediately followed by a decrease towards the baseline level indicating proper glucose disposal. In contrast, glycaemia of HFD mice peaked at approximately 300 mg/dL and showed weak glucose disposal during the time. As expected, HFD feeding markedly increased glycemic levels over time while OEA treatment ameliorates glucose disposal, improving glucose homeostasis (Fig 6.2A). OEA markedly decreased fasting glycemic levels, incremented by HFD (Fig. 6.2B). Similar data were obtained considering the AUC measured from all animals of the groups (fig. 6.2B).

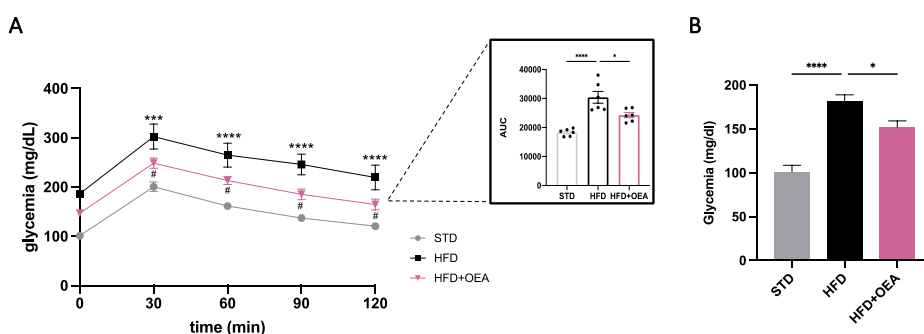


Fig 6.2 OEA ameliorates glucose disposal in obese mice. Before sacrifice, OGTT was performed in all groups of animals (A). Glucose levels in fasted mice are also shown (B). Results are shown as mean \pm S.E.M (* $P < 0,05$ and **** $P < 0,0001$ vs STD; # $P < 0,05$ vs HFD).

6.1.3 OEA BALANCES THE ALTERATION OF METABOLIC MEDIATORS IN THE HEART

The detrimental increase of fatty acids induced by HFD leads to the dysregulated secretion of adipokines, resulting in maladaptive

mechanisms in the heart that cannot counteract the metabolic alterations. So, to evaluate the OEA impact on the heart ventricle, we examined the gene transcription of two pivotal adipokines: adiponectin and meteorin-like. In figure 6.3 A-B, we showed that in HFD mice, there was a compensatory protective mechanism to counteract myocardial dysfunction related to increased transcripts of these adipokines, whose levels were normalized following OEA treatment.

As known, in cardiomyocytes, the fatty acids flux is mainly regulated by the fatty acid translocase CD36. To define the involvement of OEA in lipid metabolism, we determined the mRNA expression of CD36. Indeed, its overexpression in the ventricles of HFD-fed mice suggests an excessive lipid accumulation that was instead downregulated in OEA-treated mice (Fig. 6.3 C).

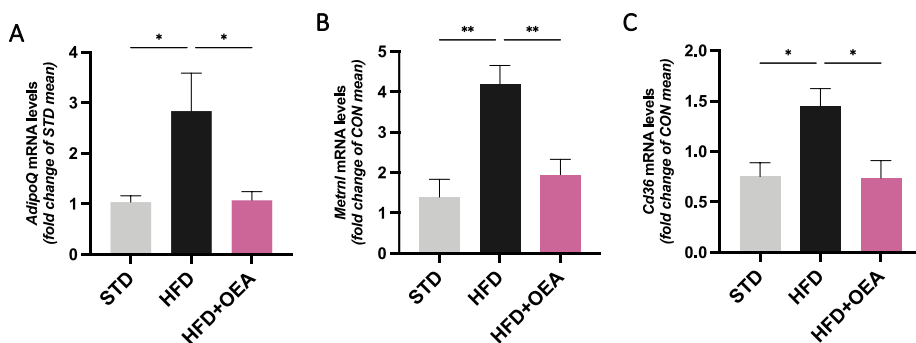
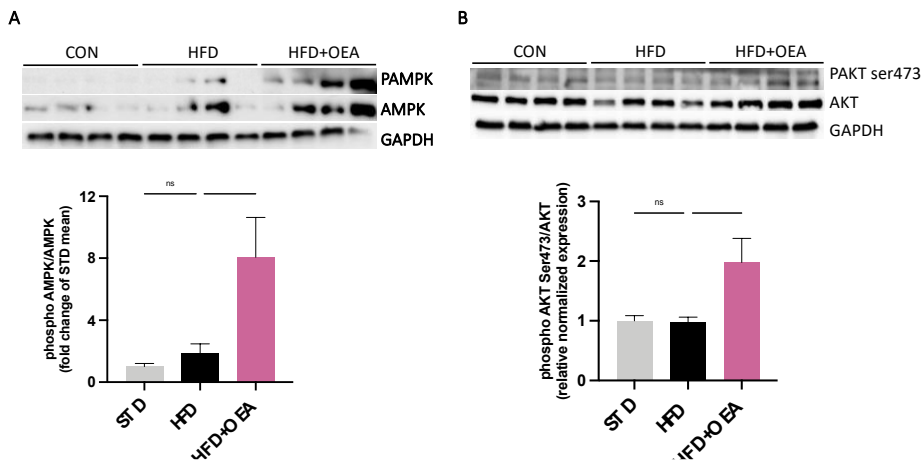


Fig 6.3 OEA normalized the expression of cardiac metabolic mediators up-regulated by HFD. OEA treatment reduced the gene expression of the cardiac adipokines adiponectin (*AdipoQ*) (A) and meteorin-like protein (*Metrnl*) (B), and the fatty acid transporter CD36 (C), which were overexpressed in HFD mice. Results are shown as mean \pm S.E.M (* $P<0,05$ and ** $P<0,01$).

6.1.4 OEA INCREASES MYOCARDIAL GLUCOSE UPTAKE ACTIVATING AMPK-AKT-AS160 SIGNALLING

To define the OEA effect on cardiac energy metabolism, we evaluated the expression of the phosphorylated AMPK and AKT. The activation of cardiac AMPK was induced by OEA, indicating an improvement in glucose and lipid homeostasis (Fig. 6.4 A). Moreover, OEA increased the phosphorylation of the Ser473 and Thr308, sites related to the activation of AKT, which plays a key role in maintaining the physiological cardiac function (Fig 6.4 B-C). Besides, the activation of AMPK and AKT converges towards As160 phosphorylation, a kinase involved in translocating the glucose transporter (GLUT) 4 to the cardiomyocyte membrane. HFD determined a significant reduction in the phosphorylation of AS160 in the ventricles of obese mice compared to STD ones, while OEA treatment restored As160 activation (Fig. 6.4 D). These results suggest that OEA treatment determines an improvement in glucose metabolism.



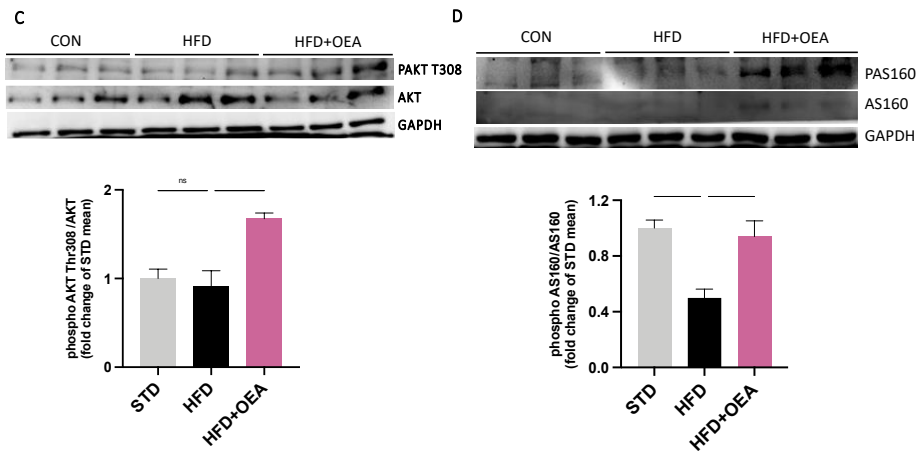


Fig 6.4 OEA induces the activation of AMPK-AKT-AS160 pathways. Phosphorylation of AMPK (A), AKT serine 473 (B), AKT threonine 308 (C) and AS160 (D) was detected in cardiac ventricles. OEA was able to increase the activation of the pathway. Results are shown as mean \pm S.E.M (* $P < 0,05$ and ** $P < 0,01$).

6.1.5 OEA EFFECTS ON LIPID PROFILE IN OBESE MICE

Lipid accumulation in the heart has been observed under elevated plasma-free fatty acids, such as in obesity, type 2 diabetes mellitus and chronic high-fat feeding [Dirkx et al., 2011]. To better explore the impact of OEA treatment on cardiac lipid profile in HFD-induced obesity, a lipidomic study was conducted on the whole lipid composition of the heart following the eight-week daily treatment of OEA.

OEA is an endogenous metabolite belonging to the NAE family, and thus, it is constitutively synthesized at the cardiac level and, as expected, OEA was considerably increased, as well as all NAEs, in mice receiving its chronic treatment (Fig. 6.5 A-B). We found that OEA induced a significant reduction in cardiac saturated triacylglyceride content (Fig. 6.5 C) and

limited the accumulation of cholesteryl ester (ChoE) (Fig. 6.5 D), lipids that were increased by HFD in obese mice.

Moreover, the ratio of fatty acid 18:3 (linoleic acid) and 18:2 (γ -linoleic acid) was higher in obese mice and significantly decreased in OEA-treated mice (Fig. 6.5 E). As known, this ratio represents an index of the activation of Δ -6-desaturase (D6D) that catalyzes the endogenous synthesis of long-chain PUFA from the essential fatty acids. Likewise, the ratio among arachidonic acid (AA), that is, a polyunsaturated ω -6 fatty acid 20:4(ω -6), and its saturated counterpart, namely the arachidic acid 22:4(ω -6), was increased in OEA-treated mice (Fig. 6.5 F). HFD-mediated dysregulation of sphingomyelin (SM) metabolism contributes to obesity-related cardiovascular disease [Xu et al., 2013]. SMs are structural components of membranes and have been linked to insulin resistance, oxidative stress, inflammation, and cardiac steatosis. The marked decrease in the SM pool in obese mice, compared to the STD group, was blunted in OEA-treated mice (Fig. 6.5 G-I).

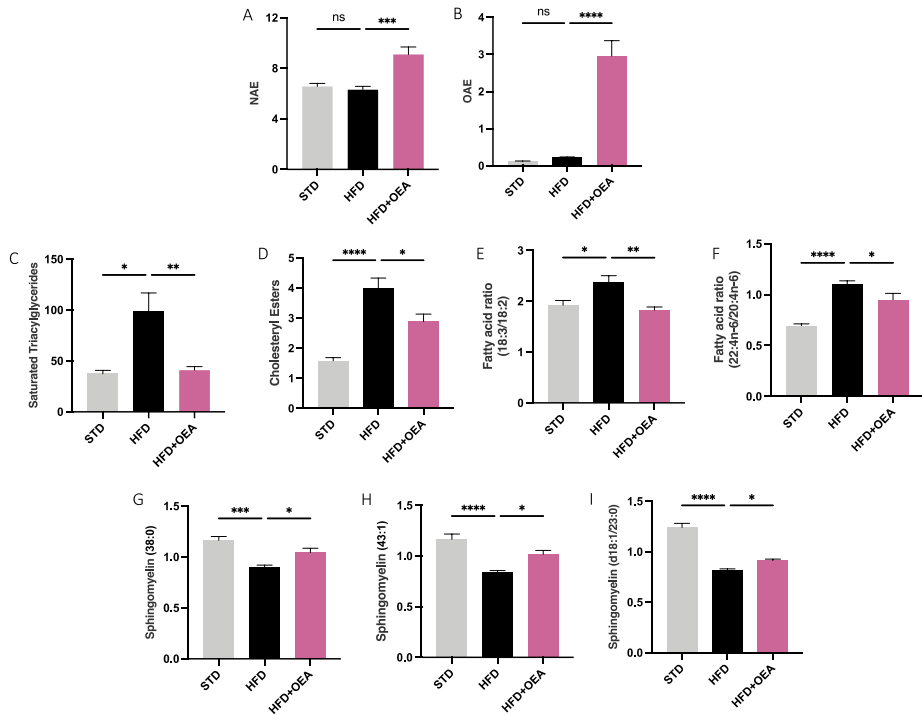


Fig 6.5 OEA affects the levels of several lipids in cardiac tissues of obese mice. Chronic OEA treatment increased NAE levels (A) and OEA (B) in cardiac tissue. OEA decreases the content of saturated triglyceride content (C) and Cholesteryl Esters (D) in the heart. OEA normalized the ratio of fatty acid (18:3/18:2) (E) and fatty acid (22:4n-6/20:4n-6) (F) in the cardiac tissues of obese mice. Additionally, OEA significantly increased the content of sphingomyelin 38:0 (G), 43:1 (H) and d18:1/23:0 (I). Results are shown as mean \pm S.E.M (* P <0,05, ** P <0,01, *** P <0,001, and **** P <0,0001).

6.1.6 OEA LIMITS INFLAMMATORY AND FIBROSIS IN CARDIAC TISSUE

Low-grade chronic inflammation has been indicated as a detrimental process in obesity-induced cardiac dysfunction [Zhang et al., 2020]. HFD leads to increased production of inflammatory cytokines and chemokines, namely IL-1, IL-6 and (MCP)-1, that predispose to myocardial fibrosis and cardiac remodelling. OEA showed a marked anti-inflammatory effect in

the ventricle by reducing the transcription of such pro-inflammatory mediators involved in the damage progression (Fig. 6.6 A-C).

To determine OEA involvement in heart fibrosis, we evaluated the gene expression of pro-fibrotic markers, such as TGF- β 1 and the core components of the extracellular cardiac matrix, fibrillin and collagenase III. OEA treatment limited the detrimental increased transcription of these pro-fibrotic parameters induced by long-term HFD feeding (Fig. 6.6 D-F).

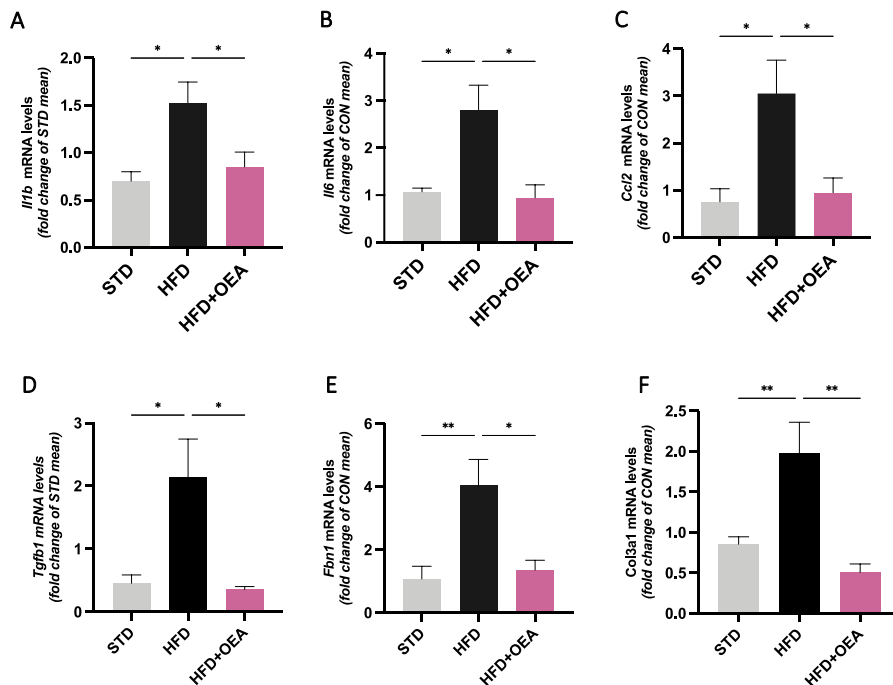


Fig 6.6 OEA reduced cardiac proinflammatory and profibrotic mediators increased in obese mice. Gene expression of cytokines, Il1b (A), Il6 (B) and Ccl2 (C) associated with fibrotic parameters, such as Tgfb1, Fbn1 and Col31a1 were markedly increased in HFD mice compared to the STD group and reduced by OEA treatment. Results are shown as mean \pm S.E.M (*P<0,05 and **P<0,01).

6.1.7 OEA INVOLVEMENT IN CARDIOMYOCYTE AUTOPHAGOSOME FORMATION

It has been reported that autophagy is decreased in metabolic disorders like obesity, leading to the aggregation of proteins and the presence of dysfunctional organelles contributing to the pathogenesis of cardiometabolic diseases [Zhang et al., 2019]. To define the effect of OEA in autophagosome formation, we determine cardiac LC3II protein level, an autophagosome membrane marker of autophagy. The ratio between isoform II and I of LC3B in the ventricle was markedly increased by OEA treatment (Fig. 6.7 A). In addition, to clarify the effect of OEA on the autophagic flux, we examined the expression of autophagy adaptor protein p62/SQSTM1 that was reduced in OEA-treated mice (Fig. 6.6 B). So, these results confirmed OEA's capability in stimulating autophagy.

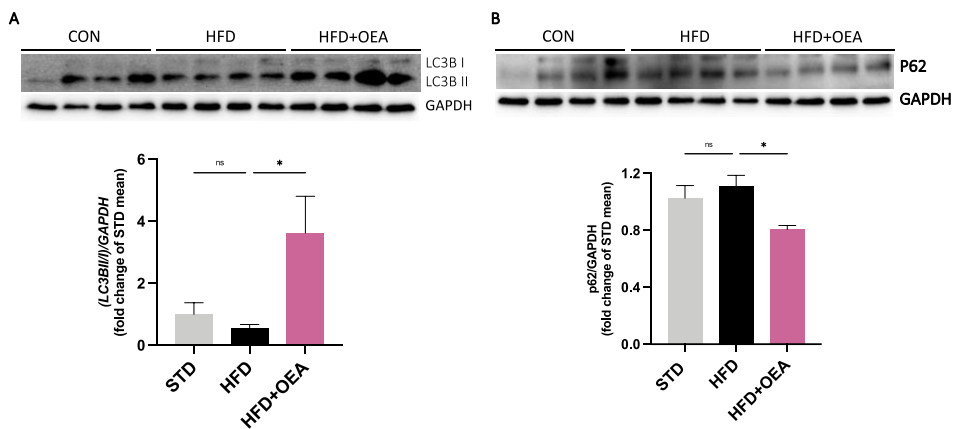


Fig 6.7 OEA affects autophagosome formation. OEA treatment modulates the protein expression of the autophagosome membrane markers of autophagy LC3II/I, increasing their ratio and decreasing the cardiac level of p62/SQSTM1, an autophagy adaptor protein. Results are shown as mean \pm S.E.M (* P <0,05).

EFFECTS OF OEA ON RENAL ALTERATION RELATED TO OBESITY

6.1.8 OEA RECOVERS KIDNEY FUNCTION PERTURBED IN OBESE MICE

Mice were individually housed in metabolic cages for 24 h to assess water intake and to collect urine. Long-term HFD feeding determined an alteration of kidney function resulting in reduced water intake and urine output, while OEA restored these parameters (Fig. 6.8 A-B). In addition, we investigated the main serum parameters of kidney function, namely serum creatinine and BUN. Creatinine level was increased in HFD-fed mice compared to the STD group and was lowered by OEA treatment (Fig. 6.8 C). Consistently, BUN levels were significantly lower in OEA-treated mice than in HFD ones (Fig. 6.8 D).

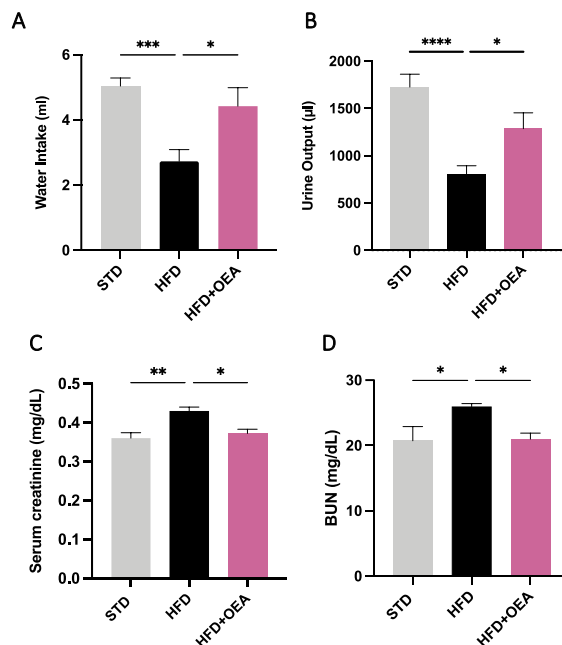


Fig 6.8 OEA treatment preserves kidney function altered by HFD. At the end of the experimental period, mice were placed in metabolic cages to assess water intake (A) and urine output (B). Serum levels of kidney function markers, creatinine (C) and BUN (D) were evaluated. OEA normalized the expression of

these parameters. Results are shown as mean \pm S.E.M (* $P < 0,05$ and ** $P < 0,01$, *** $P < 0,001$, and **** $P < 0,0001$).

6.1.9 OEA LIMITS INFLAMMATION AND FIBROSIS INDUCED BY HFD

The chronic low-grade inflammation observed in obesity induced the activation of the pro-inflammatory cascade, leading to inflammatory cell secretion of many cytokines and chemokines and the production of profibrotic mediators that, along with excessive deposition of extracellular matrix, contribute to renal fibrosis [Decl`ves et al., 2011; Kim et al., 2019]. To evaluate the effect of OEA on renal cell recruitment and inflammation in response to HFD, we measured mRNA expression of IL-1 β (Fig.6.9 A), IL-6 (Fig.6.9 B), TNF α (Fig.6.9 C), monocyte chemoattractant protein (MCP)-1 (Fig.6.9 D) and macrophage marker F4/80 (Fig.6.9 E) in the kidney. RT-qPCR results confirmed that the gene expression levels of these markers were highly up-regulated in the kidney of HFD-fed mice and greatly reduced in mice treated with OEA. Moreover, HFD feeding markedly induced the transcription of TLR4 and NF- κ B in kidney tissue compared to the STD group, while OEA treatment attenuated their induced expression (Fig. 6.9 F-G). Furthermore, we investigated the expression of TGF- β 1, which played a crucial role in the pathogenesis of renal fibrosis that resulted markedly increased in obese mice and significantly reduced in OEA-treated mice (Fig. 6.9 H). These data indicate that OEA exerted reno-protective effects, suppressing the inflammatory response.

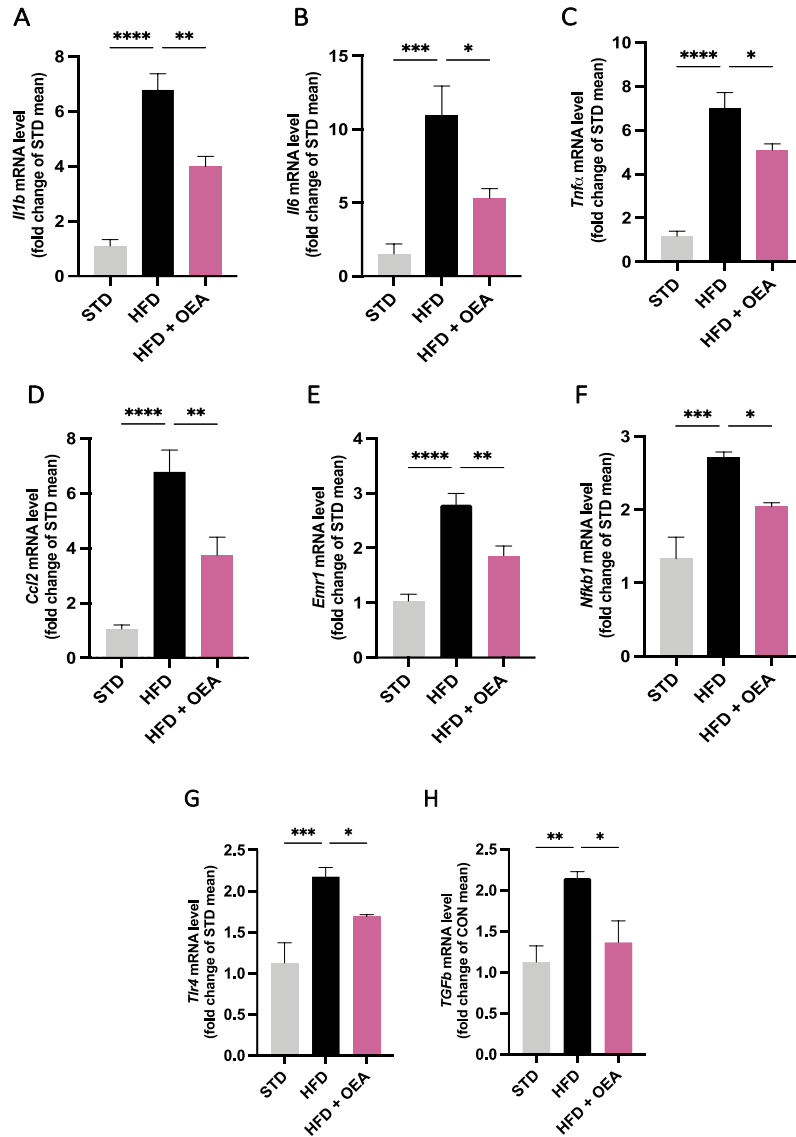


Fig 6.9 OEA moderates the inflammatory and fibrotic responses in obese mice. The increased mRNA expression of proinflammatory parameters *Il1b* (A), *Il6* (B), *Tnfα* (C), *Ccl2* (D), *Emr1* (E), *NFkb1* (F), *Tlr4* (G) and *Tgfb1* (H) found in the HFD-fed mice, was markedly reduced by OEA treatment. Results are shown as mean \pm S.E.M (* P <0,05, ** P <0,01, *** P <0,001 and **** P <0,0001).

6.2 OEA COUNTERACTS FA-INDUCED RENAL DAMAGE IN MICE

6.2.1 OEA IMPROVES RENAL FUNCTION IMPAIRED BY FA

The injection of a high dose of FA induces a macroscopic reduction in kidney volume that appears visibly restored by OEA treatment (Fig 6.10 A). However, the kidney-to-body weight ratio remains unchanged among the experimental groups (data not shown). Vehicle in the control group or OEA treatment alone did not affect kidney morphology.

Moreover, the detrimental FA challenge establishes increased water intake and urine excretion, which was reverted in OEA mice (Fig 6.10 B and C). FA-induced CKD was confirmed by increased renal function biomarkers, such as serum creatinine (Cr) and serum urea expressed as BUN [Zaghloul et al., 2019]. As shown in (Fig 6.10 D and E), kidney function was restored by the reduction of BUN concentration and serum creatinine level in mice treated with OEA.

To further determine the effect of OEA on kidney function, 24hr urinary albumin excretion and albumin to creatinine ratio (UACR) were measured in the urine at the time of sacrifice. OEA significantly increased the 24-hour urinary albumin excretion (Fig 6.10 F) and UACR (Fig 6.10 G) in FA-injured mice.

To better define the renoprotective effect of OEA, real-time PCR was performed to identify tubular injury markers, i.e kidney injury molecule-1 (KIM-1) (Fig 6.10 H) and neutrophil gelatinase-associated lipocalin (NGAL) (Fig 6.10 I), which resulted increased after kidney injury and restored by OEA treatment.

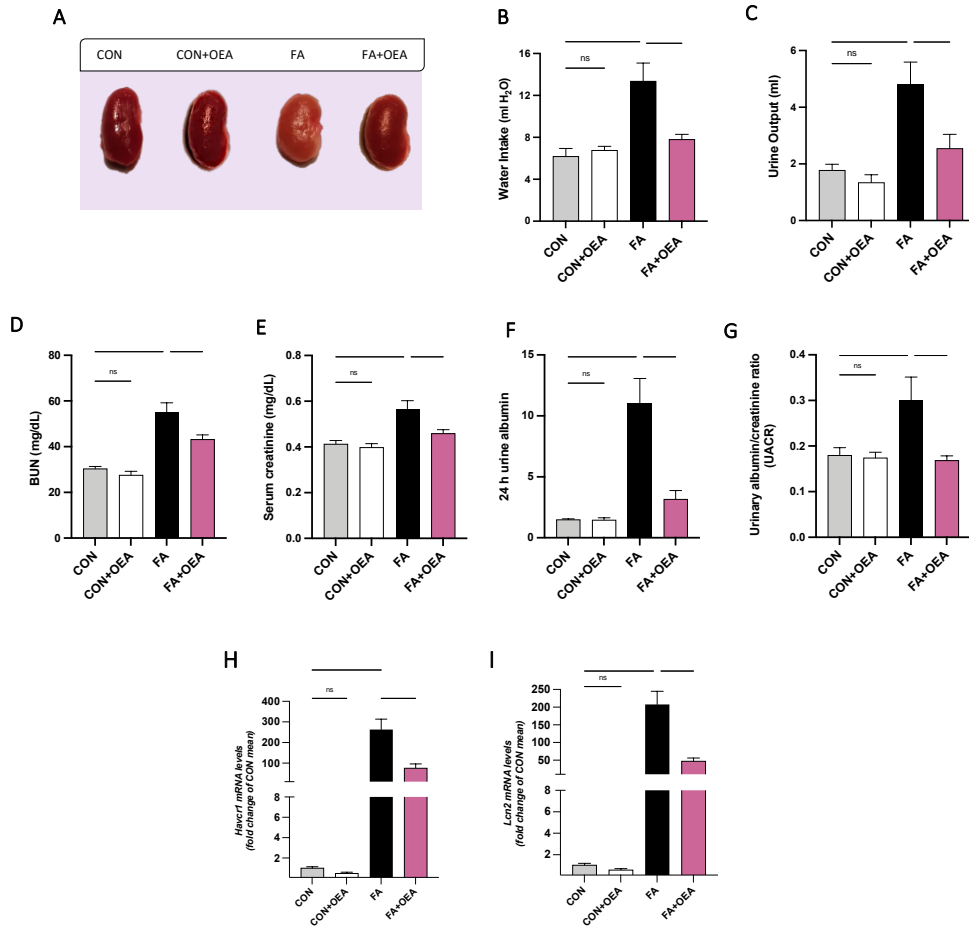


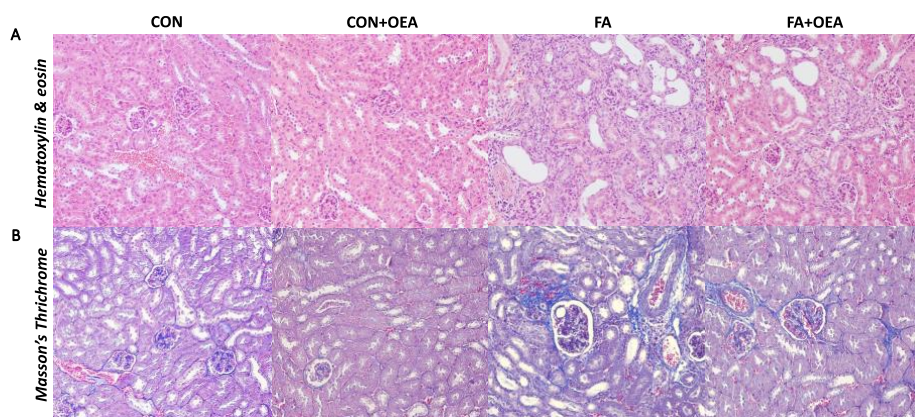
Fig 6.10 Effects of OEA treatment on *in vivo* parameters of FA-insulted mice. OEA restored the normal volume of the kidney, which was shrunk as a result of the damage by FA (A), water intake (B) and urine output (C). Renal function parameters, BUN (D), serum creatinine (E), 24h urine albumin (F) and urinary albumin to creatinine ratio (G) were also evaluated. mRNA expression of molecular markers of tubular injury, KIM-1 (H) and NGAL (I) were determined in kidney tissue. Results are shown as mean \pm S.E.M (* $P < 0,05$, ** $P < 0,01$, *** $P < 0,001$ and **** $P < 0,0001$).

6.2.2 OEA ATTENUATES TUBULOINTERSTITIAL INJURY INDUCED BY FA

We next performed histological staining to confirm the alleviation of kidney injury after OEA treatment. The examination showed that FA

induced severe lesions in the TECs and interstitium through hematoxylin and eosin (H&E) staining lumen (Fig. 6.11 A) and Masson's Trichrome staining lumen (Fig. 6.11 B), including severe tubular epithelial cell necrosis, significant tubular dilation, lots of casts and a large number of inflammatory cells infiltration into the interstitium.

Statistical analysis showed a significantly higher percentage of epithelial vacuolization (Fig. 6.11 C), dilation of the tubular lumen (Fig. 6.11 D) and cast formation (Fig. 6.11 E) in the FA group than those detected in other groups ($P<0.05$), instead no statistically significant differences were observed between the control and OEA treated groups. In addition, mice insulted by FA and treated with OEA showed a substantial reduction in inflammation (Fig. 6.11 F), fibrosis (Fig. 6.11 G), and necrosis (Fig. 6.11 H) compared with the FA group. The results of the histological examination are summarized as a median value in table 6.1.



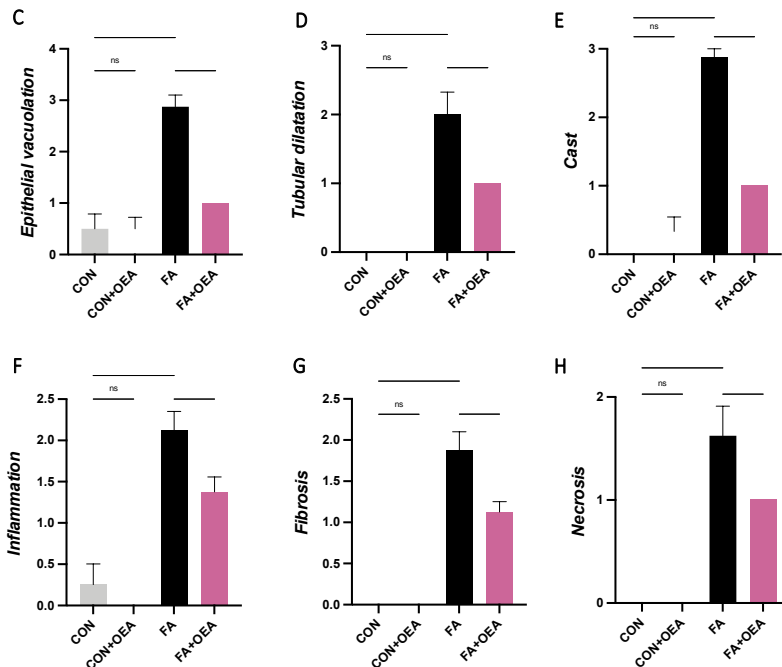


Fig 6.11 OEA mitigated pathological renal injury induced by FA. Representative photomicrographs of hematoxylin and eosin (HE) (A) and Masson’s Trichrome (B) stained kidney sections. FA damage caused a significant increase in epithelial vacuolization (C), necrosis (D), tubular dilatation (E), inflammation (F), cast (G) and fibrosis (H), which were restored by OEA treatment. Results are shown as mean \pm S.E.M (* P <0,05, ** P <0,01 and **** P <0,0001).

	Epithelial vacuolization*	Necrosis	Tubular dilatation*	Cast*	Inflammation*	Fibrosis*
CON	0,5	0	0	0	0	0
CON+OEA	0,5	0	0	0	0	0
FA	3	1	2	3	2	2
FA+OEA	1	1	1	1	1	1

Table 6.1 Median for each assess group (* p <0,05)

6.2.3 OEA INHIBITS PROINFLAMMATORY PARAMETERS AND CELL RECRUITMENT IN KIDNEY OF FA MICE

To investigate whether OEA exerts an anti-inflammatory effect, the inflammatory cell infiltration and pro-inflammatory cytokine expression in

the kidney tissues were analyzed using qRT-PCR. So, we evaluated the transcription of renal monocyte chemoattractant protein (MCP)-1 and macrophage marker F4/80, which play an important role in renal inflammation in several models of kidney injury. Gene expression of IL-1 β (Fig 6.12 A), IL-6 (Fig 6.12 B), TNF α (Fig 6.12 C) and Ccl2 (Fig 6.12 D) was significantly increased in FA animals compared to the control group and attenuated by OEA treatment. Moreover, renal RNA expression of IFN- γ and the macrophage marker Emr1 was increased in FA mice and significantly reduced by OEA treatment (Fig 6.12 E and F, respectively). Recent studies have found that mast cells (MCs) degranulation promotes the occurrence and progression of inflammation and fibrosis (Jiang et al., 2018). On this basis, we evaluated the gene transcription of Cma1 (Fig 6.12 G) and tpsb2 (Fig 6.12 H), whose increase in FA mice was blunted by OEA treatment. These data suggested that OEA reduces the inflammatory response as demonstrated by the reduction of macrophage infiltration, proinflammatory cytokine and mast cell activation in the kidney of FA mice.

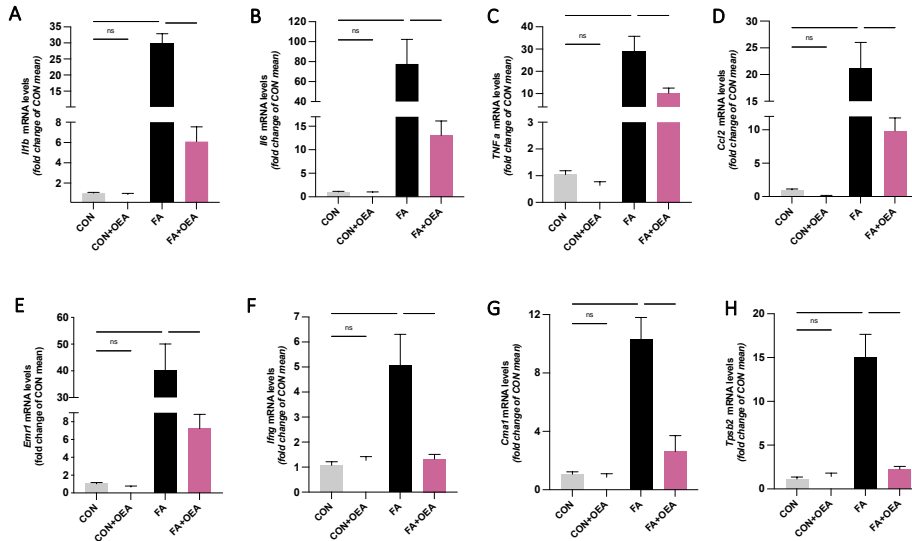


Fig 6.12 OEA prevents inflammatory responses induced by FA. Quantitative RT-PCR showed increased mRNA expression of cytokines, such as Il-1b (A), IL-6 (B), TNF α (C), MCP1(D), F4-80 (E) IFN γ (F) and mast cell markers, chymase 1 (G) and tryptase (H) in FA insulted mice that were significantly reduced by OEA treatment. Results are shown as mean \pm S.E.M (* P <0,05, ** P <0,01, *** P <0,001 and **** P <0,0001).

6.2.4 OEA SUPPRESSES RENAL FIBROTIC RESPONSE IN FA MICE

Renal fibrosis is a common feature of CKD in which tissue architecture is progressively replaced by type IV collagen and other extracellular matrix (ECM) proteins, such as fibronectin and collagen IV [Liu, 2011].

To elucidate the involvement of TGF- β 1 in the mechanism by which OEA limits renal fibrosis, we have also examined the mRNA expression of this factor. Indeed, TGF- β 1 acts as an important mediator in kidney disease, given its multiple functions in inflammation, cell growth, apoptosis, and differentiation. The increased expression of TGF- β 1 in FA mice was markedly reduced in OEA-treated mice (Fig. 6.13 A). These data show that OEA prevents the development of FA-induced renal fibrosis through the

inhibition of TGF- β 1 expression and extracellular matrix deposition. In addition, to further determine whether OEA was able to limit renal fibrosis, we evaluated its activity on the expression of Col4a1 and Fn1, two major constituents of ECM. According to previous findings, significant induction of both mRNAs was observed in the kidney of FA-treated animals compared with controls. Notably, the administration of OEA significantly inhibited gene transcription of both pro-fibrotic markers (Fig. 6.13 B and C).

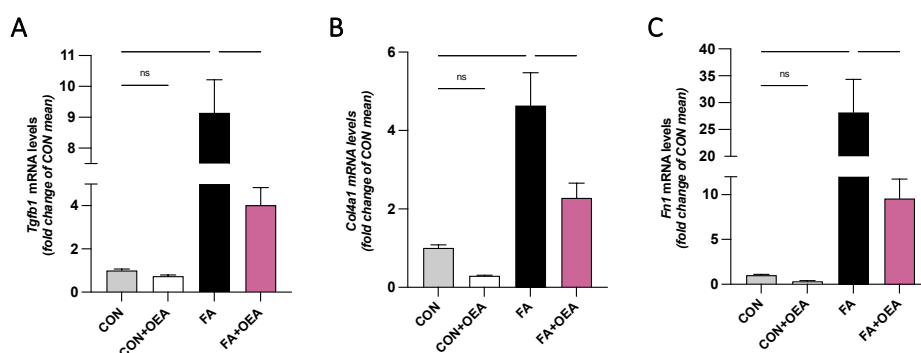


Fig 6.13 OEA inhibits the upregulation of TGF- β 1 and the extracellular matrix deposition in FA mice. Renal gene expression of Tgfb1 (A), Col4a1 (B) and Fn1 (C) was assessed by RT-PCR. OEA-treated FA mice showed a reduction of these parameters involved in renal fibrosis. Results are shown as mean \pm S.E.M (* P <0,05, ** P <0,01, *** P <0,001 and **** P <0,0001).

6.2.5 OEA COUNTERS OXIDATIVE STRESS RELATED TO FA-INDUCED KIDNEY DAMAGE

Due to the crosstalk among oxidative stress, inflammation, and fibrosis, leading to the progression of kidney disease, we evaluated the protein expression of the scavenger enzyme superoxide dismutase (SOD)2 evaluated in the kidney by Western Blot. OEA treatment recovered the reduction of the enzyme level induced by the FA challenge (Fig 6.14 A).

According to this result, we examined ROS levels in the kidney by a colorimetric assay. The significant increase in ROS kidneys from FA mice was blunted by OEA treatment (Fig 6.14 B).

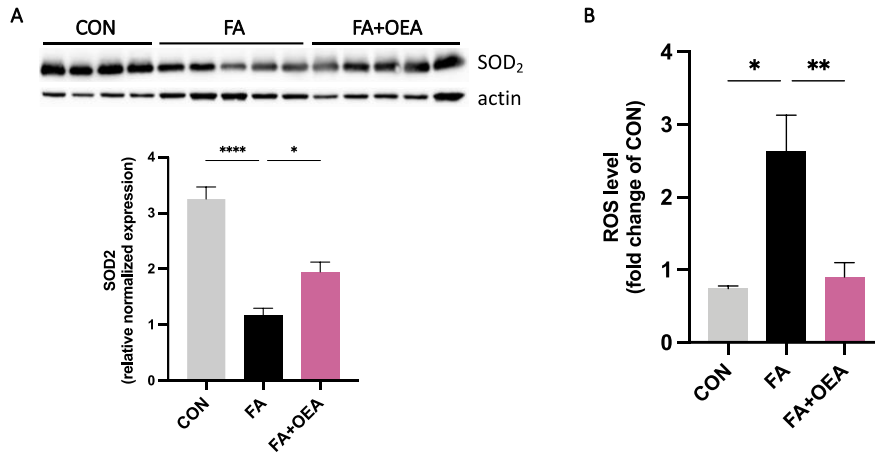


Fig 6.14 OEA limits oxidative stress in kidney of FA mice. OEA increased SOD2 protein expression (A), evaluated through Western Blot. Similar results were obtained measuring the renal ROS levels: FA mice showed a marked increase in ROS that was limited in OEA-treated mice. Results are shown as mean \pm S.E.M (* P <0,05, ** P <0,01 and **** P <0,0001).

6.2.6 EFFECTS OF OEA ON PPAR- α AND TRPV1 TRANSCRIPTION

To define the capability of OEA to affect the expression of its target receptors was evaluated the gene expression of kidney TRPV1 and PPAR- α .

TRPV1 hyperfunction contributes to renal tubular damage, as demonstrated by Lu et al. [2021]. Therefore, blunting TRPV1 transcription in OEA-treated mice attenuates nephropathy (Fig. 6.15 A).

Previous research has shown that PPAR- α induction protects renal hemodynamics in various models of renal damage [Gao et al., 2022]. OEA

treatment induced a considerable increase of PPAR- α mRNA in kidney tissue, indicating a renoprotective role (Fig. 6.15 B).

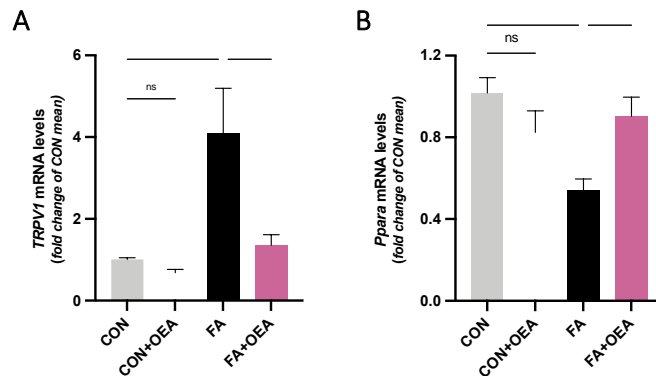


Fig 6.15 Effect of OEA on PPAR- α and TRPV1 transcription in kidney. The gene expression of *Trpv1* (A) and *Ppara* (B) was detected by RT-PCR. OEA downregulated TRPV1 transcription induced by FA. The expression of PPAR- α , reduced in FA mice, was significantly increased in OEA-treated FA mice. Results are shown as mean \pm S.E.M (* $P < 0,05$ and ** $P < 0,01$).

6.3 PPAR α INVOLVEMENT IN OEA RENO-PROTECTIVE EFFECTS

IN VIVO EXPERIMENTS

To investigate the mechanism of action of OEA, which is an endogenous ligand of PPAR- α , we employed mice that did not genetically express this receptor. For this purpose, many aspects investigated in the kidneys of wild-type (WT) C57/BL6J mice were respectively analyzed in PPAR- α null (KO) mice in the murine model of renal fibrosis induced by FA.

6.3.1 OEA FAILS IN RESTORING KIDNEY FUNCTION IN PPAR- α KO MICE

PPAR- α KO mice received a high dose injection of FA, resulting in kidney damage that appears milder when compared with WT mice (data not shown). The high dose of FA provoked a considerable reduction in water intake and increased urine excretion that was not reverted by OEA treatment (Fig 6.16 A-B).

Moreover, renal function was assessed by measuring BUN and serum creatinine levels. OEA treatment was unable to restore these markers that were significantly increased in FA-insulted mice compared with the control group (Fig 6.16 C-D).

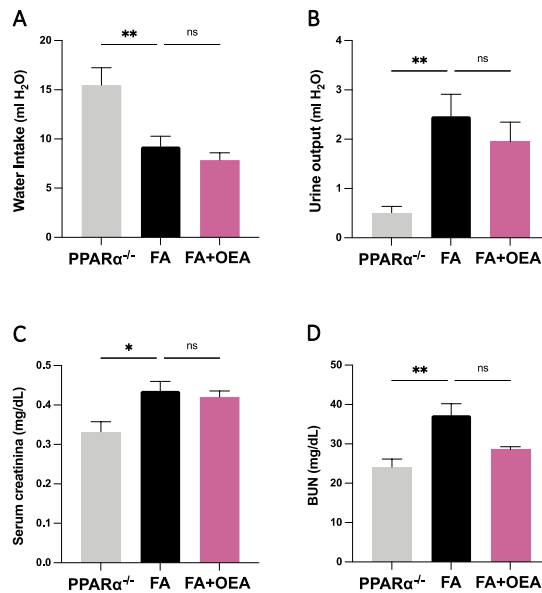


Fig 6.16 OEA failed to restore kidney function in PPAR- α KO mice. At the end of the experimental period, mice were placed in metabolic cages to assess metabolic parameters: water intake (A) and urine output (B). OEA treatment was unable to re-establish the altered metabolic parameters induced by FA challenge compared to the control group in PPAR- α KO mice. Renal function parameters, BUN, and serum creatinine increased in FA mice compared to the control group was not recovered in OEA mice (C and D). Results are shown as mean \pm S.E.M (* P <0,05 and ** P <0,01).

6.3.2 PPAR- α BLUNTING LIMITS OEA ANTI-INFLAMMATORY AND ANTI-FIBROTIC EFFECTS

To assess PPAR- α involvement in renal anti-inflammatory and anti-fibrotic OEA effects we employed mice lacking this receptor. Chronic inflammation and levels of inflammatory mediators have been identified as playing an important role in the onset, development, and progression of kidney damage [Li et al., 2021]. Here, the pro-inflammatory factors MCP-1 (Fig. 6.17 A), IL-1 β (Fig. 6.17 B), and F4-80 (Fig. 6.17 C) were increased upon FA in PPAR- α KO mice, and OEA treatment did not significantly limit the increased transcription. The activated inflammatory cells also produce profibrotic factors, such as TGF- β 1, and excessive extracellular matrix deposition, revealed by the increased collagen IV and fibronectin deposition. PPAR- α was involved in the OEA anti-fibrotic effect of FA challenge in mice since OEA treatment did not lessen the gene expression of all these factors in mice lacking PPAR- α (Fig 6.17D, E and F).

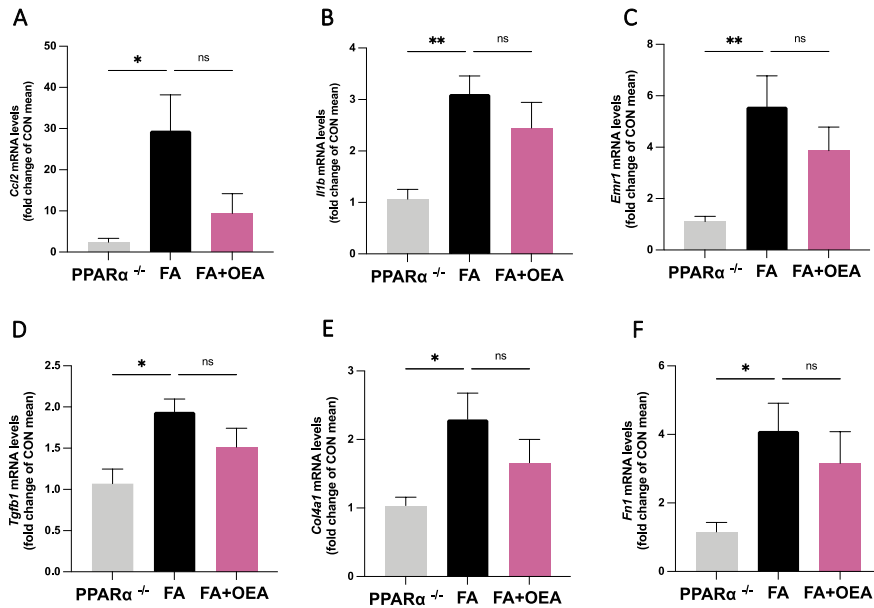


Fig 6.17 OEA did not limit inflammatory and fibrotic parameters in PPAR- α KO mice. OEA treatment did not reduce the increased levels of Ccl2 (A), Il1b (B), Emr1 (C), Tgfb1 (D), Col4a1 (E) and Fn1 (F) mRNAs, induced by FA challenge in PPAR- α KO mice. Results are shown as mean \pm S.E.M (* P <0,05, ** P <0,01, and *** P <0,001).

IN VITRO EXPERIMENT

6.3.3 EFFECTS OF OEA ON TGFB1-INDUCED FIBROSIS IN HK-2 CELLS

TGF- β 1 signalling pathway, the master regulator of fibrosis, was examined in human proximal tubular (HK-2) cells *in vitro* to define the direct antifibrotic effects of OEA on tubular cells and to investigate, as mechanistic insight, the involvement of PPAR- α , through its receptor antagonist, GW6471.

First, an MTT assay was carried out to determine the appropriate OEA concentration that did not alter cell viability. HK-2 cells were treated with various concentrations of OEA (1, 3, 10, 30 μ M), and the results showed

that OEA concentrations $>10 \mu\text{M}$ caused a sharp decrease in cell viability; thus, $5 \mu\text{M}$ OEA was chosen for subsequent experiments.

Cell viability was not altered at OEA concentrations between 1 and $10 \mu\text{M}$ both in control or treated cells, either with TGF- β 1 or with TGF- β 1 and GW6471, while OEA $30 \mu\text{M}$ significantly reduced the cell survival rate.

According to numerous studies, TGF- β 1 (10ng/ml) is sufficient to induce an EMT in HK-2 cells over a 24-h period [Wang et al., 2014; You et al., 2016; Xu et al., 2019; Tang et al., 2018].

Cell morphology showed that HK-2 cells lost their epithelial appearance and presented elongated and spindle-shaped morphology after being stimulated with TGF- β 1 (10ng/ml) for 24h, while OEA ($5 \mu\text{M}$) significantly reduced spindle-like morphology.

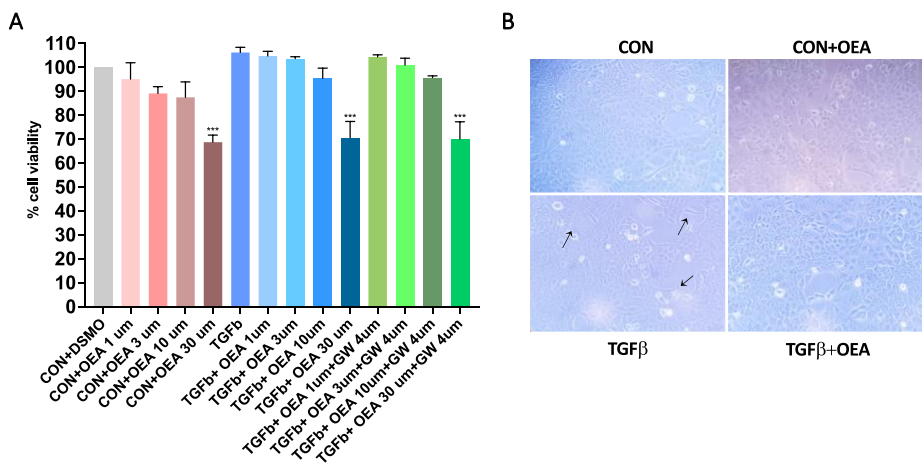


Fig 6.18 Effect of OEA on TGF- β 1-induced cell fibrosis *in vitro*. MTT assay was performed to determine the appropriate OEA concentration that did not alter cell viability. OEA concentrations tested were: 1, 3, 10 and $30 \mu\text{M}$, with or without TGF- β 1 (10ng/ml) for 24h (A). Microscopy images (B) showing morphological changes of HK-2 cells treated with TGF- β 1 for 24 h, pretreated or not with OEA for 12h. Elongated and spindle-like cells are indicated by arrows (B). Results are

representative of three replicate experiments. All data are shown as mean \pm S.E.M (***) $P < 0.001$.

6.3.4 PPAR- α INVOLVEMENT IN THE INHIBITION EFFECT OF OEA ON FIBROSIS AND INFLAMMATION INDUCED BY TGF- β 1 EXPOSURE

As shown in fig. 6.19, TGF- β 1 induced epithelial-mesenchymal transition (EMT) and fibrotic process in HK-2 cells. OEA inhibited the increased gene expression of MCP1, IL-1 β , type IV collagen and fibronectin stimulated by TGF- β 1 (fig. 6.19 A-D).

To assess the role of PPAR- α in the antifibrotic effect of OEA, HK-2 cells were pretreated with the PPAR- α antagonist GW6471 before OEA treatment. We showed that GW6471 almost completely abolished the inhibitory effect of OEA on Ccl2 and Fn1 gene expression (Fig 5.20 E and F).

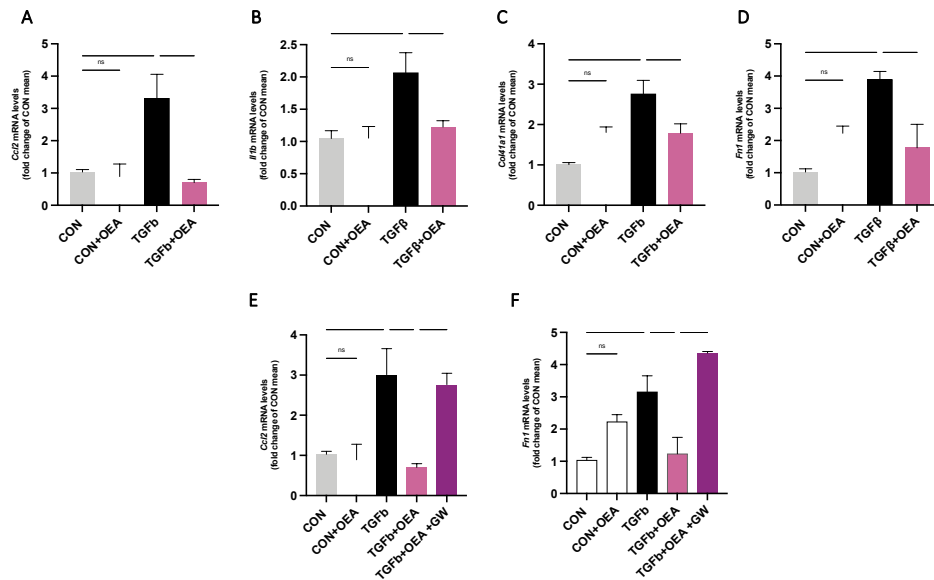


Fig 6.19 OEA limits inflammatory and fibrotic responses induced by TGF- β 1 in HK-2 cells. The increased mRNA levels of the inflammatory genes, including MCP1 (Ccl2) (A) and IL-1 β (Il1b) (B) and epithelial-mesenchymal transition markers,

Collagenase IV (Col4a1) (C) and fibronectin (Fn1) (D), following TGF- β 1 stimulation in HK2 were significantly decreased by OEA pre-treatment. OEA effect on Ccl2 (E) and Fn1 (F) was blunted by GW6471 incubation. Results are representative of three replicate experiments. Results are shown as mean \pm S.E.M (*P<0,05, **P<0,01, ***P<0,001 and ****P<0,0001).

6.3.5 OEA INHIBITS EFFECT ON THE TGF- β 1/SMAD AND MAPK SIGNALLING PATHWAYS IN HK-2 CELLS THROUGH THE PPAR- α

Exposure to TGF- β 1 led to a marked increase of SMAD3 phosphorylation and of the mitogen-activated protein kinases (MAPKs), namely Erk1/2 and p38, after the 30-min incubation period, compared with untreated cells (fig. 6.20 A and B). As shown, the addition of OEA for 1 h significantly downregulated this signalling pathway; nevertheless, pretreatment with the PPAR- α -antagonist GW6471 prevented OEA effects. Taken together, these results confirm the role of PPAR- α in mediating the damping effect of OEA on TGF- β 1 signalling via Smad and MAPK pathway in HK2 cells.

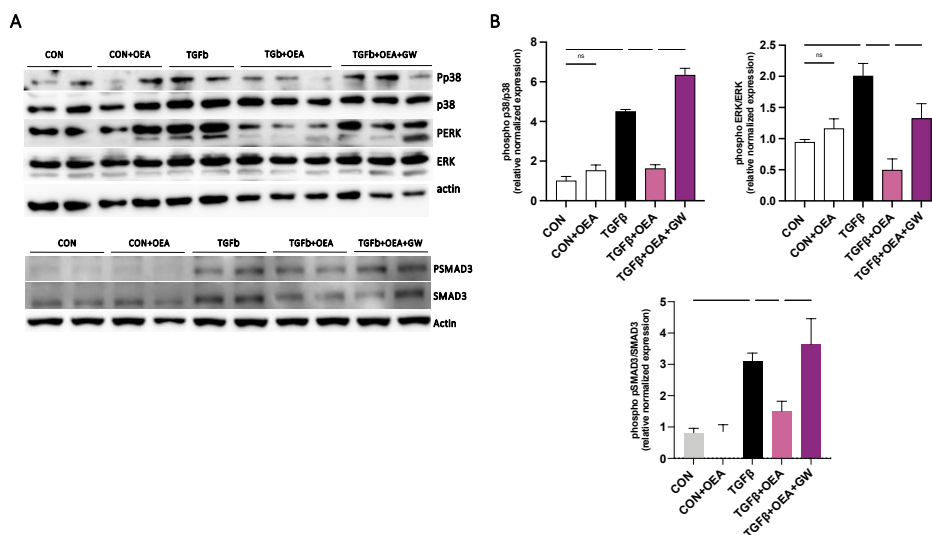


Fig 6.20 OEA inhibits the TGF- β 1/Smad and MAPK signalling pathways in HK-2 cells through PPAR- α activation. Representative Western blot of p38, ERK and SMAD3 (A) and the relative levels of phosphorylated and total proteins (B) are

shown. OEA significantly inhibited TGF- β /Smad and MAPK signalling pathways. In contrast, pretreatment with the PPAR- α -antagonist GW-6471 inhibited OEA inhibitory activity on gene expression. The data were normalized to the intensity of total protein and expressed relative to the value of the control (CON) group. Results are representative of three replicate experiments. All data were presented as mean \pm S.E.M (*P<0,05, **P<0,01, ***P<0,001 and ****P<0,0001).

SUPPLEMENTARY RESULTS

6.4 OEA AND EGB ASSOCIATION DOES NOT SHOW SYNERGISTIC EFFECTS

IN OBESE MOUSE MODEL

6.4.1 OEA AND EGB COMBINATION FAILS TO RESTORE THE METABOLIC ALTERATION IN HFD MICE

The combination of OEA with EGb was tested in HFD-induced obesity in mice. Long-term HFD resulted in a significant increase in body weight which was only reduced by OEA treatment but not in mice treated with EGB alone or with an OEA-EGb combination (Fig. 6.21 A). In addition, the combination only partially limited the increase of systolic pressure induced by the HFD recorded at the end of the treatment period (Fig. 6.21 B). Moreover, the effect on food and water intake was assessed by metabolic cages. HFD determined an increase in food intake that was counteracted only in OEA-treated mice (fig. 6.21C) and a reduction in water intake that was restored solely by OEA treatment. In addition, to assess kidney function, urine output and proteinuria were evaluated; both parameters were significantly altered in obese mice and restored only by OEA but not in OEA-EGb co-treated mice (fig. 6.21E and F).

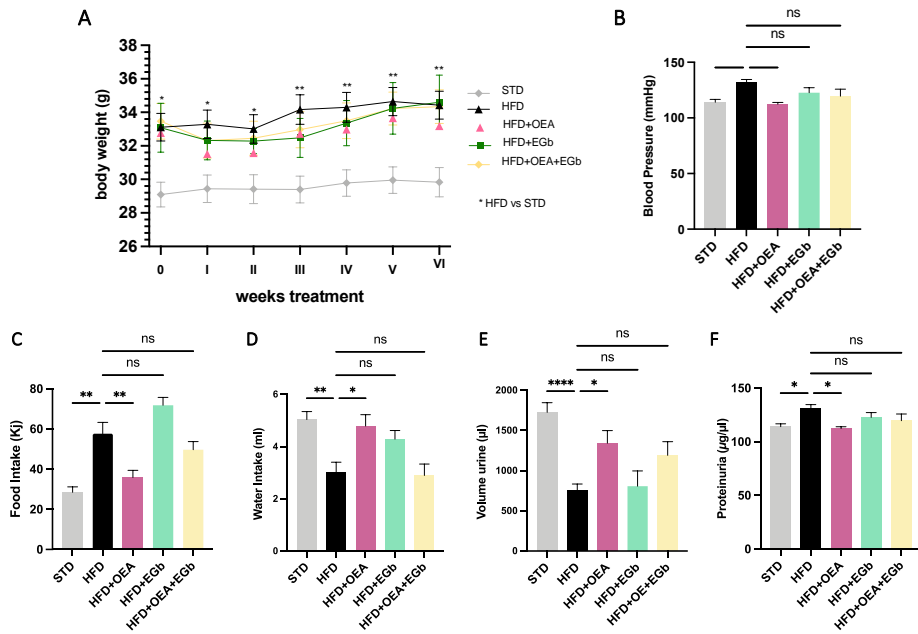


Fig 6.21 OEA and EGb association does not restore metabolic impairment induced by HFD. Body weight (A), blood pressure recorded at the end of the treatment (B), food intake (C), water intake (D), volume urine (E) and proteinuria (F) are reported. Results are shown as mean \pm S.E.M (* $P < 0,05$, ** $P < 0,01$, *** $P < 0,001$ and **** $P < 0,0001$).

IN CKD MOUSE MODEL

6.4.2 OEA AND EGB ASSOCIATION DOES NOT REGENERATE KIDNEY IMPAIRMENT IN FA MICE

The effect of the OEA and EGb combination was also evaluated in the FA model of CKD. As shown in figure 6.22, the co-treatment of OEA and EGb was unable to reduce water intake and urine output, which increased in FA-insulted mice (fig. 6.22A and B). In addition, mice receiving OEA in combination with EGb did not exhibit a reduction of BUN and serum creatinine, which markedly increased in the HFD group (fig. 6.22C and D).

These results indicate that OEA and EGb, in combination, did not show a promising renoprotective synergic effect also in short-term treatment.

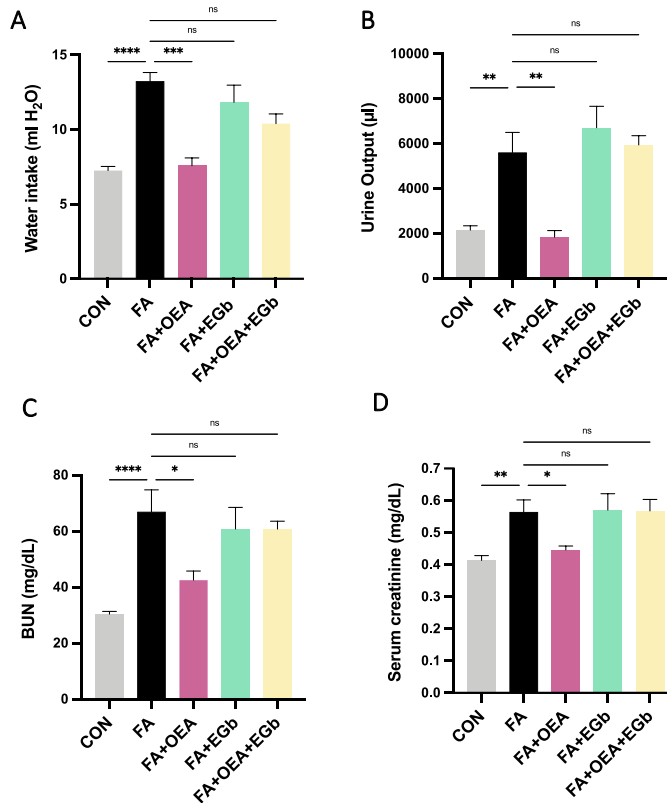


Fig 6.22 OEA and EGb association fails to recover kidney parameters worsened in FA mice. Water intake (A), urine output (B), BUN (C) and serum Cr (D) are shown. Results are shown as mean \pm S.E.M (* $P < 0,05$, ** $P < 0,01$, *** $P < 0,001$ and **** $P < 0,0001$).

6.4.3 OEA AND EGB COMBINATION DOES NOT LIMITS KIDNEY INFLAMMATION AND FIBROSIS IN FA MICE

To investigate the effects of OEA in combination with EGb, we examined the expression of proinflammatory and profibrotic markers in kidney tissue. Mice insulted with FA induced an increase of Emr1 (Fig. 6.23 A), Fn1

(Fig. 6.23 B) and Col4a1 (Fig. 6.23 C) that were markedly reduced in OEA-treated mice and partially in the EGb group, but not in mice receiving the combination.

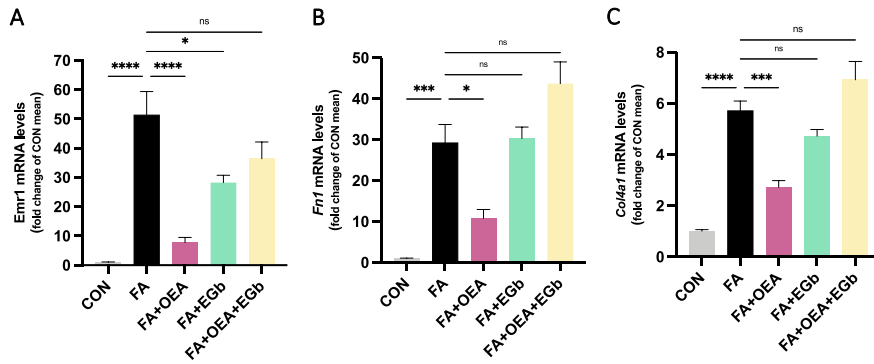


Fig 6.23 OEA and EGb association fails to reduce proinflammatory and profibrotic markers in FA mice. Transcription of renal *Emr1*(A), *Fn1* (B), *Col4a1* (C) is shown. Results are shown as mean \pm S.E.M (* P <0,05, *** P <0,001 and **** P <0,0001).

6.4.4 EGB CAN NOT RESTORE INFLAMMATION, FIBROSIS, AND OXIDATIVE STRESS IN FA MICE

Since we have validated that the combination of OEA and EGb has not found any synergistic or potentiating effects, we have evaluated the treatment with EGb alone in the FA mice model. Inflammation and fibrosis mediators were examined in kidney tissue. Gene expression of IL-1b (Fig. 6.24 A), *ccl2* (Fig. 6.24 B), *Emr1* (Fig. 6.24 C), *Fn1* (Fig. 6.24 D) and TGF- β 1 (Fig. 6.24 E) was strongly up-regulated by FA challenge, but only partially limited in EGb treated mice. Similarly, EGb does not affect protein expression of the scavenger enzyme, SOD2, suggesting no effect on oxidative stress.

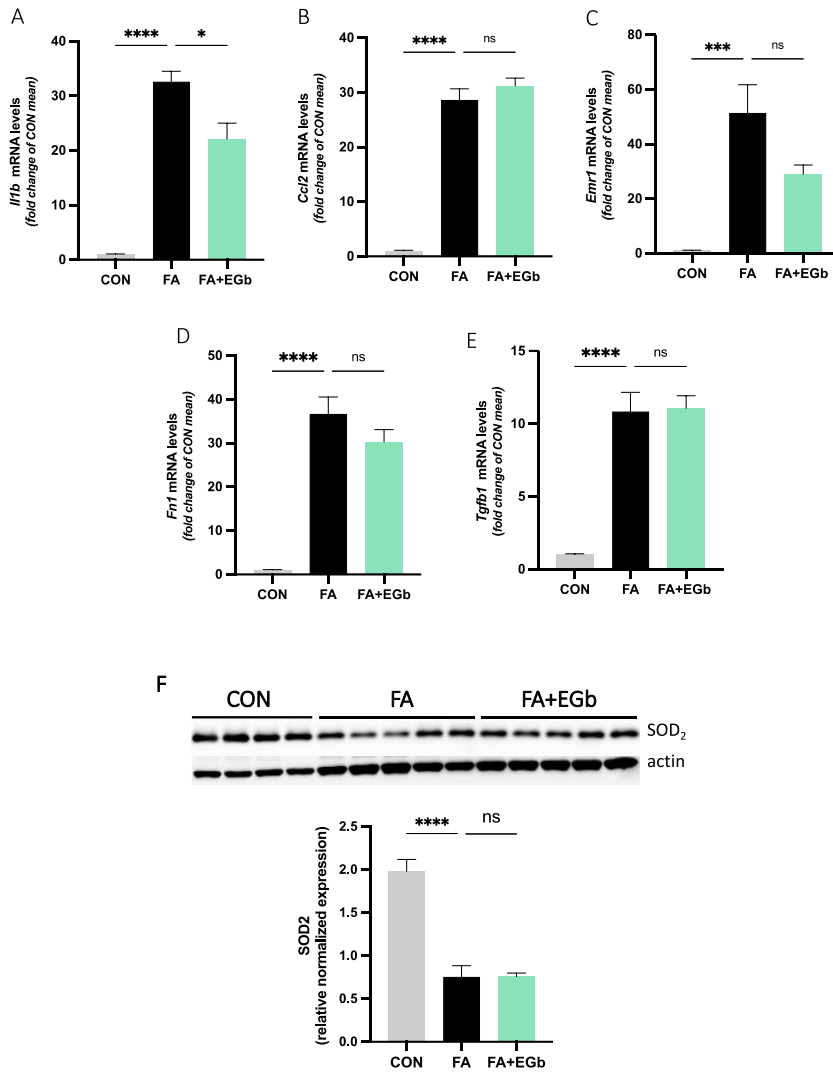


Fig 6.24 EGb treatment does not recover kidney alterations induced by FA. Gene expression of *Il1b* (A), *Ccl2* (B), *Emr1* (C), *Fn1* (D) and *Tgfb1* (E) in renal tissue is shown. Protein level of SOD2 (F) in the kidney is also shown. Results are shown as mean \pm S.E.M (* $P < 0,05$, ** $P < 0,001$ and **** $P < 0,0001$).

7. DISCUSSION

Obesity has reached epidemic proportions worldwide with numerous risks and consequences, including other metabolic disorders, such as type 2 diabetes, non-alcoholic fatty liver disease, and cardiovascular and chronic kidney diseases.

Insights from epidemiological, clinical, and basic research illuminate the interplay between metabolic disorders and obesity that contribute to the cluster of interactive maladaptive cardiovascular and kidney diseases that constitute the CardioRenal Metabolic Syndrome (CRMetS) [Connell et al., 2014].

The mechanisms involved in cardiorenal syndrome progression are multifaceted. Fat accumulation is driven by an energy imbalance between food intake and calories consumed, leading to metabolic dysfunctions related to inflammation and oxidative stress, often resulting in fibrosis which, in turn, determines anatomical-functional cardiac and renal damage. Encompassing complex and multifactorial pathophysiology, the cardio-renal syndrome is a clinical challenge. It is a common feature in heart failure and chronic kidney disease. Diagnostic, prognostic, and therapeutic measures are limited in the cardiorenal syndrome setting. Current pharmacological therapies are powerful but insufficient to reverse or mitigate the progression of cardiorenal syndrome satisfactorily; thus, it is a high-priority area for drug discovery and new therapeutic strategies. Separate heart and kidney transplants are options for end-stage patients. Double transplant involving both organs is much less considered.

Insight into the pathological process has revealed that oxidative stress and the inflammatory and fibrotic signalling pathways associated with glucose

and lipid metabolism alterations play a central role in the progression of chronic kidney disease. To date, kidney transplantation and dialysis are the only options for end-stage kidney disease; therefore, strategies to prevent chronic kidney diseases are needed. Therefore, the development of integrative/adjunctive treatment targeting the underlying mechanisms of progressive kidney disease is needed.

7.1. LACK OF SYNERGY BETWEEN OEA AND EGB ON KIDNEY DAMAGE

Preclinical testing of potential therapeutics through experimental *in vitro* and *in vivo* models offers support for translating of research findings into clinical trials and practice. Here, we tried to validate, through valuable model systems for the experimental nephrology field, the potential of a novel combination of OEA and EGb, based on sound scientific evidence of their possible efficacy in renal disease [Izzedine et al., 2004; Li et al., 2013]. In particular, both OEA and EGb extracts alone or in combination were tested either in a diet-induced obesity model of renal damage or a non-metabolic FA-induced kidney fibrosis model in mice. Notably, these models of kidney damage recapitulate chronic kidney injury through activating similar pathways, although evoked by divergent stimuli. Moreover, both models allow functional readouts regarding water intake and urine output beyond evaluating molecular inflammatory and fibrotic markers.

In our experimental conditions, following 12 weeks of high-fat diet feeding EGb alone or in combination with OEA did not significantly affect the examined parameters after a 6-week treatment. No difference was shown among HFD-fed mice and EGb- or EGb and OEA-treated mice in metabolic

(body weight and food intake), cardiovascular (blood pressure), and renal functional (water intake, urine output) parameters. Similarly, the evaluation of molecular markers related to macrophage recruitment (Emr1 gene expression) or fibrosis (Fn1 and Col4a1 transcription) did not show any potential of EGb or EGb/OEA combination in damping renal damage. The failure of any synergic effect could be ascribed to the chosen doses for both components of the combination or the duration of the treatment. However, while EGb dosage was in the average of those found in the literature [Lu et al., 2007; Lu et al., 2015], particular care was taken in selecting the OEA dose based on its anorectic effect. In fact, 2.5 mg/kg is not a common OEA dose used here to avoid profound weight loss.

Conversely, OEA treatment significantly increased water intake and urine output, consistently with a reduction of F4/80, Fn1 and Col4a transcription. Although no promising data on the activity of EGb alone or in combination with OEA were shown, the same treatments were also performed in the model of kidney damage induced by FA, where a direct fibrotic challenge is evoked regardless of metabolic alterations. These experiments confirmed the ineffectiveness of EGb, and the lack of a synergic effect with OEA in hematic or functional parameters associated with kidney damage, as well as in modulating pro-inflammatory or pro-fibrotic markers altered in FA-insulted mice. Taken together, these findings indicate the lack of a potential synergistic effect of the combination; however, in both models of kidney damage, OEA exhibited a renoprotective marked impact instead.

7.2. OEA PROTECTIVE EFFECT IN HFD-INDUCED HEART DAMAGE

OEA effect was also evaluated in the HFD-induced obesity model to assess its potential in the cardiac dysfunction induced by dysfunctional metabolism.

Following long-term HFD feeding, mice show metabolic alterations comparable to the metabolic syndrome in humans, i.e. obesity, insulin resistance, glucose intolerance, and altered serum biochemical parameters [Fraulob et al., 2010; Della Vedova et al., 2016]. Weight gain is an obligatory feature of the development of the metabolic syndrome and is observed in all the studies that model metabolic syndrome and type 2 diabetes by keeping animals on HFD [Wang et al., 2013].

In our experimental conditions, OEA shows a decrease in body weight and weight gain starting from the third week of the study. In line, OEA countered the increase in food intake, serum cholesterol and fat mass accumulation associated with obesity. Moreover, in our study, HFD-fed animals developed elevated fasting glucose and markedly increased glucose levels over time after glucose load, while OEA treatment ameliorates glucose disposal improving blood glucose.

The detrimental increase in fatty acids and dysregulated adipokine secretion induced by HFD determines the maladaptive mechanisms in the heart unable to counteract the metabolic alterations [Dirkx et al., 2011]. In cardiomyocytes, the flux of fatty acids is mainly regulated by the fatty acid translocase CD36 [Glatz et al., 2020]. Here, in HFD mice, its increased expression is suggestive of an excessive lipid accumulation and the formation of lipotoxic species associated with myocardial contractile dysfunction, also contributing to insulin resistance. This increased

expression of CD36 was instead downregulated in OEA-treated mice, indicating a re-established homeostasis of the cardiac fatty acid flux. Moreover, OEA was shown to induce significant changes in the cardiac levels of different classes of lipids in HFD-fed mice. The hearts of mice on HFD had an increased content of saturated triacylglycerols and cholesteryl esters that OEA normalized. Moreover, analyzing the lipidomic profile, it appears that OEA alters mainly classes of glycerophospholipids containing highly unsaturated fatty acids. The ratio of the fatty acid linoleic acid and γ -linoleic acid and the ratio of the polyunsaturated fatty acid arachidonic acid ω -6 and saturated arachidic acid ω -6 were both significantly decreased in cardiac tissue of HFD mice upon OEA treatment. Moreover, OEA modulates the cardiac content of three classes of sphingomyelins, a lipid class that is part of the typical composition of the lipid bilayer of the cell membrane.

AMPK phosphorylation is a central regulator of mammalian cellular energy metabolism; in fact, it is activated after an acute increase in the cellular [AMP]/[ATP] ratio [Zhao et al., 2020; Hardie et al., 2012]. In cardiac muscle, the AMPK protein has a specific role in the regulation of cardiomyocyte metabolism. Several lines of evidence have shown that an increase in AMPK activity in cardiomyocytes results in an increase in the rate of transport of cardiomyocytes glucose [Salt et al., 2017; Russell et al., 1999; Kramer et al., 2006; Ginion et al., 2011]. The increased phosphorylated state of AMPK in the heart from OEA-treated mice suggests the potential stimulation of glucose uptake. Consistently, OEA increased Akt phosphorylation as well. Previous studies reported that increased Akt expression could promote glucose utilization in peripheral tissues, reduces

insulin resistance, enhance cardiac energy supply, preventing cardiac insufficiency [Zhu et al., 2011]. Thus, both pathways activated by OEA treatment and converging in AS160 activation could synergize in improving insulin sensitivity and glucose uptake in cardiac tissue, inducing the translocation of GLUT4 to the cardiomyocyte membrane [Heim et al., 2020; Shoop et al., 2019; Feijóo-Bandín et al., 2013].

An increase in adiponectin transcription and meteorin-like (Metrnl) was shown in the heart from HFD, normalized by OEA treatment. Indeed, it was shown that the heart has a local adiponectin signalling system; in fact, cardiomyocyte-derived adiponectin has a cardioprotective role through an autocrine/paracrine mechanism, directly impacting cardiac metabolism and preventing cardiovascular dysfunction. As adiponectin, Metrnl is another newly discovered cardioprotective factor with insulin-sensitizing and anti-inflammatory properties. Possibly the induction of both adipokines in HFD could represent a compensatory protective mechanism in order to counteract myocardial dysfunction. On the other hand, HFD also leads to increased production of inflammatory cytokines IL-1 and IL-6 and MCP-1, which play an important role in cell recruitment involving increased inflammatory cell infiltration, compromising normal cardiomyocyte function and leading to myocardial fibrosis and cardiac remodelling [Bujak et al., 2007]. We showed that OEA exhibits a marked anti-inflammatory effect by reducing the transcription in the ventricle of such pro-inflammatory mediators involved in the progression of heart damage.

To determine OEA capability in limiting heart fibrosis, we evaluated the gene expression of TGF- β , fibrillin and collagen III that participate in

forming the extracellular cardiac matrix. OEA was able to reduce the expression of all the profibrotic markers that were markedly increased in the heart from HFD mice.

The basal autophagy process constitutes an essential mechanism in cardiomyocyte function since the renewal and recycling of cytoplasmic components, organelles or protein aggregates whose accumulation can be toxic to cells, is particularly relevant to quiescent and differentiated cells such as cardiomyocytes [Terman et al., 2010]. The degradation products generated after autophagy have the function of providing substrates for the biosynthesis of new molecules and organelles and the generation of energy; so autophagy constitutes a pivotal process to ensure energy supply under stressful conditions and to control cardiomyocyte size, function, and homeostasis [Loos et al., 2013; Nakai et al., 2007]. We showed that OEA stimulates the autophagic process, modulating the processing of LC3 protein and the expression of p62 protein. LC3 protein is initially synthesized as an unprocessed proLC3 form, which undergoes a proteolytic modification that removes several amino acids from the C-terminal end, producing the soluble cytosolic form LC3I [Kabeja et al., 2000]. During the induction of the autophagic process, LC3I undergoes covalent lipidation producing the conjugated form LC3II located in the autophagic membranes associated with the autophagosome. Interestingly, this lipidation process can be determined by Western Blot since the lipidated form has a lower molecular weight, so both the free and the lipidated form of LC3 [Klionsky et al., 2016] can be estimated. The use of LC3II as an autophagic marker is useful because it provides an approximate interpretation of phagosome numbers, although it does not

provide information on autophagic flux [Esteban et al., 2004]. The p62 protein, also called sequestosoma 1 (SQSTM1), is another marker to monitor the autophagic process. In fact, it is degraded by the autophagosome thanks to an interaction with LC3, and its quantity is, therefore, inversely proportional to the level of cellular autophagy [Katsuragi et al., 2015].

7.3. OEA EFFECT ON KIDNEY DAMAGE

As aforementioned, in HFD-induced kidney damage, OEA treatment exhibited a renoprotective effect, as suggested by preliminary data showing an increase in water intake and urine output, consistently with a reduction of F4/80, Fn1 and Col4a transcription. These results on improving kidney function and reducing molecular markers of fibrosis prompted further investigation of the possible direct renoprotective activity of OEA. Therefore, the study of the OEA effect in the FA model was undertaken to address whether this ethanolamide improves functional and pathological kidney injury in a non-metabolic model of fibrotic renal injury. Here, we showed not only the protective effect of OEA in the kidney but also the possible underlying mechanisms. Indeed, our study has first demonstrated that OEA significantly reduced water intake, urine output, serum urea nitrogen and creatinine following the FA challenge. Subsequently, our findings showed that OEA attenuated inflammation, matrix protein expression, and thus renal fibrosis. In line with this, OEA significantly lessened histologic injury, as shown by reduced epithelial vacuolization, tubular dilation, and cylindrical structures formed from

coagulated protein, all features induced after FA exposure. In addition, Masson's trichrome, immunohistochemical staining, and gene transcription data revealed that OEA inhibited *tgfb1* expression and the deposition of ECM components, such as fibronectin and collagen 4a. In addition, the reduced transcription of *Ccl2*, *Emr1*, *Cma1* and *Tpsb2* upon OEA treatment demonstrated that OEA could attenuate the accumulation of inflammatory cells in the injured kidney and hence reduce the inflammatory process fostered by cell recruitment. Inflammation is a pivotal event in the pathophysiology of kidney injury's acute phase [Akca et al., 2009]. It is associated with tissue destruction in the acute phase and determines the long-term outcome since unresolved inflammation represents the main culprit of the fibrotic process [Venkatachalam et al., 2010]. Actually, the acute stage of FA-induced kidney damage ends within three days from the challenge, starting the transition into the chronic stage. Thus, it is conceivable to hypothesize that prompt treatment during the acute phase not only attenuates the early inflammatory injury but also attenuates kidney fibrosis in the chronic phase (at day 14). These data imply that OEA could represent an effective agent for preventing the progression of kidney injury after the acute phase, affecting the delicate transition mechanisms.

OEA has been shown to have anti-inflammatory and/or anti-fibrotic effects also in the liver. Indeed, OEA was shown to significantly attenuate the progress of liver fibrosis in two experimental animal models by blocking the activation of hepatic stellate cells [Chen et al., 2015]. In particular, OEA reduced the expression of genes involved in hepatic fibrosis, inflammation and extracellular matrix remodelling in a mouse

model of fibrosis induced by a methionine choline-deficient (MCD) diet or thioacetamide (TAA) treatment [Chen et al., 2015]. Similar data were obtained by Lin et al. [2022]; the authors demonstrated that after exposure of mice to HFD, subchronic OEA administration reduced lipid accumulation, inflammatory responses, and fibrosis in the liver. Notably, a triple-blind randomized controlled clinical trial was performed to assess the combination of OEA treatment and calorie restriction on several parameters related to inflammation and hepatic fibrosis in steatotic obese patients [Tutunchi et al., 2021]. In this 12-week randomized clinical trial, 76 obese patients newly diagnosed with NAFLD were randomly allocated into either OEA or placebo group. Actually, no significant within-and between-group differences were observed in the NAFLD fibrosis score at the end of the trial. However, the treatment with OEA, along with weight-loss intervention, significantly improved inflammation and body composition in patients with NAFLD.

Up to date, OEA has proven to be a multi-target compound: the main pharmacological effects of OEA are mediated by the activation of PPAR- α [Fu et al., 2005], a transcription factor involved in the regulation of gene networks, which controls metabolism and inflammation [Montaigne et al., 2021; Li et al., 2013].

Here, we have also demonstrated that the positive effect exerted by OEA is contingent on PPAR- α activation since OEA treatment failed to induce its renoprotective activity in PPAR- α KO mice. Notably, OEA did not significantly affect water intake or urine output in FA-insulted PPAR- α KO mice. Consistently, OEA did not improve serum creatinine either, while a not significant trend of reduction was shown in BUN concentration. The

evaluation of the transcription of *Ccl2* and *Emr1* revealed that OEA failed in reducing chemotaxis and monocyte/macrophage recruitment in the kidney of PPAR- α null mice. Consistently, the reduction in renal fibrosis by OEA treatment was also contingent on PPAR- α expression since OEA treatment failed to inhibit *tgb1*, *col4a*, and *fn1* transcription, indicating an obligatory involvement of PPAR- α in OEA effect. According to these results, we found significantly lower PPAR- α mRNA expression in the kidney of wt FA-insulted mice that was increased after OEA treatment. However, we cannot exclude the involvement of other OEA binding receptors, in particular of vanilloid TRPV1, abundantly expressed at the renal level, whose OEA binding antagonist activity has to be taken into account as a potential additional mechanism underlying the renoprotective effect.

A role for PPAR- α has been clearly ascribed in kidney function. Intriguingly, transgenic expression of proximal tubule PPAR- α in mice was noted to confer protection against acute kidney injury [Li et al., 2009]. Moreover, PPAR- α activation resulted in a reduction of oxidative stress and inflammation, common features of renal damage [Hou et al., 2010; Wanner and Krane, 2011]. Actually, the central role of PPAR- α in lipid metabolism indicated the potential of PPAR- α agonists in the management of kidney damage when associated with metabolic impairment, considering renal lipid accumulation-induced lipotoxicity one of the pathogenic mechanisms underlying nephropathy [Balakumar et al., 2012; Hiukka et al., 2010; Mattace Raso et al., 2013]. Indeed, PPAR- α agonists, such as fenofibrate or berberine, ameliorate kidney damage or tubular cell alterations by enhancing lipolysis [Tanaka et al., 2011; Gelosa et al., 2010].

Here, we clearly indicate the intrinsic direct renoprotective properties of OEA, demonstrating its effect on renal damage in FA-insulted mice, a non-metabolic model of renal fibrosis, where the downregulation of triglyceride metabolism and lipid accumulation in proximal tubules do not constitute the causative pathogenic mechanisms. This conclusion was further strengthened by *in vitro* results, where we clearly showed that OEA blunted TGF- β -induced alterations and signalling in human tubular HK-2. TGF- β is a crucial detrimental factor in kidney damage due to its involvement in fibrosis, inflammation, apoptosis, and differentiation, regardless of the initial cause of kidney disease [Bottinger & Bitzer, 2002; Meng, & Chung, 2013]. Notably, treatment of HK-2 with OEA reduced inflammatory- (Ccl2 and Il1b) and fibrotic- (Col4a1 and Fn1) associated gene expression, indicating a direct anti-inflammatory and anti-fibrotic activity of OEA. To further investigate at the mechanistic level, the effect of OEA on TGF- β 1 signalling was also evaluated. Indeed, TGF- β 1 signalling could involve small mothers against decapentaplegic (Smad)-dependent or independent pathways [Lan and Chung, 2012]. Downstream phosphorylation of Smad2 and Smad3 factors upon TGF- β 1 pathway activation results in phosphorylated Smad transfer and accumulation into the nucleus, where they control gene transcription. While Smad2 was reported to counteract renal fibrosis [Lan et al., 2012] beneficially, Smad3 has a detrimental role. On the other hand, TGF- β 1 can also activate the non-Smad signalling pathway involving MAPks Erk1/2 and p38 [Zhang, 2009]. Here, we demonstrated that OEA inhibited TGF- β 1-induced gene transcription through both Smad3 and non-Smad MAPk activation, as shown by Western blot analysis of phosphorylated forms of TGF- β 1

downstream player. Therefore, OEA could be considered an anti-fibrotic tool, able to reduce *tgfb1* gene transcription *in vivo* and *in vitro* and to dampen TGF- β 1 downstream signalling pathway. Moreover, the acylethanolamide receptor blockade by the PPAR- α antagonist GW blunted both Smad3 and MAPk phosphorylation and gene transcription (Ccl2 and Fn1) evoked by TGF- β 1 stimulation of HK-2, indicating once again the involvement of PPAR- α in OEA activity.

8. GENERAL CONCLUSIONS

In conclusion, OEA, when used in combination with EGb, does not show a protective effect either in the HFD-mediated model of cardiorenal metabolic alterations or in the FA-mediated model of CKD. This may be mainly due to the dose chosen considering a potential combinatorial and potentiating effect and avoiding unpleasant side effects. It could also be related to the duration of treatment which may not have been long enough to detect any possible combined positive effects. So, the following investigations were mainly focused on evaluating the effects of OEA as it had shown, for the first time, a profound protective effect, at renal level, as at cardiac level, even at a dose considered sub-therapeutic in other conditions.

Here, it has been demonstrated that OEA reduced body weight and weight gain and improved the cardiac metabolism altered by HFD, counteracting the inflammatory and fibrotic processes. Furthermore, we demonstrated that OEA regulates energy metabolism by normalizing the altered lipid profile, inducing glucose uptake, and inducing the autophagic process.

Moreover, our study demonstrates that OEA could attenuate kidney injury after divergent detrimental stimuli secondary or not to metabolic impairment through mouse models of diet-induced obesity or FA challenge, respectively. OEA alleviates renal tubular epithelial cell damage, promotes the process of recovery, ameliorates inflammatory response, and prevents long-term kidney fibrosis. The renoprotective effect is mediated by the inhibition of TGF- β 1 expression and signalling pathway and involves the expression of PPAR- α .

Taken together, our findings suggest that OEA might represent an effective therapeutic strategy for preventing acute injury aggravation and subsequent progression in chronic disease.

9. KEY POINTS

- Cardiorenal metabolic syndrome (CRmetS) indicates a metabolic syndrome with cardio-renal comorbidities.
- Oleoylethanolamide is an endogenous lipid mediator and a PPAR- α agonist.
- Cardiovascular and renal disorders share common pathophysiological pathways.
- Oleoylethanolamide exerts a renoprotective effect, through the involvement of PPAR- α , *in vivo* and *in vitro*.
- Oleoylethanolamide enhances cardiac metabolism-regulating energy homeostasis, and limits inflammation and fibrosis.
- Oleoylethanolamide and extract of *Ginkgo biloba* leaves have no synergic effect in managing metabolic and non-metabolic kidney dysfunction.

10. REFERENCES

Abramowicz, D. et al. European Renal Best Practice Guideline on kidney donor and recipient evaluation and perioperative care. *Nephrol. Dial. Transplant.* 30, 1790–1797 (2015).

Afshin A, Reitsma MB, Murray CJL. Health Effects of Overweight and Obesity in 195 Countries. *N Engl J Med.* 2017 Oct 12;377(15):1496-7. doi: 10.1056/NEJMc1710026. PMID: 29020584.

Ahern GP. Activation of TRPV1 by the satiety factor oleoylethanolamide. *J Biol Chem.* 2003 Aug 15;278(33):30429-34. doi: 10.1074/jbc.M305051200. Epub 2003 May 21. PMID: 12761211.

Akcay A, Nguyen Q, Edelstein CL. Mediators of inflammation in acute kidney injury. *Mediators Inflamm.* 2009;2009:137072. doi: 10.1155/2009/137072. Epub 2010 Feb 21. PMID: 20182538; PMCID: PMC2825552.

Akgun E, Boyacioglu M, Kum S. The potential protective role of folic acid against acetaminophen-induced hepatotoxicity and nephrotoxicity in rats. *Exp Anim.* 2021;70(1):54-62. doi:10.1538/expanim.20-0075

Al-Rubaye H, McGlone ER, Farzaneh B, Mustafa L, Johnson M, Kayal A, et al. Roux-En-Y Gastric Bypass or Sleeve Gastrectomy for Obstructive Sleep Apnea: A Systematic Review and Meta-Analysis. *Laparoscopic Endoscopic Robotic Surg* (2019) 2(3):53–8. doi: 10.1016/j.lers.2019.05.002

Aminian A, Zelisko A, Kirwan JP, Brethauer SA, Schauer PR. Exploring the Impact of Bariatric Surgery on High Density Lipoprotein. *Surg Obes Relat Dis* (2015) 11:238–47. doi: 10.1016/j.soard.2014.07.017

Annuzzi G, Piscitelli F, Di Marino L, Patti L, Giacco R, Costabile G, Bozzetto L, Riccardi G, Verde R, Petrosino S, Rivellese AA, Di Marzo V. Differential alterations of the concentrations of endocannabinoids and related lipids in the subcutaneous adipose tissue of obese diabetic patients. *Lipids Health Dis.* 2010 Apr 28;9:43. doi: 10.1186/1476-511X-9-43. PMID: 20426869; PMCID: PMC2868848.

Antón M, Alén F, Gómez de Heras R, Serrano A, Pavón FJ, Leza JC, García-Bueno B, Rodríguez de Fonseca F, Orio L. Oleoylethanolamide prevents neuroimmune HMGB1/TLR4/NF-κB danger signaling in rat frontal cortex and depressive-like

behavior induced by ethanol binge administration. *Addict Biol.* 2017 May;22(3):724-741. doi: 10.1111/adb.12365. Epub 2016 Feb 9. PMID: 26857094.

Aparicio-Trejo OE, Avila-Rojas SH, Tapia E, et al. Chronic impairment of mitochondrial bioenergetics and beta-oxidation promotes experimental AKI-to-CKD transition induced by folic acid. *Free Radic Biol Med.* 2020;154:18-32. doi:10.1016/j.freeradbiomed.2020.04.016

Aparicio-Trejo OE, Reyes-Fermin LM, Briones-Herrera A, et al. Protective effects of N-acetyl-cysteine in mitochondria bioenergetics, oxidative stress, dynamics and S-glutathionylation alterations in acute kidney damage induced by folic acid. *Free Radic Biol Med.* 2019;130:379-396. doi:10.1016/j.freeradbiomed.2018.11.005

Astarita G, Rourke BC, Andersen JB, Fu J, Kim JH, Bennett AF, Hicks JW, Piomelli D. Postprandial increase of oleoylethanolamide mobilization in small intestine of the Burmese python (*Python molurus*). *Am J Physiol Regul Integr Comp Physiol.* 2006 May;290(5):R1407-12. doi: 10.1152/ajpregu.00664.2005. Epub 2005 Dec 22. PMID: 16373434.

Aviello G, Matias I, Capasso R, Petrosino S, Borrelli F, Orlando P, Romano B, Capasso F, Di Marzo V, Izzo AA. Inhibitory effect of the anorexic compound oleoylethanolamide on gastric emptying in control and overweight mice. *J Mol Med (Berl).* 2008 Apr;86(4):413-22. doi: 10.1007/s00109-008-0305-7. Epub 2008 Feb 16. PMID: 18278475.

Aydin D, Peker EG, Karakurt MD, Gurel A, Ayyildiz M, Cevher ŞC, Agar E, Dane S. Effects of Ginkgo biloba extract on brain oxidative condition after cisplatin exposure. *Clin Invest Med.* 2016 Dec 1;39(6):27511. PMID: 27917801.

Aziz TA, Hussain SA, Mahwi TO, Ahmed ZA. Efficacy and safety of *Ginkgo biloba* extract as an "add-on" treatment to metformin for patients with metabolic syndrome: a pilot clinical study. *Ther Clin Risk Manag.* 2018 Jul 11;14:1219-1226. doi: 10.2147/TCRM.S169503. PMID: 30034238; PMCID: PMC6047609.

Bachinskaya N, Hoerr R, Ihl R. Alleviating neuropsychiatric symptoms in dementia: the effects of Ginkgo biloba extract EGb 761. Findings from a randomized controlled trial. *Neuropsychiatr Dis Treat.* 2011;7:209-15. doi: 10.2147/NDT.S18741. Epub 2011 Apr 20. PMID: 21573082; PMCID: PMC3090284.

Balakumar P, Kadian S, Mahadevan N. Are PPAR alpha agonists a rational therapeutic strategy for preventing abnormalities of the diabetic kidney? *Pharmacol Res.* 2012 Apr;65(4):430-6. doi: 10.1016/j.phrs.2012.01.004. Epub 2012 Jan 21. PMID: 22285932.

Balvers MG, Wortelboer HM, Witkamp RF, Verhoeckx KC. Liquid chromatography-tandem mass spectrometry analysis of free and esterified fatty acid N-acyl ethanolamines in plasma and blood cells. *Anal Biochem.* 2013 Mar 15;434(2):275-83. doi: 10.1016/j.ab.2012.11.008. Epub 2012 Nov 29. PMID: 23201387.

Banin RM, Hirata BK, Andrade IS, Zemdegs JC, Clemente AP, Dornellas AP, Boldarine VT, Estadella D, Albuquerque KT, Oyama LM, Ribeiro EB, Telles MM. Beneficial effects of Ginkgo biloba extract on insulin signaling cascade, dyslipidemia, and body adiposity of diet-induced obese rats. *Braz J Med Biol Res.* 2014 Sep;47(9):780-8. doi: 10.1590/1414-431x20142983. Epub 2014 Jul 25. PMID: 25075573; PMCID: PMC4143206.

Bao YW, Yuan Y, Chen JH, Lin WQ. Kidney disease models: tools to identify mechanisms and potential therapeutic targets. *Zool Res.* 2018;39(2):72-86. doi:10.24272/j.issn.2095-8137.2017.055

Belwal, Tarun, et al. "Ginkgo biloba." *Nonvitamin and nonmineral nutritional supplements.* Academic Press, 2019. 241-250.

Berger J, Moller DE. The mechanisms of action of PPARs. *Annu Rev Med.* 2002;53:409-35. doi: 10.1146/annurev.med.53.082901.104018. PMID: 11818483.

Bhargava P, Schnellmann RG. Mitochondrial energetics in the kidney. *Nat Rev Nephrol.* 2017 Oct;13(10):629-646. doi: 10.1038/nrneph.2017.107. Epub 2017 Aug 14. PMID: 28804120; PMCID: PMC5965678.

Bikbov B, Purcell CA, Levey AS, et al. Global, regional, and national burden of chronic kidney disease, 1990–2017: a systematic analysis for the Global Burden of Disease Study 2017. *Lancet* 2020; 395: 709–33.

Boateng ID. A critical review of ginkgolic acids in *Ginkgo biloba* leaf extract (EGb): toxicity and technologies to remove ginkgolic acids and their promising bioactivities. *Food Funct.* 2022 Sep 22;13(18):9226-9242. doi: 10.1039/d2fo01827f. PMID: 36065842.

Bobulescu IA. Renal lipid metabolism and lipotoxicity. *Curr Opin Nephrol Hypertens*. 2010 Jul;19(4):393-402. doi: 10.1097/MNH.0b013e32833aa4ac. PMID: 20489613; PMCID: PMC3080272.

Bookout A. L., Y. Jeong, M. Downes, R. T. Yu, R. M. Evans, and D. J. Mangelsdorf, "Anatomical profiling of nuclear receptor expression reveals a hierarchical transcriptional network," *Cell*, vol. 126, no. 4, pp. 789–799, 2006

Boor P, Floege J. The renal (myo-)fibroblast: a heterogeneous group of cells. *Nephrol Dial Transplant*. 2012 Aug;27(8):3027-36. doi: 10.1093/ndt/gfs296. PMID: 22851626.

Böttinger EP, Bitzer M. TGF-beta signaling in renal disease. *J Am Soc Nephrol*. 2002 Oct;13(10):2600-10. doi: 10.1097/01.asn.0000033611.79556.ae. PMID: 12239251.

Bowen KJ, Kris-Etherton PM, Shearer GC, West SG, Reddivari L, Jones PJH. Oleic acid-derived oleoylethanolamide: A nutritional science perspective. *Prog Lipid Res*. 2017 Jul;67:1-15. doi: 10.1016/j.plipres.2017.04.001. Epub 2017 Apr 5. PMID: 28389247.

Brade W, Herken H, Merker HJ. [Lesion and regeneration of renal tubule cells following administration of folic acid]. *Naunyn Schmiedebergs Arch Exp Pathol Pharmacol*. 1969;262(2):228- 250. Schädigung und Regeneration renaler Tubuluszellen nach Folsäuregabe.

Braissant O, Foufelle F, Scotto C, Dauça M, Wahli W. Differential expression of peroxisome proliferator-activated receptors (PPARs): tissue distribution of PPAR-alpha, -beta, and -gamma in the adult rat. *Endocrinology*. 1996 Jan;137(1):354-66. doi: 10.1210/endo.137.1.8536636. PMID: 8536636.

Bünger M, van den Bosch HM, van der Meijde J, Kersten S, Hooiveld GJ, Müller M. Genome-wide analysis of PPARalpha activation in murine small intestine. *Physiol Genomics*. 2007 Jul 18;30(2):192-204. doi: 10.1152/physiolgenomics.00198.2006. Epub 2007 Apr 10. PMID: 17426115.

Burgos-Silva M, Semedo-Kuriki P, Donizetti-Oliveira C, et al. Adipose tissue-derived stem cells reduce acute and chronic kidney damage in mice. *PLoS One*. 2015;10(11):e0142183. doi:10.1371/ journal.pone.0142183

Capasso R, Matias I, Lutz B, Borrelli F, Capasso F, Marsicano G, Mascolo N, Petrosino S, Monory K, Valenti M, Di Marzo V, Izzo AA. Fatty acid amide hydrolase

controls mouse intestinal motility in vivo. *Gastroenterology*. 2005 Sep;129(3):941-51. doi: 10.1053/j.gastro.2005.06.018. PMID: 16143133.

Chan LS, Wells RA. Cross-Talk between PPARs and the Partners of RXR: A Molecular Perspective. *PPAR Res*. 2009;2009:925309. doi: 10.1155/2009/925309. Epub 2009 Dec 20. PMID: 20052392; PMCID: PMC2801013.

Chan PC, Xia Q, Fu PP. Ginkgo biloba leave extract: biological, medicinal, and toxicological effects. *J Environ Sci Health C Environ Carcinog Ecotoxicol Rev*. 2007 Jul-Sep;25(3):211-44. doi: 10.1080/10590500701569414. PMID: 17763047.

Chen HW, Yang MY, Hung TW, Chang YC, Wang CJ. Nelumbo nucifera leaves extract attenuate the pathological progression of diabetic nephropathy in high-fat diet-fed and streptozotocin-induced diabetic rats. *J Food Drug Anal*. 2019 Jul;27(3):736-748. doi: 10.1016/j.jfda.2018.12.009. Epub 2019 Jan 8. PMID: 31324289; PMCID: PMC9307034.

Chen L, Li L, Chen J, Li L, Zheng Z, Ren J, Qiu Y. Oleoylethanolamide, an endogenous PPAR- α ligand, attenuates liver fibrosis targeting hepatic stellate cells. *Oncotarget*. 2015 Dec 15;6(40):42530-40. doi: 10.18632/oncotarget.6466. PMID: 26729705; PMCID: PMC4767450.

Chung KW, Lee EK, Lee MK, Oh GT, Yu BP, Chung HY. Impairment of PPAR α and the Fatty Acid Oxidation Pathway Aggravates Renal Fibrosis during Aging. *J Am Soc Nephrol*. 2018 Apr;29(4):1223-1237. doi: 10.1681/ASN.2017070802. Epub 2018 Feb 12. PMID: 29440279; PMCID: PMC5875952.

Cignarelli M, Lamacchia O. Obesity and kidney disease. *Nutri Metab Cardiovasc Dis*. (2007) 17:757–62. doi: 10.1016/j.numecd.2007.03.003

Das UN. Essential fatty acids: biochemistry, physiology and pathology. *Biotechnol J*. 2006 Apr;1(4):420-39. doi: 10.1002/biot.200600012. PMID: 16892270.

Davison SN, Levin A, Moss AH, et al. Executive summary of the KDIGO Controversies Conference on Supportive Care in Chronic Kidney Disease: developing a roadmap to improving quality care. *Kidney Int*. 2015;88: 447–459.

De Caterina R, Zampolli A. From asthma to atherosclerosis--5-lipoxygenase, leukotrienes, and inflammation. *N Engl J Med*. 2004 Jan 1;350(1):4-7. doi: 10.1056/NEJMp038190. PMID: 14702420.

Declèves AE, Mathew AV, Cunard R, Sharma K. AMPK mediates the initiation of kidney disease induced by a high-fat diet. *J Am Soc Nephrol*. 2011 Oct;22(10):1846-55. doi: 10.1681/ASN.2011010026. Epub 2011 Sep 15. PMID: 21921143; PMCID: PMC3187184.

Dell'Agli, M., & Bosisio, E. (2002). Biflavones of Ginkgo biloba stimulate lipolysis in 3T3-L1 adipocytes. *Planta Medica*, 68(1), 76–79. [https:// doi.org/10.1055/s-2002-19876](https://doi.org/10.1055/s-2002-19876)

Della Vedova MC, Muñoz MD, Santillan LD, Plateo-Pignatari MG, Germanó MJ, Rinaldi Tosi ME, Garcia S, Gomez NN, Fornes MW, Gomez Mejiba SE, Ramirez DC. A Mouse Model of Diet-Induced Obesity Resembling Most Features of Human Metabolic Syndrome. *Nutr Metab Insights*. 2016 Dec 5;9:93-102. doi: 10.4137/NMI.S32907. PMID: 27980421; PMCID: PMC5140012.

Di Marzo V, Bisogno T, Melck D, Ross R, Brockie H, Stevenson L, Pertwee R, De Petrocellis L. Interactions between synthetic vanilloids and the endogenous cannabinoid system. *FEBS Lett*. 1998 Oct 9;436(3):449-54. doi: 10.1016/s0014-5793(98)01175-2. PMID: 9801167.

Dirkx E, Schwenk RW, Glatz JF, Luiken JJ, van Eys GJ.

Dixon ED, Nardo AD, Claudel T, Trauner M. The Role of Lipid Sensing Nuclear Receptors (PPARs and LXR) and Metabolic Lipases in Obesity, Diabetes and NAFLD. *Genes (Basel)*. 2021 Apr 26;12(5):645. doi: 10.3390/genes12050645. PMID: 33926085; PMCID: PMC8145571.

Doi K, Okamoto K, Negishi K, et al. Attenuation of folic acid- induced renal inflammatory injury in platelet-activating factor receptor-deficient mice. *Am J Pathol*. 2006;168(5):1413-1424. doi:10.2353/ajpath.2006.050634

Ducker GS, Rabinowitz JD. One-carbon metabolism in health and disease. *Cell Metab*. 2017;25(1):27-42. doi:10.1016/j.cmet. 2016.08.009

Drieu K, Vranckx R, Benassayad C, Haourigi M, Hassid J, Yoa RG, Rapin JR, Nunez EA. Effect of the extract of Ginkgo biloba (EGb 761) on the circulating and cellular profiles of polyunsaturated fatty acids: correlation with the anti-oxidant properties of the extract. *Prostaglandins Leukot Essent Fatty Acids*. 2000 Nov;63(5):293-300. doi: 10.1054/plf.2000.0217. PMID: 11090256.

Esteban V, Lorenzo O, Rupérez M, Suzuki Y, Mezzano S, Blanco J, Kretzler M, Sugaya T, Egido J, Ruiz-Ortega M. Angiotensin II, via AT1 and AT2 receptors and

NF-kappaB pathway, regulates the inflammatory response in unilateral ureteral obstruction. *J Am Soc Nephrol.* 2004 Jun;15(6):1514-29. doi: 10.1097/01.asn.0000130564.75008.f5. PMID: 15153562.

Evans S, Ma X, Wang X, Chen Y, Zhao C, Weinheimer CJ, Kovacs A, Finck B, Diwan A, Mann DL. Targeting the Autophagy-Lysosome Pathway in a Pathophysiologically Relevant Murine Model of Reversible Heart Failure. *JACC Basic Transl Sci.* 2022 Oct 19;7(12):1214-1228. doi: 10.1016/j.jacbts.2022.06.003. PMID: 36644282; PMCID: PMC9831862.

Ewees MG, Messiha BAS, Abdel-Bakky MS, Bayoumi AMA, Abo-Saif AA. Tempol, a superoxide dismutase mimetic agent, reduces cisplatin-induced nephrotoxicity in rats. *Drug Chem Toxicol.* 2019 Nov;42(6):657-664. doi: 10.1080/01480545.2018.1485688. Epub 2018 Aug 1. PMID: 30067109.

Feijóo-Bandín S, Rodríguez-Penas D, García-Rúa V, Mosquera-Leal A, Otero MF, Pereira E, et al. Nesfatin-1 in human and murine cardiomyocytes: synthesis, secretion, and mobilization of GLUT-4. *Endocrinology.* 2013;154(12):4757-67.

Feng Z, Sun Q, Chen W, Bai Y, Hu D, Xie X. The neuroprotective mechanisms of ginkgolides and bilobalide in cerebral ischemic injury: a literature review. *Mol Med.* 2019 Dec 21;25(1):57. doi: 10.1186/s10020-019-0125-y. PMID: 31864312; PMCID: PMC6925848.

Fiorentino TV, Prioletta A, Zuo P, Folli F. Hyperglycemia-induced oxidative stress and its role in diabetes mellitus related cardiovascular diseases. *Curr Pharm Des.* 2013;19(32):5695-703. doi: 10.2174/1381612811319320005. PMID: 23448484.

Fontaine DA, Davis DB. Attention to Background Strain Is Essential for Metabolic Research: C57BL/6 and the International Knockout Mouse Consortium. *Diabetes.* 2016 Jan;65(1):25-33. doi: 10.2337/db15-0982. PMID: 26696638; PMCID: PMC4686949.

Forbes JM, Cooper ME. Mechanisms of diabetic complications. *Physiol Rev.* 2013 Jan;93(1):137-88. doi: 10.1152/physrev.00045.2011. PMID: 23303908.

Foreman KJ, Marquez N, Dolgert A, et al. Forecasting life expectancy, years of life lost, and all-cause and cause-specific mortality for 250 causes of death: reference and alternative scenarios for 2016-40 for 195 countries and territories. *Lancet* 2018; 392: 2052-90.

Fraulob JC, Ogg-Diamantino R, Fernandes-Santos C, Aguila MB, Mandarim-de-Lacerda CA. A Mouse Model of Metabolic Syndrome: Insulin Resistance, Fatty Liver and Non-Alcoholic Fatty Pancreas Disease (NAFPD) in C57BL/6 Mice Fed a High Fat Diet. *J Clin Biochem Nutr.* 2010 May;46(3):212-23. doi: 10.3164/jcbn.09-83. Epub 2010 Apr 10. PMID: 20490316; PMCID: PMC2872226.

Fu J, Astarita G, Gaetani S, Kim J, Cravatt BF, Mackie K, Piomelli D. Food intake regulates oleoylethanolamide formation and degradation in the proximal small intestine. *J Biol Chem.* 2007 Jan 12;282(2):1518-28. doi: 10.1074/jbc.M607809200. Epub 2006 Nov 22. PMID: 17121838; PMCID: PMC1764767.

Fu J, Astarita G, Gaetani S, Kim J, Cravatt BF, Mackie K, Piomelli D. Food intake regulates oleoylethanolamide formation and degradation in the proximal small intestine. *J Biol Chem.* 2007 Jan 12;282(2):1518-28. doi: 10.1074/jbc.M607809200. Epub 2006 Nov 22. PMID: 17121838; PMCID: PMC1764767.

Fu J, Dipatrizio NV, Guijarro A, Schwartz GJ, Li X, Gaetani S, Astarita G, Piomelli D. Sympathetic activity controls fat-induced oleoylethanolamide signaling in small intestine. *J Neurosci.* 2011 Apr 13;31(15):5730-6. doi: 10.1523/JNEUROSCI.5668-10.2011. PMID: 21490214; PMCID: PMC3084524.

Fu J, Gaetani S, Oveisi F, Lo Verme J, Serrano A, Rodríguez De Fonseca F, Rosengarth A, Luecke H, Di Giacomo B, Tarzia G, Piomelli D. Oleylethanolamide regulates feeding and body weight through activation of the nuclear receptor PPAR-alpha. *Nature.* 2003 Sep 4;425(6953):90-3. doi: 10.1038/nature01921. PMID: 12955147.

Fu J, Gaetani S, Oveisi F, Lo Verme J, Serrano A, Rodríguez De Fonseca F, Rosengarth A, Luecke H, Di Giacomo B, Tarzia G, Piomelli D. Oleylethanolamide regulates feeding and body weight through activation of the nuclear receptor PPAR-alpha. *Nature.* 2003 Sep 4;425(6953):90-3. doi: 10.1038/nature01921. PMID: 12955147.

Fu J, Gaetani S, Oveisi F, Lo Verme J, Serrano A, Rodríguez De Fonseca F, Rosengarth A, Luecke H, Di Giacomo B, Tarzia G, Piomelli D. Oleylethanolamide regulates feeding and body weight through activation of the nuclear receptor PPAR-alpha. *Nature.* 2003 Sep 4;425(6953):90-3. doi: 10.1038/nature01921. PMID: 12955147.

Fu J, Kim J, Oveisi F, Astarita G, Piomelli D. Targeted enhancement of oleoylethanolamide production in proximal small intestine induces across-meal satiety in rats. *Am J Physiol Regul Integr Comp Physiol*. 2008 Jul;295(1):R45-50. doi: 10.1152/ajpregu.00126.2008. Epub 2008 Apr 23. PMID: 18434444; PMCID: PMC2494809.

Fu J, Oveisi F, Gaetani S, Lin E, Piomelli D. Oleoylethanolamide, an endogenous PPAR-alpha agonist, lowers body weight and hyperlipidemia in obese rats. *Neuropharmacology*. 2005 Jun;48(8):1147-53. doi: 10.1016/j.neuropharm.2005.02.013. Epub 2005 Apr 21. PMID: 15910890.

Fu J, Oveisi F, Gaetani S, Lin E, Piomelli D. Oleoylethanolamide, an endogenous PPAR-alpha agonist, lowers body weight and hyperlipidemia in obese rats. *Neuropharmacology*. 2005 Jun;48(8):1147-53. doi: 10.1016/j.neuropharm.2005.02.013. Epub 2005 Apr 21. PMID: 15910890.

Gaetani S, Fu J, Cassano T, Dipasquale P, Romano A, Righetti L, Cianci S, Laconca L, Giannini E, Scaccianoce S, Mairesse J, Cuomo V, Piomelli D. The fat-induced satiety factor oleoylethanolamide suppresses feeding through central release of oxytocin. *J Neurosci*. 2010 Jun 16;30(24):8096-101. doi: 10.1523/JNEUROSCI.0036-10.2010. PMID: 20554860; PMCID: PMC2900249.

Gaetani S, Oveisi F, Piomelli D. Modulation of meal pattern in the rat by the anorexic lipid mediator oleoylethanolamide. *Neuropsychopharmacology*. 2003 Jul;28(7):1311-6. doi: 10.1038/sj.npp.1300166. Epub 2003 Apr 2. PMID: 12700681.

Galan-Rodriguez B, Suarez J, Gonzalez-Aparicio R, Bermudez-Silva FJ, Maldonado R, Robledo P, Rodriguez de Fonseca F, Fernandez-Espejo E. Oleoylethanolamide exerts partial and dose-dependent neuroprotection of substantia nigra dopamine neurons. *Neuropharmacology*. 2009 Mar;56(3):653-64. doi: 10.1016/j.neuropharm.2008.11.006. Epub 2008 Dec 7. PMID: 19070629.

Gao J, Gu Z. The Role of Peroxisome Proliferator-Activated Receptors in Kidney Diseases. *Front Pharmacol*. 2022 Mar 4;13:832732. doi: 10.3389/fphar.2022.832732. PMID: 35308207; PMCID: PMC8931476.

Gelosa P, Banfi C, Gianella A, Brioschi M, Pignieri A, Nobili E, Castiglioni L, Cimino M, Tremoli E, Sironi L. Peroxisome proliferator-activated receptor {alpha} agonism prevents renal damage and the oxidative stress and inflammatory processes affecting the brains of stroke-prone rats. *J Pharmacol Exp Ther*. 2010

Nov;335(2):324-31. doi: 10.1124/jpet.110.171090. Epub 2010 Jul 29. PMID: 20671072.

Ginion A, Auquier J, Benton CR, Mouton C, Vanoverschelde JL, Hue L, Horman S, Beauloye C, Bertrand L. Inhibition of the mTOR/p70S6K pathway is not involved in the insulin-sensitizing effect of AMPK on cardiac glucose uptake. *Am J Physiol Heart Circ Physiol*. 2011 Aug;301(2):H469-77. doi: 10.1152/ajpheart.00986.2010. Epub 2011 May 20. PMID: 21602475.

Ginsberg HN, MacCallum PR. The obesity, metabolic syndrome, and type 2 diabetes mellitus pandemic: Part I. Increased cardiovascular disease risk and the importance of atherogenic dyslipidemia in persons with the metabolic syndrome and type 2 diabetes mellitus. *J Cardiometab Syndr*. 2009 Spring;4(2):113-9. doi: 10.1111/j.1559-4572.2008.00044.x. PMID: 19614799; PMCID: PMC2901596.

Glatz JFC, Luiken JJFP, Nabben M. CD36 (SR-B2) as a Target to Treat Lipid Overload-Induced Cardiac Dysfunction. *J Lipid Atheroscler*. 2020 Jan;9(1):66-78. doi: 10.12997/jla.2020.9.1.66. Epub 2020 Jan 8. PMID: 32821722; PMCID: PMC7379071.

Gomez G, Stanford FC. US health policy and prescription drug coverage of FDA-approved medications for the treatment of obesity. *Int J Obes (Lond)*. 2018 Mar;42(3):495-500. doi: 10.1038/ijo.2017.287. Epub 2017 Nov 20. PMID: 29151591; PMCID: PMC6082126.

Gong S, Ye T, Wang M, Wang M, Li Y, Ma L, Yang Y, Wang Y, Zhao X, Liu L, Yang M, Chen H, Qian J. Traditional Chinese Medicine Formula *Kang Shuai Lao Pian* Improves Obesity, Gut Dysbiosis, and Fecal Metabolic Disorders in High-Fat Diet-Fed Mice. *Front Pharmacol*. 2020 Mar 25;11:297. doi: 10.3389/fphar.2020.00297. PMID: 32269525; PMCID: PMC7109517.

Gonzalez-Aparicio R, Blanco E, Serrano A, Pavon FJ, Parsons LH, Maldonado R, Robledo P, Fernandez-Espejo E, de Fonseca FR. The systemic administration of oleoylethanolamide exerts neuroprotection of the nigrostriatal system in experimental Parkinsonism. *Int J Neuropsychopharmacol*. 2014 Mar;17(3):455-68. doi: 10.1017/S1461145713001259. Epub 2013 Oct 29. PMID: 24169105.

González-Guerrero C, Morgado-Pascual JL, Cannata-Ortiz P, et al. CCL20 blockade increases the severity of nephrotoxic folic acid-induced acute kidney injury. *J Pathol*. 2018;246(2):191-204. doi:10.1002/path.5132

Goossens JF, Thuru X, Bailly C. Properties and reactivity of the folic acid and folate photoproduct 6-formylpterin. *Free Radic Biol Med.* 2021;171:1-10. doi:10.1016/j.freeradbiomed.2021.05.002

Greenway FL, Aronne LJ, Raben A, Astrup A, Apovian CM, Hill JO, et al. A Randomized, Double-Blind, Placebo-Controlled Study of Gelesis100: A Novel Nonsystemic Oral Hydrogel for Weight Loss. *Obes (Silver Spring)* (2019) 27:205–16. doi: 10.1002/oby.22347

Gregg EW, Shaw JE. Global Health Effects of Overweight and Obesity. *N Engl J Med.* 2017 Jul 6;377(1):80-81. doi: 10.1056/NEJMe1706095. Epub 2017 Jun 12. PMID: 28604226.

Guan Y, Zhang Y, Davis L, Breyer MD. Expression of peroxisome proliferator-activated receptors in urinary tract of rabbits and humans. *Am J Physiol.* 1997 Dec;273(6):F1013-22. doi: 10.1152/ajprenal.1997.273.6.F1013. PMID: 9435691.

Guellich A, Damy T, Lecarpentier Y, Conti M, Claes V, Samuel JL, Quillard J, Hébert JL, Pineau T, Coirault C. Role of oxidative stress in cardiac dysfunction of PPARalpha-/- mice. *Am J Physiol Heart Circ Physiol.* 2007 Jul;293(1):H93-H102. doi: 10.1152/ajpheart.00037.2007. Epub 2007 Mar 16. PMID: 17369471.

Guo L. and R. Tabrizchi, "Peroxisome proliferator-activated receptor gamma as a drug target in the pathogenesis of insulin resistance," *Pharmacology and Therapeutics*, vol. 111, no. 1, pp. 145–173, 2006.

Gupta A, Puri V, Sharma R, Puri S. Folic acid induces acute renal failure (ARF) by enhancing renal prooxidant state. *Exp Toxicol Pathol.* 2012;64(3):225-232. doi:10.1016/j.etp.2010.08.010

Gupta A, Puri V, Sharma R, Puri S. Folic acid induces acute renal failure (ARF) by enhancing renal prooxidant state. *Exp Toxicol Pathol.* 2012;64(3):225-232. doi:10.1016/j.etp.2010.08.010

Guzmán M, Lo Verme J, Fu J, Oveisi F, Blázquez C, Piomelli D. Oleoylethanolamide stimulates lipolysis by activating the nuclear receptor peroxisome proliferator-activated receptor alpha (PPAR-alpha). *J Biol Chem.* 2004 Jul 2;279(27):27849-54. doi: 10.1074/jbc.M404087200. Epub 2004 Apr 26. PMID: 15123613.

Hansen, H. S., Diep, T. A. (2009) N-acylethanolamines, anandamide and food intake. *Biochem.Pharmacol.* 78, 553–560.

Hardie DG, Ross FA, Hawley SA. AMPK: a nutrient and energy sensor that maintains energy homeostasis. *Nat Rev Mol Cell Biol.* 2012 Mar 22;13(4):251-62. doi: 10.1038/nrm3311. PMID: 22436748; PMCID: PMC5726489.

Heim P, Morandi C, Brouwer GR, Xu L, Montessuit C, Brink M. Neuregulin-1 triggers GLUT4 translocation and enhances glucose uptake independently of insulin receptor substrate and ErbB3 in neonatal rat cardiomyocytes. *Biochim Biophys acta Mol cell Res.* 2020;1867(3):118562.

Hiukka A, Maranghi M, Matikainen N, Taskinen MR. PPARalpha: an emerging therapeutic target in diabetic microvascular damage. *Nat Rev Endocrinol.* 2010 Aug;6(8):454-63. doi: 10.1038/nrendo.2010.89. Epub 2010 Jun 22. Erratum in: *Nat Rev Endocrinol.* 2010 Sep;6(9):476. PMID: 20567246.

Hodgkins, K. S. & Schnaper, H. W. Tubulointerstitial injury and the progression of chronic kidney disease. *Pediatr. Nephrol.* 27, 901–909 (2012).

Hong F, Pan S, Guo Y, Xu P, Zhai Y. PPARs as Nuclear Receptors for Nutrient and Energy Metabolism. *Molecules.* 2019 Jul 12;24(14):2545. doi: 10.3390/molecules24142545. PMID: 31336903; PMCID: PMC6680900.

Hou X, Shen YH, Li C, Wang F, Zhang C, Bu P, Zhang Y. PPARalpha agonist fenofibrate protects the kidney from hypertensive injury in spontaneously hypertensive rats via inhibition of oxidative stress and MAPK activity. *Biochem Biophys Res Commun.* 2010 Apr 9;394(3):653-9. doi: 10.1016/j.bbrc.2010.03.043. Epub 2010 Mar 11. PMID: 20226762.

Hsueh W, Rostorfer HH. Chemically induced renal hypertrophy in the rat. *Lab Invest.* 1973 Nov;29(5):547-55. PMID: 4753020.

Hu L, Ding M, He W. Emerging Therapeutic Strategies for Attenuating Tubular EMT and Kidney Fibrosis by Targeting Wnt/ β -Catenin Signaling. *Front Pharmacol.* 2022 Jan 10;12:830340. doi: 10.3389/fphar.2021.830340. PMID: 35082683; PMCID: PMC8784548.

Humphreys BD. Mechanisms of Renal Fibrosis. *Annu Rev Physiol.* 2018 Feb 10;80:309-326. doi: 10.1146/annurev-physiol-022516-034227. Epub 2017 Oct 25. PMID: 29068765.

Hwang SY, Siow YL, Au-Yeung KKW, House J, O K. Folic acid supplementation inhibits NADPH oxidase-mediated superoxide anion production in the kidney. *Am*

J Physiol Renal Physiol. 2011;300(1):F189-F198.
doi:10.1152/ajprenal.00272.2010

induced diabetic cardiomyopathy. Prostaglandins Leukot Essent Fatty Acids. 2011 Nov;85(5):219-25. doi: 10.1016/j.plefa.2011.04.018. Epub 2011 May 14. PMID: 21571515.

Iwaki T, Bennion BG, Stenson EK, Lynn JC, Otinga C, Djukovic D, Raftery D, Fei L, Wong HR, Liles WC, Standage SW. PPAR α contributes to protection against metabolic and inflammatory derangements associated with acute kidney injury in experimental sepsis. *Physiol Rep*. 2019 May;7(10):e14078. doi: 10.14814/phy2.14078. PMID: 31102342; PMCID: PMC6525329.

Izquierdo-Lahuerta A, Martínez-García C, Medina-Gómez G. Lipotoxicity as a trigger factor of renal disease. *J Nephrol*. 2016 Oct;29(5):603-10. doi: 10.1007/s40620-016-0278-5. Epub 2016 Mar 8. PMID: 26956132.

Izzedine H, Launay-Vacher V, Baumelou A, Deray G. Renal effects of PPAR α agonists. *Minerva Urol Nefrol*. 2004 Dec;56(4):339-42. PMID: 15785426.

Ji, S., He, D.D., Wang, T.Y., Han, J., Li, Z., Du, Y., Zou, J.H., Guo, M.Z., Tang, D.Q., 2017. Separation and characterization of chemical constituents in Ginkgo biloba extract by off-line hydrophilic interaction reversed-phase two-dimensional liquid chromatography coupled with quadrupole-time of flight mass spectrometry.

Jia G, DeMarco VG, Sowers JR. Insulin resistance and hyperinsulinaemia in diabetic cardiomyopathy. *Nat Rev Endocrinol*. 2016 Mar;12(3):144-53. doi: 10.1038/nrendo.2015.216. Epub 2015 Dec 18. PMID: 26678809; PMCID: PMC4753054.

Jiang K, Ponzo TA, Tang H, Mishra PK, Macura SI, Lerman LO. Multiparametric MRI detects longitudinal evolution of folic acid-induced nephropathy in mice. *Am J Physiol Renal Physiol*. 2018;315(5):F1252-F1260. doi:10.1152/ajprenal.00128.2018

Jie, L., & Hai, H. (2005). Clinical observation of Ginkgo biloba extract injection in treating early diabetic nephropathy. *Chinese Journal of Integrative Medicine*, 11(3), 226–228.

Jin P, Yu HL, Tian-Lan, Zhang F, Quan ZS. Antidepressant-like effects of oleylethanolamide in a mouse model of chronic unpredictable mild stress.

Pharmacol Biochem Behav. 2015 Jun;133:146-54. doi: 10.1016/j.pbb.2015.04.001. Epub 2015 Apr 10. PMID: 25864425.

Joles JA, Kunter U, Janssen U, Kriz W, Rabelink TJ, Koomans HA, Floege J. Early mechanisms of renal injury in hypercholesterolemic or hypertriglyceridemic rats. *J Am Soc Nephrol.* 2000 Apr;11(4):669-683. doi: 10.1681/ASN.V114669. PMID: 10752526.

Kabeya Y, Mizushima N, Ueno T, Yamamoto A, Kirisako T, Noda T, et al. LC3, a mammalian homologue of yeast Apg8p, is localized in autophagosome membranes after processing. *EMBO J.* 2000;19(21):5720–8.

Kadowaki T, Maegawa H, Watada H, Yabe D, Node K, Murohara T, Wada J. Interconnection between cardiovascular, renal and metabolic disorders: A narrative review with a focus on Japan. *Diabetes Obes Metab.* 2022 Dec;24(12):2283-2296. doi: 10.1111/dom.14829. Epub 2022 Aug 25. PMID: 35929483; PMCID: PMC9804928.

Kalantar-Zadeh K, Jafar TH, Nitsch D, Neuen BL, Perkovic V. Chronic kidney disease. *Lancet.* 2021 Aug 28;398(10302):786-802. doi: 10.1016/S0140-6736(21)00519-5. Epub 2021 Jun 24. PMID: 34175022.

Kamijo Y, Hora K, Tanaka N, Usuda N, Kiyosawa K, Nakajima T, Gonzalez FJ, Aoyama T. Identification of functions of peroxisome proliferator-activated receptor alpha in proximal tubules. *J Am Soc Nephrol.* 2002 Jul;13(7):1691-702. doi: 10.1097/01.asn.0000018403.61042.56. PMID: 12089364.

Kang, H. (2017). Hypocholesterolemic effect of Ginkgo biloba seeds extract from high fat diet mice. *Biomedical Science Letters*, 23(2), 138–143. doi: BSL-23-138

Kao MP, Ang DS, Pall A, Struthers AD. Oxidative stress in renal dysfunction: mechanisms, clinical sequelae and therapeutic options. *J Hum Hypertens.* 2010 Jan;24(1):1-8. doi: 10.1038/jhh.2009.70. PMID: 19727125.

Karri S, Sharma S, Hatware K, Patil K. Natural anti-obesity agents and their therapeutic role in management of obesity: A future trend perspective. *Biomed Pharmacother.* 2019 Feb;110:224-238. doi: 10.1016/j.biopha.2018.11.076. Epub 2018 Nov 24. PMID: 30481727.

Karwi QG, Sun Q, Lopaschuk GD. The Contribution of Cardiac Fatty Acid Oxidation to Diabetic Cardiomyopathy Severity. *Cells.* 2021 Nov 21;10(11):3259. doi: 10.3390/cells10113259. PMID: 34831481; PMCID: PMC8621814.

Katsuragi Y, Ichimura Y, Komatsu M. p62/SQSTM1 functions as a signaling hub and an autophagy adaptor. *FEBS J.* 2015 Dec;282(24):4672-8. doi: 10.1111/febs.13540. Epub 2015 Oct 16. PMID: 26432171.

Kaur N, Dhiman M, Perez-Polo JR, Mantha AK. Ginkgolide B revamps neuroprotective role of apurinic/aprimidinic endonuclease 1 and mitochondrial oxidative phosphorylation against A β 25-35 -induced neurotoxicity in human neuroblastoma cells. *J Neurosci Res.* 2015 Jun;93(6):938-47. doi: 10.1002/jnr.23565. Epub 2015 Feb 9. PMID: 25677400.

Kazancioğlu R. Risk factors for chronic kidney disease: an update. *Kidney Int Suppl* (2011). 2013 Dec;3(4):368-371. doi: 10.1038/kisup.2013.79. PMID: 25019021; PMCID: PMC4089662.

Kikas P, Chalikias G, Tziakas D. Cardiovascular Implications of Sphingomyelin Presence in Biological Membranes. *Eur Cardiol.* 2018 Aug;13(1):42-45. doi: 10.15420/ecr.2017:20:3. PMID: 30310470; PMCID: PMC6159463.

Kim SR, Jiang K, Ogrodnik M, Chen X, Zhu XY, Lohmeier H, Ahmed L, Tang H, Tchkonja T, Hickson LJ, Kirkland JL, Lerman LO. Increased renal cellular senescence in murine high-fat diet: effect of the senolytic drug quercetin. *Transl Res.* 2019 Nov;213:112-123. doi: 10.1016/j.trsl.2019.07.005. Epub 2019 Jul 15. PMID: 31356770; PMCID: PMC6783353.

Kimmelman AC, White E. Autophagy and Tumor Metabolism. *Cell Metab.* 2017 May 2;25(5):1037-1043. doi: 10.1016/j.cmet.2017.04.004. PMID: 28467923; PMCID: PMC5604466.

Kirschbaum BB. Alterations of mitochondrial properties in folate nephropathy. *Nephron.* 1979;24(6):297-301. doi:10.1159/000181740

Kleberg, K.; Hassing, H.A.; Hansen, H.S. Classical endocannabinoid-like compounds and their regulation by nutrients. *Biofactors* 2014, 40, 363–372

Klionsky DJ, Abdelmohsen K, Abe A, Abedin MJ, Abeliovich H, Arozena AA, et al. Guidelines for the use and interpretation of assays for monitoring autophagy (3rd edition) [Internet]. Vol. 12, *Autophagy*. Taylor and Francis Inc.; 2016. p. 1– 222.

Kops NL, Vivan MA, Fülber ER, Fleuri M, Fagundes J, Friedman R. Preoperative Binge Eating and Weight Loss After Bariatric Surgery: A Systematic Review and Meta-Analysis. *Obes Surg* (2020) 31(3):1239–48. doi: 10.1007/s11695-020-05124-9

Kramer HF, Witczak CA, Fujii N, Jessen N, Taylor EB, Arnolds DE, Sakamoto K, Hirshman MF, Goodyear LJ. Distinct signals regulate AS160 phosphorylation in response to insulin, AICAR, and contraction in mouse skeletal muscle. *Diabetes*. 2006 Jul;55(7):2067-76. doi: 10.2337/db06-0150. PMID: 16804077.

Kramer, Karl Ulrich, and P. S. Green. "Introduction to pteridophytes and gymnosperms." *Pteridophytes and Gymnosperms*. Springer, Berlin, Heidelberg, 1990. 1-1.

Kriegelstein J, Beck T, Seibert A. Influence of an extract of Ginkgo biloba on cerebral blood flow and metabolism. *Life Sci*. 1986 Dec 15;39(24):2327-34. doi: 10.1016/0024-3205(86)90663-6. PMID: 3796196.

Kudolo GB. The effect of 3-month ingestion of Ginkgo biloba extract (EGb 761) on pancreatic beta-cell function in response to glucose loading in individuals with non-insulin-dependent diabetes mellitus. *J Clin Pharmacol*. 2001 Jun;41(6):600-11. doi: 10.1177/00912700122010483. PMID: 11402628.

Kumar D, Singla SK, Puri V, Puri S. The restrained expression of NF- κ B in renal tissue ameliorates folic acid induced acute kidney injury in mice. *PLoS One*. 2015;10(1):e115947. doi:10.1371/journal.pone.0115947

Kuwahara S, Hosojima M, Kaneko R, Aoki H, Nakano D, Sasagawa T, Kabasawa H, Kaseda R, Yasukawa R, Ishikawa T, Suzuki A, Sato H, Kageyama S, Tanaka T, Kitamura N, Narita I, Komatsu M, Nishiyama A, Saito A. Megalin-Mediated Tubuloglomerular Alterations in High-Fat Diet-Induced Kidney Disease. *J Am Soc Nephrol*. 2016 Jul;27(7):1996-2008. doi: 10.1681/ASN.2015020190. Epub 2015 Nov 3. PMID: 26534923; PMCID: PMC4926965.

Lakkis JI, Weir MR. Obesity and Kidney Disease. *Prog Cardiovasc Dis*. 2018 Jul-Aug;61(2):157-167. doi: 10.1016/j.pcad.2018.07.005. Epub 2018 Jul 5. PMID: 29981350.

Lan H, Vassileva G, Corona A, Liu L, Baker H, Golovko A, Abbondanzo SJ, Hu W, Yang S, Ning Y, Del Vecchio RA, Poulet F, Lavery M, Gustafson EL, Hedrick JA, Kowalski TJ. GPR119 is required for physiological regulation of glucagon-like peptide-1 secretion but not for metabolic homeostasis. *J Endocrinol*. 2009 May;201(2):219-30. doi: 10.1677/JOE-08-0453. Epub 2009 Mar 12. PMID: 19282326.

Lan HY, Chung AC. TGF- β /Smad signaling in kidney disease. *Semin Nephrol*. 2012 May;32(3):236-43. doi: 10.1016/j.semnephrol.2012.04.002. PMID: 22835454.

Lasaitė, L., Spadiene, A., Savickienė, N., Skesters, A., & Silova, A. (2014). The effect of Ginkgo biloba and Camellia sinensis extracts on psychological state and glycemic control in patients with type 2 diabetes mellitus. *Natural Product Communications*, 9(9), 1934578X1400900

Lee EY, Yoon KH. Epidemic Obesity in Children and Adolescents: Risk Factors and Prevention. *Front Med* (2018) 12(6):658–66. doi: 10.1007/s11684-018-0640-1

Lee SY, Kim SI, Choi ME. Therapeutic targets for treating fibrotic kidney diseases. *Transl Res*. 2015 Apr;165(4):512-30. doi: 10.1016/j.trsl.2014.07.010. Epub 2014 Aug 13. PMID: 25176603; PMCID: PMC4326607.

Lee WS, Kim J. Peroxisome Proliferator-Activated Receptors and the Heart: Lessons from the Past and Future Directions. *PPAR Res*. 2015;2015:271983. doi: 10.1155/2015/271983. Epub 2015 Oct 26. PMID: 26587015; PMCID: PMC4637490.

Lefebvre P, Chinetti G, Fruchart JC, Staels B. Sorting out the roles of PPAR alpha in energy metabolism and vascular homeostasis. *J Clin Invest*. 2006 Mar;116(3):571-80. doi: 10.1172/JCI27989. PMID: 16511589; PMCID: PMC1386122.

Li S, Mariappan N, Megyesi J, Shank B, Kannan K, Theus S, Price PM, Duffield JS, Portilla D. Proximal tubule PPAR α attenuates renal fibrosis and inflammation caused by unilateral ureteral obstruction. *Am J Physiol Renal Physiol*. 2013 Sep 1;305(5):F618-27. doi: 10.1152/ajprenal.00309.2013. Epub 2013 Jun 26. PMID: 23804447; PMCID: PMC3761210.

Li S, Mariappan N, Megyesi J, Shank B, Kannan K, Theus S, Price PM, Duffield JS, Portilla D. Proximal tubule PPAR α attenuates renal fibrosis and inflammation caused by unilateral ureteral obstruction. *Am J Physiol Renal Physiol*. 2013 Sep 1;305(5):F618-27. doi: 10.1152/ajprenal.00309.2013. Epub 2013 Jun 26. PMID: 23804447; PMCID: PMC3761210.

Li S, Nagothu KK, Desai V, Lee T, Branham W, Moland C, Megyesi JK, Crew MD, Portilla D. Transgenic expression of proximal tubule peroxisome proliferator-activated receptor-alpha in mice confers protection during acute kidney injury. *Kidney Int*. 2009 Nov;76(10):1049-62. doi: 10.1038/ki.2009.330. Epub 2009 Aug 26. PMID: 19710628; PMCID: PMC3244273.

Li S, Nagothu KK, Desai V, Lee T, Branham W, Moland C, Megyesi JK, Crew MD, Portilla D. Transgenic expression of proximal tubule peroxisome proliferator-

activated receptor-alpha in mice confers protection during acute kidney injury. *Kidney Int.* 2009 Nov;76(10):1049-62. doi: 10.1038/ki.2009.330. Epub 2009 Aug 26. PMID: 19710628; PMCID: PMC3244273.

Li X, Zou Y, Fu YY, Xing J, Wang KY, Wan PZ, Wang M, Zhai XY. Ibudilast Attenuates Folic Acid-Induced Acute Kidney Injury by Blocking Pyroptosis Through TLR4-Mediated NF- κ B and MAPK Signaling Pathways. *Front Pharmacol.* 2021 May 7;12:650283. doi: 10.3389/fphar.2021.650283. PMID: 34025417; PMCID: PMC8139578.

Li Y, Xiong Y, Zhang H, Li J, Wang D, Chen W, Yuan X, Su Q, Li W, Huang H, Bi Z, Liu L, Wang C. Ginkgo biloba extract EGb761 attenuates brain death-induced renal injury by inhibiting pro-inflammatory cytokines and the SAPK and JAK-STAT signalings. *Sci Rep.* 2017 Mar 23;7:45192. doi: 10.1038/srep45192. PMID: 28332628; PMCID: PMC5362910.

Li, X.-S., Zheng, W.-Y., Lou, S.-X., Lu, X.-W., & Ye, S.-H. (2009). Effect of Ginkgo leaf extract on vascular endothelial function in patients with early stage diabetic nephropathy. *Chinese Journal of Integrative Medicine*, 15(1), 26–29.

Lieberman M, Marks AD. Marks' Basic Medical Biochemistry: A clinical Approach. 4th ed. Wolters Kluwer/Lippincott Williams & Wilkins; 2013.

Lin X, Li H. Obesity: Epidemiology, Pathophysiology, and Therapeutics. *Front Endocrinol (Lausanne).* 2021 Sep 6;12:706978. doi: 10.3389/fendo.2021.706978. PMID: 34552557; PMCID: PMC8450866.

Lin Y, Wang Y, Li PF. PPAR α : An emerging target of metabolic syndrome, neurodegenerative and cardiovascular diseases. *Front Endocrinol (Lausanne).* 2022 Dec 16;13:1074911. doi: 10.3389/fendo.2022.1074911. PMID: 36589809; PMCID: PMC9800994.

Liu M, Liu SW, Wang LJ, Bai YM, Zeng XY, Guo HB, Liu YN, Jiang YY, Dong WL, He GX, Zhou MG, Yu SC. Burden of diabetes, hyperglycaemia in China from to 2016: Findings from the 1990 to 2016, global burden of disease study. *Diabetes Metab.* 2019 Jun;45(3):286-293. doi: 10.1016/j.diabet.2018.08.008. Epub 2018 Sep 6. PMID: 30196138.

Liu Y, Xin H, Zhang Y, Che F, Shen N, Cui Y. Leaves, seeds and exocarp of Ginkgo biloba L. (Ginkgoaceae): A Comprehensive Review of Traditional Uses, phytochemistry, pharmacology, resource utilization and toxicity. *J*

Ethnopharmacol. 2022 Nov 15;298:115645. doi: 10.1016/j.jep.2022.115645. Epub 2022 Aug 19. PMID: 35988840.

Liu Y. Cellular and molecular mechanisms of renal fibrosis. *Nat Rev Nephrol*. 2011 Oct 18;7(12):684-96. doi: 10.1038/nrneph.2011.149. PMID: 22009250; PMCID: PMC4520424.

Lobos P, Regulska-Ilow B. Link between methyl nutrients and the DNA methylation process in the course of selected diseases in adults. *Rocz Panstw Zakl Hig*. 2021;72(2):123-136. doi:10.32394/rpzh.2021.0157

Loos B, Engelbrecht A-M, Lockshin RA, Klionsky DJ, Zakari Z. The variability of autophagy and cell death susceptibility. *Autophagy*. 2013;9(9):1270–85.

Lopaschuk GD, Karwi QG, Tian R, Wende AR, Abel ED. Cardiac Energy Metabolism in Heart Failure. *Circ Res*. 2021 May 14;128(10):1487-1513. doi: 10.1161/CIRCRESAHA.121.318241. Epub 2021 May 13. PMID: 33983836; PMCID: PMC8136750.

LoVerme J, Guzmán M, Gaetani S, Piomelli D. Cold exposure stimulates synthesis of the bioactive lipid oleoylethanolamide in rat adipose tissue. *J Biol Chem*. 2006 Aug 11;281(32):22815-8. doi: 10.1074/jbc.M604751200. Epub 2006 Jun 19. PMID: 16785227.

Lu Q, Zuo WZ, Ji XJ, Zhou YX, Liu YQ, Yao XQ, Zhou XY, Liu YW, Zhang F, Yin XX. Ethanolic Ginkgo biloba leaf extract prevents renal fibrosis through Akt/mTOR signaling in diabetic nephropathy. *Phytomedicine*. 2015 Nov 15;22(12):1071-8. doi: 10.1016/j.phymed.2015.08.010. Epub 2015 Sep 6. PMID: 26547529.

luJung JH, Choi JE, Song JH, Ahn SH. Human CD36 overexpression in renal tubules accelerates the progression of renal diseases in a mouse model of folic acid-induced acute kidney injury. *Kidney Res Clin Pract*. 2018;37(1):30-40. doi:10.23876/j.krcp.2018.37.1.30

Mahadevan S, Park Y. Multifaceted therapeutic benefits of Ginkgo biloba L.: chemistry, efficacy, safety, and uses. *J Food Sci*. 2008 Jan;73(1):R14-9. doi: 10.1111/j.1750-3841.2007.00597.x. PMID: 18211362.

Mariani MM, Malm T, Lamb R, Jay TR, Neilson L, Casali B, Medarametla L, Landreth GE. Neuronally-directed effects of RXR activation in a mouse model of Alzheimer's disease. *Sci Rep*. 2017 Feb 16;7:42270. doi: 10.1038/srep42270. PMID: 28205585; PMCID: PMC5311933.

Martínez-García C, Izquierdo-Lahuerta A, Vivas Y, Velasco I, Yeo TK, Chen S, Medina-Gomez G. Renal Lipotoxicity-Associated Inflammation and Insulin Resistance Affects Actin Cytoskeleton Organization in Podocytes. *PLoS One*. 2015 Nov 6;10(11):e0142291. doi: 10.1371/journal.pone.0142291. PMID: 26545114; PMCID: PMC4636358.

Marx N, Duez H, Fruchart JC, Staels B. Peroxisome proliferator-activated receptors and atherogenesis: regulators of gene expression in vascular cells. *Circ Res*. 2004 May 14;94(9):1168-78. doi: 10.1161/01.RES.0000127122.22685.0A. PMID: 15142970.

Mattace Raso G, Simeoli R, Russo R, Santoro A, Pirozzi C, d'Emmanuele di Villa Bianca R, Mitidieri E, Paciello O, Pagano TB, Orefice NS, Meli R, Calignano A. N-Palmitoylethanolamide protects the kidney from hypertensive injury in spontaneously hypertensive rats via inhibition of oxidative stress. *Pharmacol Res*. 2013 Oct;76:67-76. doi: 10.1016/j.phrs.2013.07.007. Epub 2013 Aug 2. PMID: 23917217.

Mattina A, Argano C, Brunori G, Lupo U, Raspanti M, Lo Monaco M, Bocchio RM, Natoli G, Giusti MA, Corrao S. Clinical complexity and diabetes: a multidimensional approach for the management of cardiorenal metabolic syndrome. *Nutr Metab Cardiovasc Dis*. 2022 Dec;32(12):2730-2738. doi: 10.1016/j.numecd.2022.09.008. Epub 2022 Sep 27. PMID: 36328836.

McKinney MK, Cravatt BF. Structure and function of fatty acid amide hydrolase. *Annu Rev Biochem*. 2005;74:411-32. doi: 10.1146/annurev.biochem.74.082803.133450. PMID: 15952893.

Meng XM, Chung AC, Lan HY. Role of the TGF- β /BMP-7/Smad pathways in renal diseases. *Clin Sci (Lond)*. 2013 Feb;124(4):243-54. doi: 10.1042/CS20120252. PMID: 23126427.

Meng, X.-M., Nikolic-Paterson, D. J. & Lan, H. Y. Inflammatory processes in renal fibrosis. *Nat. Rev. Nephrol*. 10, 493–503 (2014).

Michalik L., J. Auwerx, J. P. Berger et al., "International union of pharmacology. LXI. Peroxisome proliferator-activated receptors," *Pharmacological Reviews*, vol. 58, no. 4, pp. 726–741, 2006.

Mock ED, Gaggestein B, van der Stelt M. Anandamide and other N-acyl ethanolamines: A class of signaling lipids with therapeutic opportunities. *Prog*

Lipid Res. 2022 Sep 20:101194. doi: 10.1016/j.plipres.2022.101194. Epub ahead of print. PMID: 36150527.

Mohanta TK, Occhipinti A, Atsbaha Zebelo S, Foti M, Fliegmann J, Bossi S, Maffei ME, Berteza CM. Ginkgo biloba responds to herbivory by activating early signaling and direct defenses. *PLoS One*. 2012;7(3):e32822. doi: 10.1371/journal.pone.0032822. Epub 2012 Mar 20. PMID: 22448229; PMCID: PMC3308967.

Montaigne D, Butruille L, Staels B. PPAR control of metabolism and cardiovascular functions. *Nat Rev Cardiol*. 2021 Dec;18(12):809-823. doi: 10.1038/s41569-021-00569-6. Epub 2021 Jun 14. PMID: 34127848.

Nabavi SM, Habtemariam S, Daglia M, Braidy N, Loizzo MR, Tundis R, Nabavi SF. Neuroprotective Effects of Ginkgolide B Against Ischemic Stroke: A Review of Current Literature. *Curr Top Med Chem*. 2015;15(21):2222-32. doi: 10.2174/1568026615666150610142647. PMID: 26059355.

Nacu, Anatolie, and Robert Hoerr. "Neuropsychiatric symptoms in dementia and the effects of Ginkgo biloba extract EGb 761® treatment: additional results from a 24-week randomized, placebo-controlled trial." *Open Access Journal of Clinical Trials* 8 (2016): 1-6.

Nakai A, Yamaguchi O, Takeda T, Higuchi Y, Hikoso S, Taniike M, et al. The role of autophagy in cardiomyocytes in the basal state and in response to hemodynamic stress. *Nat Med*. 2007;13(5):619–24.

Napryeyenko O, Borzenkol. Ginkgo biloba special extract in dementia with neuropsychiatric features. A randomised, placebo-controlled, double-blind clinical trial. *Arzneimittelforschung* 2007;57:4–11.

Nguyen B, Clements J. Obesity Management Among Patients With Type 2 Diabetes and Prediabetes: A Focus on Lifestyle Modifications and Evidence of Antiobesity Medications. *Expert Rev Endocrinol Metab* (2017) 12(5):303–13. doi: 10.1080/17446651.2017.1367285

Nicholson A, Reifsnyder PC, Malcolm RD, Lucas CA, MacGregor GR, Zhang W, Leiter EH. Diet-induced obesity in two C57BL/6 substrains with intact or mutant nicotinamide nucleotide transhydrogenase (Nnt) gene. *Obesity (Silver Spring)*. 2010 Oct;18(10):1902-5. doi: 10.1038/oby.2009.477. Epub 2010 Jan 7. PMID: 20057372; PMCID: PMC2888716.

Nikolic T, Petrovic D, Matic S, et al. The influence of folic acid- induced acute kidney injury on cardiac function and redox status in rats. *Naunyn Schmiedebergs Arch Pharmacol.* 2020;393(1):99- 109. doi:10.1007/s00210-019-01717-z

Nowak A, Kojder K, Zielonka-Brzezicka J, Wróbel J, Bosiacki M, Fabiańska M, Wróbel M, Sołek-Pastuszka J, Klimowicz A. The Use of Ginkgo Biloba L. as a Neuroprotective Agent in the Alzheimer's Disease. *Front Pharmacol.* 2021 Nov 4;12:775034. doi: 10.3389/fphar.2021.775034. PMID: 34803717; PMCID: PMC8599153.

Oguntibeju OO. Type 2 diabetes mellitus, oxidative stress and inflammation: examining the links. *Int J Physiol Pathophysiol Pharmacol.* 2019 Jun 15;11(3):45-63. PMID: 31333808; PMCID: PMC6628012.

Ortega A, Rámila D, Ardura JA, et al. Role of parathyroid hormone- related protein in tubulointerstitial apoptosis and fibrosis after folic acid-induced nephrotoxicity. *J Am Soc Nephrol.* 2006;17(6):1594- 1603. doi:10.1681/ASN.2005070690

Osto M, Abegg K, Bueter M, le Roux CW, Cani PD, Lutz TA. Roux-En-Y Gastric Bypass Surgery in Rats Alters Gut Microbiota Profile Along the Intestine. *Physiol Behav* (2013) 119:92–6. doi: 10.1016/j.physbeh.2013.06.008

Oveisi F, Gaetani S, Eng KT, Piomelli D. Oleoylethanolamide inhibits food intake in free-feeding rats after oral administration. *Pharmacol Res.* 2004 May;49(5):461-6. doi: 10.1016/j.phrs.2003.12.006. PMID: 14998556.

Overton HA, Babbs AJ, Doel SM, Fyfe MC, Gardner LS, Griffin G, Jackson HC, Procter MJ, Rasamison CM, Tang-Christensen M, Widdowson PS, Williams GM, Reynet C. Deorphanization of a G protein-coupled receptor for oleoylethanolamide and its use in the discovery of small-molecule hypophagic agents. *Cell Metab.* 2006 Mar;3(3):167-75. doi: 10.1016/j.cmet.2006.02.004. PMID: 16517404.

Pagliarini DJ, Calvo SE, Chang B, Sheth SA, Vafai SB, Ong SE, Walford GA, Sugiana C, Boneh A, Chen WK, Hill DE, Vidal M, Evans JG, Thorburn DR, Carr SA, Mootha VK. A mitochondrial protein compendium elucidates complex I disease biology. *Cell.* 2008 Jul 11;134(1):112-23. doi: 10.1016/j.cell.2008.06.016. PMID: 18614015; PMCID: PMC2778844.

Patel DK. Biological Importance of a Biflavonoid 'Bilobetin' in the Medicine: Medicinal Importance, Pharmacological Activities and Analytical Aspects. *Infect*

Disord Drug Targets. 2022;22(5):22-30. doi: 10.2174/1871526522666220321152036. PMID: 35319397.

Petersen G, Sørensen C, Schmid PC, Artmann A, Tang-Christensen M, Hansen SH, Larsen PJ, Schmid HH, Hansen HS. Intestinal levels of anandamide and oleoylethanolamide in food-deprived rats are regulated through their precursors. *Biochim Biophys Acta*. 2006 Feb;1761(2):143-50; discussion 141-2. doi: 10.1016/j.bbaliip.2005.12.011. Epub 2006 Jan 26. PMID: 16478679.

Pettersson US, Waldén TB, Carlsson PO, Jansson L, Phillipson M. Female mice are protected against high-fat diet induced metabolic syndrome and increase the regulatory T cell population in adipose tissue. *PLoS One*. 2012;7(9):e46057. doi: 10.1371/journal.pone.0046057. Epub 2012 Sep 25. PMID: 23049932; PMCID: PMC3458106.

Prasad R, Jha RK, Keerti A. Chronic Kidney Disease: Its Relationship With Obesity. *Cureus*. 2022 Oct 21;14(10):e30535. doi: 10.7759/cureus.30535. PMID: 36415443; PMCID: PMC9675899.

Proulx K, Cota D, Castañeda TR, Tschöp MH, D'Alessio DA, Tso P, Woods SC, Seeley RJ. Mechanisms of oleoylethanolamide-induced changes in feeding behavior and motor activity. *Am J Physiol Regul Integr Comp Physiol*. 2005 Sep;289(3):R729-37. doi: 10.1152/ajpregu.00029.2005. Epub 2005 May 5. PMID: 15879057.

Radunz CL, Okuyama CE, Branco-Barreiro FCA, Pereira RMS, Diniz SN. Clinical randomized trial study of hearing aids effectiveness in association with Ginkgo biloba extract (EGb 761) on tinnitus improvement. *Braz J Otorhinolaryngol*. 2020 Nov-Dec;86(6):734-742. doi: 10.1016/j.bjorl.2019.05.003. Epub 2019 Jun 18. PMID: 31300303; PMCID: PMC9422696.

Raso GM, Esposito E, Vitiello S, Iacono A, Santoro A, D'Agostino G, Sasso O, Russo R, Piazza PV, Calignano A, Meli R. Palmitoylethanolamide stimulation induces allopregnanolone synthesis in C6 Cells and primary astrocytes: involvement of peroxisome-proliferator activated receptor- α . *J Neuroendocrinol*. 2011 Jul;23(7):591-600. doi: 10.1111/j.1365-2826.2011.02152.x. PMID: 21554431.

Rebello CJ, Greenway FL. Obesity medications in development. *Expert Opin Investig Drugs*. 2020 Jan;29(1):63-71. doi: 10.1080/13543784.2020.1705277. Epub 2019 Dec 19. PMID: 31847611; PMCID: PMC6990416.

Ren T, Ma A, Zhuo R, Zhang H, Peng L, Jin X, Yao E, Yang L. Oleoylethanolamide Increases Glycogen Synthesis and Inhibits Hepatic Gluconeogenesis via the LKB1/AMPK Pathway in Type 2 Diabetic Model. *J Pharmacol Exp Ther*. 2020 Apr;373(1):81-91. doi: 10.1124/jpet.119.262675. Epub 2020 Feb 5. PMID: 32024803.

Reuter T. Y., 2007. Diet-induced models for obesity and type 2 diabetes. *Drug Discov. Today Dis. Models* 4, 3-8.

Rhee KJ, Lee CG, Kim SW, Gim DH, Kim HC, Jung BD. Extract of Ginkgo Biloba Ameliorates Streptozotocin-Induced Type 1 Diabetes Mellitus and High-Fat Diet-Induced Type 2 Diabetes Mellitus in Mice. *Int J Med Sci*. 2015 Nov 23;12(12):987-94. doi: 10.7150/ijms.13339. PMID: 26664261; PMCID: PMC4661298.

Ridge, Robert W., et al. *Ginkgo biloba: a global treasure: from biology to medicine*. Springer-Verlag, 1997.

Rivara MB, Mehrotra R. Timing of Dialysis Initiation: What Has Changed Since IDEAL? *Semin Nephrol*. 2017 Mar;37(2):181-193. doi: 10.1016/j.semnephrol.2016.12.008. PMID: 28410652; PMCID: PMC5407409.

Rodríguez de Fonseca F, Navarro M, Gómez R, Escuredo L, Nava F, Fu J, Murillo-Rodríguez E, Giuffrida A, LoVerme J, Gaetani S, Kathuria S, Gall C, Piomelli D. An anorexic lipid mediator regulated by feeding. *Nature*. 2001 Nov 8;414(6860):209-12. doi: 10.1038/35102582. PMID: 11700558.

Rodríguez de Fonseca F, Navarro M, Gómez R, Escuredo L, Nava F, Fu J, Murillo-Rodríguez E, Giuffrida A, LoVerme J, Gaetani S, Kathuria S, Gall C, Piomelli D. An anorexic lipid mediator regulated by feeding. *Nature*. 2001 Nov 8;414(6860):209-12. doi: 10.1038/35102582. PMID: 11700558.

Rogue A., C. Lambert, R. Josse' et al., "Comparative gene expression profiles induced by PPAR γ and PPAR α/γ agonists in human hepatocytes," *PLoS ONE*, vol. 6, no. 4, Article ID e18816, 15 pages, 2011.

Roy A, Jana M, Corbett GT, Ramaswamy S, Kordower JH, Gonzalez FJ, Pahan K. Regulation of cyclic AMP response element binding and hippocampal plasticity-related genes by peroxisome proliferator-activated receptor α . *Cell Rep*. 2013 Aug 29;4(4):724-37. doi: 10.1016/j.celrep.2013.07.028. Epub 2013 Aug 22. PMID: 23972989; PMCID: PMC3804033.

Ruggiero C, Ehrenshaft M, Cleland E, Stadler K. High-fat diet induces an initial adaptation of mitochondrial bioenergetics in the kidney despite evident oxidative stress and mitochondrial ROS production. *Am J Physiol Endocrinol Metab.* 2011 Jun;300(6):E1047-58. doi: 10.1152/ajpendo.00666.2010. Epub 2011 Mar 8. PMID: 21386058; PMCID: PMC3118596.

Russell RR 3rd, Bergeron R, Shulman GI, Young LH. Translocation of myocardial GLUT-4 and increased glucose uptake through activation of AMPK by AICAR. *Am J Physiol.* 1999 Aug;277(2):H643-9. doi: 10.1152/ajpheart.1999.277.2.H643. PMID: 10444490.

Saland JM, Pierce CB, Mitsnefes MM, Flynn JT, Goebel J, Kupferman JC, Warady BA, Furth SL; CKiD Investigators. Dyslipidemia in children with chronic kidney disease. *Kidney Int.* 2010 Dec;78(11):1154-63. doi: 10.1038/ki.2010.311. Epub 2010 Aug 25. PMID: 20736985; PMCID: PMC3222564.

Salt IP, Hardie DG. AMP-Activated Protein Kinase: An Ubiquitous Signaling Pathway With Key Roles in the Cardiovascular System. *Circ Res.* 2017 May 26;120(11):1825-1841. doi: 10.1161/CIRCRESAHA.117.309633. PMID: 28546359; PMCID: PMC5447810.

Samodelov SL, Gai Z, Kullak-Ublick GA, Visentin M. Renal reabsorption of folates: pharmacological and toxicological snapshots. *Nutrients.* 2019;11(10):2353. doi:10.3390/nu11102353

Saper, Robert B., and David Seres. "Clinical use of Ginkgo biloba." Uptodate. com Topic 1387 (2014).

Savaskan E, Mueller H, Hoerr R, von Gunten A, Gauthier S. Treatment effects of Ginkgo biloba extract EGb 761® on the spectrum of behavioral and psychological symptoms of dementia: meta-analysis of randomized controlled trials. *Int Psychogeriatr.* 2018 Mar;30(3):285-293. doi: 10.1017/S1041610217001892. Epub 2017 Sep 21. PMID: 28931444.

Saxton RA, Sabatini DM. mTOR Signaling in Growth, Metabolism, and Disease. *Cell.* 2017 Mar 9;168(6):960-976. doi: 10.1016/j.cell.2017.02.004. Erratum in: *Cell.* 2017 Apr 6;169(2):361-371. PMID: 28283069; PMCID: PMC5394987.

Sayd A, Antón M, Alén F, Caso JR, Pavón J, Leza JC, Rodríguez de Fonseca F, García-Bueno B, Orió L. Systemic administration of oleoylethanolamide protects from neuroinflammation and anhedonia induced by LPS in rats. *Int J Neuropsychopharmacol.* 2014 Dec 28;18(6):pyu111. doi: 10.1093/ijnp/pyu111.

Erratum in: *Int J Neuropsychopharmacol.* 2016;19(3). pii: pyw004. doi: 10.1093/ijnp/pyw004. PMID: 25548106; PMCID: PMC4438549.

Schneider LS, Dekosky ST, Farlow MR, Tariot PN, Hoerr R, Kieser M. A randomized, double-blind, placebo-controlled trial of two doses of Ginkgo biloba extract in dementia of the Alzheimer's type. *Curr Alzheimer Res* 2005;2:541–51.

Schneider MP, Schlaich MP, Harazny JM, et al. Folic acid treatment normalizes NOS-dependence of vascular tone in the metabolic syndrome. *Obesity.* 2011;19(5):960-967. doi:10.1038/oby.2010.210

Schwartz GJ, Fu J, Astarita G, Li X, Gaetani S, Campolongo P, Cuomo V, Piomelli D. The lipid messenger OEA links dietary fat intake to satiety. *Cell Metab.* 2008 Oct;8(4):281-288. doi: 10.1016/j.cmet.2008.08.005. PMID: 18840358; PMCID: PMC2572640.

Scripnikov A, Khomenko A, Napryeyenko O; GINDEM-NP Study Group. Effects of Ginkgo biloba extract EGb 761 on neuropsychiatric symptoms of dementia: findings from a randomised controlled trial. *Wien Med Wochenschr.* 2007;157(13-14):295-300. doi: 10.1007/s10354-007-0427-5. PMID: 17704975.

Serrano A, Pavón FJ, Tovar S, Casanueva F, Señarís R, Diéguez C, de Fonseca FR. Oleoylethanolamide: effects on hypothalamic transmitters and gut peptides regulating food intake. *Neuropharmacology.* 2011 Mar;60(4):593-601. doi: 10.1016/j.neuropharm.2010.12.007. Epub 2010 Dec 21. PMID: 21172362.

Shi R, Wang Y, An X, Ma J, Wu T, Yu X, Liu S, Huang L, Wang L, Liu J, Ge J, Qiu S, Yin H, Wang X, Wang Y, Yang B, Yu J, Sun Z. Efficacy of Co-administration of Liuwei Dihuang Pills and Ginkgo Biloba Tablets on Albuminuria in Type 2 Diabetes: A 24-Month, Multicenter, Double-Blind, Placebo-Controlled, Randomized Clinical Trial. *Front Endocrinol (Lausanne).* 2019 Feb 22;10:100. doi: 10.3389/fendo.2019.00100. PMID: 30873118; PMCID: PMC6402447.

Shoop S, Maria Z, Campolo A, Rashdan N, Martin D, Lovern P, et al. Glial Growth Factor 2 Regulates Glucose Transport in Healthy Cardiac Myocytes and During Myocardial Infarction via an Akt-Dependent Pathway. *Front Physiol.* 2019;10:189.

Sihag J, Jones PJH. Oleoylethanolamide: The role of a bioactive lipid amide in modulating eating behaviour. *Obes Rev.* 2018 Feb;19(2):178-197. doi: 10.1111/obr.12630. Epub 2017 Nov 10. PMID: 29124885.

Simon MF, Chap H, Braquet P, Douste-Blazy L. Effect of BN 52021, a specific antagonist of platelet activating factor (PAF-acether), on calcium movements and phosphatidic acid production induced by PAF-acether in human platelets. *Thromb Res.* 1987 Feb 15;45(4):299-309. doi: 10.1016/0049-3848(87)90219-2. PMID: 3576518.

Singh B, Kaur P, Gopichand, Singh RD, Ahuja PS. Biology and chemistry of Ginkgo biloba. *Fitoterapia.* 2008 Sep;79(6):401-18. doi: 10.1016/j.fitote.2008.05.007. Epub 2008 Jun 27. PMID: 18639617.

Small, Lewin, et al. "Thermoneutral housing does not influence fat mass or glucose homeostasis in C57BL/6 mice." *Journal of Endocrinology* 239.3 (2018): 313-324.

Song W, Zhao J, Yan XS, Fang X, Huo DS, Wang H, Jia JX, Yang ZJ. Mechanisms Associated with Protective Effects of Ginkgo Biloba Leaf Extracton in Rat Cerebral Ischemia Reperfusion Injury. *J Toxicol Environ Health A.* 2019;82(19):1045-1051. doi: 10.1080/15287394.2019.1686215. Epub 2019 Nov 18. PMID: 31735125.

Spiegel R, Kalla R, Mantokoudis G, Maire R, Mueller H, Hoerr R, Ihl R. *Ginkgo biloba* extract EGb 761® alleviates neurosensory symptoms in patients with dementia: a meta-analysis of treatment effects on tinnitus and dizziness in randomized, placebo-controlled trials. *Clin Interv Aging.* 2018 Jun 13;13:1121-1127. doi: 10.2147/CIA.S157877. PMID: 29942120; PMCID: PMC6005330.

Stanley WC, Recchia FA, Lopaschuk GD. Myocardial substrate metabolism in the normal and failing heart. *Physiol Rev.* 2005 Jul;85(3):1093-129. doi: 10.1152/physrev.00006.2004. PMID: 15987803.

Stasi A, Cosola C, Caggiano G, Cimmarusti MT, Palieri R, Acquaviva PM, Rana G, Gesualdo L. Obesity-Related Chronic Kidney Disease: Principal Mechanisms and New Approaches in Nutritional Management. *Front Nutr.* 2022 Jun 24;9:925619. doi: 10.3389/fnut.2022.925619. PMID: 35811945; PMCID: PMC9263700.

Stevens LA, Viswanathan G, Weiner DE. Chronic kidney disease and end-stage renal disease in the elderly population: current prevalence, future projections, and clinical significance. *Adv Chronic Kidney Dis.* 2010 Jul;17(4):293-301. doi: 10.1053/j.ackd.2010.03.010. PMID: 20610356; PMCID: PMC3160131.

Suardíaz M, Estivill-Torrús G, Goicoechea C, Bilbao A, Rodríguez de Fonseca F. Analgesic properties of oleoylethanolamide (OEA) in visceral and inflammatory

pain. *Pain*. 2007 Dec 15;133(1-3):99-110. doi: 10.1016/j.pain.2007.03.008. Epub 2007 Apr 20. PMID: 17449181.

Suárez J, Rivera P, Arrabal S, Crespillo A, Serrano A, Baixeras E, Pavón FJ, Cifuentes M, Nogueiras R, Ballesteros J, Dieguez C, Rodríguez de Fonseca F. Oleoylethanolamide enhances β -adrenergic-mediated thermogenesis and white-to-brown adipocyte phenotype in epididymal white adipose tissue in rat. *Dis Model Mech*. 2014 Jan;7(1):129-41. doi: 10.1242/dmm.013110. Epub 2013 Oct 23. PMID: 24159189; PMCID: PMC3882055.

Sun Y, Alexander SP, Garle MJ, Gibson CL, Hewitt K, Murphy SP, Kendall DA, Bennett AJ. Cannabinoid activation of PPAR alpha; a novel neuroprotective mechanism. *Br J Pharmacol*. 2007 Nov;152(5):734-43. doi: 10.1038/sj.bjp.0707478. Epub 2007 Oct 1. PMID: 17906680; PMCID: PMC2190030.

Sun Y, Ge X, Li X, He J, Wei X, Du J, Sun J, Li X, Xun Z, Liu W, Zhang H, Wang ZY, Li YC. High-fat diet promotes renal injury by inducing oxidative stress and mitochondrial dysfunction. *Cell Death Dis*. 2020 Oct 24;11(10):914. doi: 10.1038/s41419-020-03122-4. PMID: 33099578; PMCID: PMC7585574.

Suryavanshi SV, Kulkarni YA. NF- κ B: A Potential Target in the Management of Vascular Complications of Diabetes. *Front Pharmacol*. 2017 Nov 7;8:798. doi: 10.3389/fphar.2017.00798. PMID: 29163178; PMCID: PMC5681994.

Suzuki R, Kohno H, Sugie S, Sasaki K, Yoshimura T, Wada K, Tanaka T. Preventive effects of extract of leaves of ginkgo (*Ginkgo biloba*) and its component bilobalide on azoxymethane-induced colonic aberrant crypt foci in rats. *Cancer Lett*. 2004 Jul 16;210(2):159-69. doi: 10.1016/j.canlet.2004.01.034. PMID: 15183531.

Swinburn BA, Sacks G, Hall KD, McPherson K, Finegood DT, Moodie ML, Gortmaker SL. The global obesity pandemic: shaped by global drivers and local environments. *Lancet*. 2011 Aug 27;378(9793):804-14. doi: 10.1016/S0140-6736(11)60813-1. PMID: 21872749.

Tabassum Noor-E-, Das R, Lami MS, Chakraborty AJ, Mitra S, Tallei TE, Idroes R, Mohamed AA, Hossain MJ, Dhama K, Mostafa-Hedeab G, Emran TB. *Ginkgo biloba*: A Treasure of Functional Phytochemicals with Multimedicinal Applications. *Evid Based Complement Alternat Med*. 2022 Feb 28;2022:8288818. doi: 10.1155/2022/8288818. PMID: 35265150; PMCID: PMC8901348.

Tabrizi R, Nowrouzi-Sohrabi P, Hessami K, Rezaei S, Jalali M, Savardashtaki A, Shahabi S, Kolahi AA, Sahebkar A, Safiri S. Effects of Ginkgo biloba intake on cardiometabolic parameters in patients with type 2 diabetes mellitus: A systematic review and meta-analysis of clinical trials. *Phytother Res.* 2020 Oct 8. doi: 10.1002/ptr.6822. Epub ahead of print. PMID: 33090588.

Taegtmeyer H, Golfman L, Sharma S, Razeghi P, van Arsdall M. Linking gene expression to function: metabolic flexibility in the normal and diseased heart. *Ann N Y Acad Sci.* 2004 May;1015:202-13. doi: 10.1196/annals.1302.017. PMID: 15201161.

Tai T, Tsuboi K, Uyama T, Masuda K, Cravatt BF, Houchi H, Ueda N. Endogenous molecules stimulating N-acyl ethanolamine-hydrolyzing acid amidase (NAAA). *ACS Chem Neurosci.* 2012 May 16;3(5):379-85. doi: 10.1021/cn300007s. Epub 2012 Jan 27. PMID: 22860206; PMCID: PMC3382453.

Takano H, Nagai T, Asakawa M, Toyozaki T, Oka T, Komuro I, Saito T, Masuda Y. Peroxisome proliferator-activated receptor activators inhibit lipopolysaccharide-induced tumor necrosis factor- α expression in neonatal rat cardiac myocytes. *Circ Res.* 2000 Sep 29;87(7):596-602. doi: 10.1161/01.res.87.7.596. PMID: 11009565.

Tanaka Y, Kume S, Araki S, Isshiki K, Chin-Kanasaki M, Sakaguchi M, Sugimoto T, Koya D, Haneda M, Kashiwagi A, Maegawa H, Uzu T. Fenofibrate, a PPAR α agonist, has renoprotective effects in mice by enhancing renal lipolysis. *Kidney Int.* 2011 Apr;79(8):871-82. doi: 10.1038/ki.2010.530. Epub 2011 Jan 26. PMID: 21270762.

Tang M, Cao X, Zhang K, Li Y, Zheng QY, Li GQ, He QH, Li SJ, Xu GL, Zhang KQ. Celastrol alleviates renal fibrosis by upregulating cannabinoid receptor 2 expression. *Cell Death Dis.* 2018 May 22;9(6):601. doi: 10.1038/s41419-018-0666-y. PMID: 29789558; PMCID: PMC5964092.

Tao Z, Jin W, Ao M, Zhai S, Xu H, Yu L. Evaluation of the anti-inflammatory properties of the active constituents in Ginkgo biloba for the treatment of pulmonary diseases. *Food Funct.* 2019 Apr 17;10(4):2209-2220. doi: 10.1039/c8fo02506a. PMID: 30945705.

Telle-Hansen VH, Halvorsen B, Dalen KT, Narverud I, Wesseltoft-Rao N, Granlund L, Ulven SM, Holven KB. Altered expression of genes involved in lipid metabolism in obese subjects with unfavourable phenotype. *Genes Nutr.* 2013 Jul;8(4):425-

34. doi: 10.1007/s12263-012-0329-z. Epub 2013 Jan 8. PMID: 23296345; PMCID: PMC3689894.

Telles S, Gangadhar BN, Chandwani KD. Lifestyle Modification in the Prevention and Management of Obesity. *J Obes* (2016) 2016:5818601. doi: 10.1155/2016/5818601

Tellez LA, Medina S, Han W, Ferreira JG, Licona-Limón P, Ren X, Lam TT, Schwartz GJ, de Araujo IE. A gut lipid messenger links excess dietary fat to dopamine deficiency. *Science*. 2013 Aug 16;341(6147):800-2. doi: 10.1126/science.1239275. PMID: 23950538.

Terman A, Kurz T, Navratil M, Arriaga EA, Brunk UT. Mitochondrial Turnover and Aging of Long-Lived Postmitotic Cells: The Mitochondrial–Lysosomal Axis Theory of Aging. *Antioxid Redox Signal*. 2010;12(4):503–35.

Thabuis C, Destailats F, Lambert DM, Muccioli GG, Maillot M, Harach T, Tissot-Favre D, Martin JC. Lipid transport function is the main target of oral oleoylethanolamide to reduce adiposity in high-fat-fed mice. *J Lipid Res*. 2011 Jul;52(7):1373-82. doi: 10.1194/jlr.M013391. Epub 2011 Apr 24. PMID: 21515921; PMCID: PMC3111743.

Tsuboi K, Takezaki N, Ueda N. The N-acylethanolamine-hydrolyzing acid amidase (NAAA). *Chem Biodivers*. 2007 Aug;4(8):1914-25. doi: 10.1002/cbdv.200790159. PMID: 17712833.

Tucker PS, Scanlan AT, Dalbo VJ. Chronic kidney disease influences multiple systems: describing the relationship between oxidative stress, inflammation, kidney damage, and concomitant disease. *Oxid Med Cell Longev*. 2015;2015:806358. doi: 10.1155/2015/806358. Epub 2015 Mar 15. PMID: 25861414; PMCID: PMC4377508.

Tufano M, Pinna G. Is There a Future for PPARs in the Treatment of Neuropsychiatric Disorders? *Molecules*. 2020 Feb 27;25(5):1062. doi: 10.3390/molecules25051062. PMID: 32120979; PMCID: PMC7179196.

Tutunchi H, Ostadrahimi A, Saghafi-Asl M, Roshanravan N, Shakeri-Bavil A, Asghari-Jafarabadi M, Farrin N, Mobasser M. Expression of NF- κ B, IL-6, and IL-10 genes, body composition, and hepatic fibrosis in obese patients with NAFLD- Combined effects of oleoylethanolamide supplementation and calorie restriction: A triple-blind randomized controlled clinical trial. *J Cell Physiol*. 2021

Jan;236(1):417-426. doi: 10.1002/jcp.29870. Epub 2020 Jun 22. PMID: 32572955.

Ueda N, Tsuboi K, Uyama T. N-acylethanolamine metabolism with special reference to N-acylethanolamine-hydrolyzing acid amidase (NAAA). *Prog Lipid Res.* 2010 Oct;49(4):299-315. doi: 10.1016/j.plipres.2010.02.003. Epub 2010 Feb 10. PMID: 20152858.

Ueda N, Yamanaka K, Yamamoto S. Purification and characterization of an acid amidase selective for N-palmitoylethanolamine, a putative endogenous anti-inflammatory substance. *J Biol Chem.* 2001 Sep 21;276(38):35552-7. doi: 10.1074/jbc.M106261200. Epub 2001 Jul 19. PMID: 11463796.

Ueda, N., Tsuboi, K., and Uyama, T. (2013) Metabolism of endocannabinoids and related N-acylethanolamines: canonical and alternative pathways. *FEBS J.* 280, 1874–1894.

Usuda D. and T. Kanda, "Peroxisome proliferator-activated receptors for hypertension," *World Journal of Cardiology*, vol. 6, no. 8, pp. 744–754, 2014.

van Beek TA, Montoro P. Chemical analysis and quality control of Ginkgo biloba leaves, extracts, and phytopharmaceuticals. *J Chromatogr A.* 2009 Mar 13;1216(11):2002-32. doi: 10.1016/j.chroma.2009.01.013. Epub 2009 Jan 15. PMID: 19195661.

Venkatachalam MA, Griffin KA, Lan R, Geng H, Saikumar P, Bidani AK. Acute kidney injury: a springboard for progression in chronic kidney disease. *Am J Physiol Renal Physiol.* 2010 May;298(5):F1078-94. doi: 10.1152/ajprenal.00017.2010. Epub 2010 Mar 3. PMID: 20200097; PMCID: PMC2867413.

Wali JA, Jarzebska N, Raubenheimer D, Simpson SJ, Rodionov RN, O'Sullivan JF. Cardio-Metabolic Effects of High-Fat Diets and Their Underlying Mechanisms-A Narrative Review. *Nutrients.* 2020 May 21;12(5):1505. doi: 10.3390/nu12051505. PMID: 32455838; PMCID: PMC7284903.

Wang CY, Liao JK. A mouse model of diet-induced obesity and insulin resistance. *Methods Mol Biol.* 2012;821:421-33. doi: 10.1007/978-1-61779-430-8_27. PMID: 22125082; PMCID: PMC3807094.

Wang CY, Liao JK. A mouse model of diet-induced obesity and insulin resistance. *Methods Mol Biol.* 2012;821:421-33. doi: 10.1007/978-1-61779-430-8_27. PMID: 22125082; PMCID: PMC3807094.

Wang X, Miyares RL, Ahern GP. Oleoylethanolamide excites vagal sensory neurones, induces visceral pain and reduces short-term food intake in mice via capsaicin receptor TRPV1. *J Physiol.* 2005 Apr 15;564(Pt 2):541-7. doi: 10.1113/jphysiol.2004.081844. Epub 2005 Feb 3. PMID: 15695242; PMCID: PMC1464447.

Wang X, Miyares RL, Ahern GP. Oleoylethanolamide excites vagal sensory neurones, induces visceral pain and reduces short-term food intake in mice via capsaicin receptor TRPV1. *J Physiol.* 2005 Apr 15;564(Pt 2):541-7. doi: 10.1113/jphysiol.2004.081844. Epub 2005 Feb 3. PMID: 15695242; PMCID: PMC1464447.

Wanner C, Krane V. Recent advances in the treatment of atherogenic dyslipidemia in type 2 diabetes mellitus. *Kidney Blood Press Res.* 2011;34(4):209-17. doi: 10.1159/000326849. Epub 2011 Jun 21. PMID: 21691123.

Warden A, Truitt J, Merriman M, Ponomareva O, Jameson K, Ferguson LB, Mayfield RD, Harris RA. Localization of PPAR isotypes in the adult mouse and human brain. *Sci Rep.* 2016 Jun 10;6:27618. doi: 10.1038/srep27618. PMID: 27283430; PMCID: PMC4901333.

Wehrmann, M. et al. Long-term prognosis of focal sclerosing glomerulonephritis. An analysis of 250 cases with particular regard to tubulointerstitial changes. *Clin. Nephrol.* 33, 115–122 (1990).

Wei BQ, Mikkelsen TS, McKinney MK, Lander ES, Cravatt BF. A second fatty acid amide hydrolase with variable distribution among placental mammals. *J Biol Chem.* 2006 Dec 1;281(48):36569-78. doi: 10.1074/jbc.M606646200. Epub 2006 Oct 2. PMID: 17015445.

Wellner, N., Diep, T. A., Janfelt, C., and Hansen, H. S. (2013) N-acylation of phosphatidylethanolamine and its biological functions in mammals. *Biochim. Biophys. Acta* 1831, 652–662.

Whaley-Connell A, Sowers JR. Basic science: Pathophysiology: the cardiorenal metabolic syndrome. *J Am Soc Hypertens.* 2014 Aug;8(8):604-6. doi: 10.1016/j.jash.2014.07.003. Epub 2014 Jul 5. PMID: 25151323; PMCID: PMC4170524.

WHO Consultation on Obesity (1999: Geneva, Switzerland) & World Health Organization. Obesity: Preventing and Managing the Global Epidemic. Report of a WHO Consultation. World Health Organ Tech Rep Ser (2000) 894:i–xii, 1-253.

Willson T. M., P. J. Brown, D. D. Sternbach, and B. R. Henke, "The PPARs: from orphan receptors to drug discovery," *Journal of Medicinal Chemistry*, vol. 43, no. 4, pp. 527–550, 2000.

World Obesity Atlas 2022. https://s3-eu-west-1.amazonaws.com/wof-files/World_Obesity_Atlas_2022.pdf Accessed 7 November 2022

Xie Y, Bowe B, Mokdad AH, Xian H, Yan Y, Li T, Maddukuri G, Tsai CY, Floyd T, Al-Aly Z. Analysis of the Global Burden of Disease study highlights the global, regional, and national trends of chronic kidney disease epidemiology from 1990 to 2016. *Kidney Int.* 2018 Sep;94(3):567-581. doi: 10.1016/j.kint.2018.04.011. Epub 2018 Aug 3. PMID: 30078514.

Xu F, Tavintharan S, Sum CF, Woon K, Lim SC, Ong CN. Metabolic signature shift in type 2 diabetes mellitus revealed by mass spectrometry-based metabolomics. *J Clin Endocrinol Metab.* 2013 Jun;98(6):E1060-5. doi: 10.1210/jc.2012-4132. Epub 2013 Apr 30. PMID: 23633210.

Yang L, Guo H, Li Y, Meng X, Yan L, Dan Zhang, Wu S, Zhou H, Peng L, Xie Q, Jin X. Oleoylethanolamide exerts anti-inflammatory effects on LPS-induced THP-1 cells by enhancing PPAR α signaling and inhibiting the NF- κ B and ERK1/2/AP-1/STAT3 pathways. *Sci Rep.* 2016 Oct 10;6:34611. doi: 10.1038/srep34611. PMID: 27721381; PMCID: PMC5056375.

Yang Y, Chen M, Georgeson KE, Harmon CM. Mechanism of oleoylethanolamide on fatty acid uptake in small intestine after food intake and body weight reduction. *Am J Physiol Regul Integr Comp Physiol.* 2007 Jan;292(1):R235-41. doi: 10.1152/ajpregu.00270.2006. Epub 2006 Aug 10. PMID: 16902188.

Yang Y, Chen M, Georgeson KE, Harmon CM. Mechanism of oleoylethanolamide on fatty acid uptake in small intestine after food intake and body weight reduction. *Am J Physiol Regul Integr Comp Physiol.* 2007 Jan;292(1):R235-41. doi: 10.1152/ajpregu.00270.2006. Epub 2006 Aug 10. PMID: 16902188.

Yao, Z. X., Han, Z., Drieu, K., & Papadopoulos, V. (2004). Ginkgo biloba extract (Egb 761) inhibits beta-amyloid production by lowering free cholesterol levels. *The Journal of Nutritional Biochemistry*, 15(12), 749–756. <https://doi.org/10.1016/j.jnutbio.2004.06.008>

Yeo GSH, Chao DHM, Siegert AM, Koerperich ZM, Ericson MD, Simonds SE, Larson CM, Luquet S, Clarke I, Sharma S, Clément K, Cowley MA, Haskell-Luevano C, Van Der Ploeg L, Adan RAH. The melanocortin pathway and energy homeostasis: From discovery to obesity therapy. *Mol Metab.* 2021 Jun;48:101206. doi: 10.1016/j.molmet.2021.101206. Epub 2021 Mar 6. PMID: 33684608; PMCID: PMC8050006.

Yu D, Zhang P, Li J, Liu T, Zhang Y, Wang Q, Zhang J, Lu X, Fan X. Neuroprotective effects of *Ginkgo biloba* dropping pills in Parkinson's disease. *J Pharm Anal.* 2021 Apr;11(2):220-231. doi: 10.1016/j.jpha.2020.06.002. Epub 2020 Jun 20. PMID: 34012698; PMCID: PMC8116202.

Yuan Q, Tang B, Zhang C. Signaling pathways of chronic kidney diseases, implications for therapeutics. *Signal Transduct Target Ther.* 2022 Jun 9;7(1):182. doi: 10.1038/s41392-022-01036-5. PMID: 35680856; PMCID: PMC9184651.

Zaghloul MS, Abdelrahman RS. Nilotinib ameliorates folic acid-induced acute kidney injury through modulation of TWEAK and HSP-70 pathways. *Toxicology.* 2019 Nov 1;427:152303. doi: 10.1016/j.tox.2019.152303. Epub 2019 Oct 5. PMID: 31593741.

Zannad F, Rossignol P. Cardiorenal Syndrome Revisited. *Circulation.* 2018 Aug 28;138(9):929-944. doi: 10.1161/CIRCULATIONAHA.117.028814. PMID: 30354446.

Zarantonello D, Rhee CM, Kalantar-Zadeh K, Brunori G. Novel conservative management of chronic kidney disease via dialysis-free interventions. *Curr Opin Nephrol Hypertens.* 2021 Jan;30(1):97-107. doi: 10.1097/MNH.0000000000000670. PMID: 33186220.

Zeisberg, M. & Kalluri, R. Cellular mechanisms of tissue fibrosis. 1. Common and organ-specific mechanisms associated with tissue fibrosis. *Am. J. Physiol. Cell Physiol.* 304, C216–C225 (2012).

Zhang H, Cai L. Zinc homeostasis plays an important role in the prevention of obesity-induced cardiac inflammation, remodeling and dysfunction. *J Trace Elem Med Biol.* 2020 Dec;62:126615. doi: 10.1016/j.jtemb.2020.126615. Epub 2020 Jul 10. PMID: 32683230.

Zhang Y, Whaley-Connell AT, Sowers JR, Ren J. Autophagy as an emerging target in cardiorenal metabolic disease: From pathophysiology to management.

Pharmacol Ther. 2018 Nov;191:1-22. doi: 10.1016/j.pharmthera.2018.06.004. Epub 2018 Jun 22. PMID: 29909238; PMCID: PMC6195437.

Zhang YE. Non-Smad pathways in TGF- β signalling. *Cell Research*. 2009 19(1):128-139.

Zhang YE. Non-Smad Signaling Pathways of the TGF- β Family. *Cold Spring Harb Perspect Biol*. 2017 Feb 1;9(2):a022129. doi: 10.1101/cshperspect.a022129. PMID: 27864313; PMCID: PMC5287080.

Zhao P, Sun X, Chaggan C, Liao Z, In Wong K, He F, Singh S, Loomba R, Karin M, Witztum JL, Saltiel AR. An AMPK-caspase-6 axis controls liver damage in nonalcoholic steatohepatitis. *Science*. 2020 Feb 7;367(6478):652-660. doi: 10.1126/science.aay0542. PMID: 32029622; PMCID: PMC8012106.

Zhao, Y., Yu, J., Liu, J., & An, X. (2016). The role of Liuwei Dihuang pills and Ginkgo leaf tablets in treating diabetic complications. *Evidence-Based Complementary and Alternative Medicine*, 2016(7931314), 1–8.

Zhou X, Qi Y, Chen T. Long-term pre-treatment of antioxidant Ginkgo biloba extract EGb-761 attenuates cerebral-ischemia-induced neuronal damage in aged mice. *Biomed Pharmacother*. 2017 Jan;85:256-263. doi: 10.1016/j.biopha.2016.11.013. Epub 2016 Nov 15. PMID: 27863840.

Zhou Y, Yang L, Ma A, Zhang X, Li W, Yang W, Chen C, Jin X. Orally administered oleylethanolamide protects mice from focal cerebral ischemic injury by activating peroxisome proliferator-activated receptor α . *Neuropharmacology*. 2012 Aug;63(2):242-9. doi: 10.1016/j.neuropharm.2012.03.008. Epub 2012 Mar 28. PMID: 22480617.

Zhu F, Chong Lee Shin OL, Xu H, et al. Melatonin promoted renal regeneration in folic acid-induced acute kidney injury via inhibiting nucleocytoplasmic translocation of HMGB1 in tubular epithelial cells. *Am J Transl Res*. 2017;9(4):1694-1707.

Zhu S, Sun F, Li W, Cao Y, Wang C, Wang Y, Liang D, Zhang R, Zhang S, Wang H, Cao F. Apelin stimulates glucose uptake through the PI3K/Akt pathway and improves insulin resistance in 3T3-L1 adipocytes. *Mol Cell Biochem*. 2011 Jul;353(1-2):305-13. doi: 10.1007/s11010-011-0799-0. Epub 2011 Apr 2. PMID: 21461612.

Zoccali C, Mallamaci F. Uric acid, hypertension, and cardiovascular and renal complications. *Curr Hypertens Rep.* 2013 Dec;15(6):531-7. doi: 10.1007/s11906-013-0391-y. PMID: 24072559.

Zoccali C, Vanholder R, Massy ZA, Ortiz A, Sarafidis P, Dekker FW, Fliser D, Fouque D, Heine GH, Jager KJ, Kanbay M, Mallamaci F, Parati G, Rossignol P, Wiecek A, London G; European Renal and Cardiovascular Medicine (EURECA-m) Working Group of the European Renal Association – European Dialysis Transplantation Association (ERA-EDTA). The systemic nature of CKD. *Nat Rev Nephrol.* 2017 Jun;13(6):344-358. doi: 10.1038/nrneph.2017.52. Epub 2017 Apr 24. PMID: 28435157.